Heating Dynamics and Thermalization of Interacting Luttinger Liquids

Heizdynamik und Thermalisierung Wechselwirkender Luttinger Liquids

Master's thesis

Sebastian Huber

Chair of Theoretical Solid State Physics
Faculty of Physics
Ludwig-Maximilians-University Munich

First Supervisor: Prof. Dr. J. von Delft
Second Supervisor: Prof. Dr. S. Diehl

May 05, 2015

Contents

Chapter 1

Introduction

The high degree of tunability and control associated with ultracold gases[1,2] offer a platform to study challenging phenomena as many-body localization[3] and dynamics of interacting quantum systems[4,5]. Since in such experiments the system is often not completely decoupled from the environment, strong theoretical effort has been spent during the last decades to develop possible concepts to capture nonequilbrium phenomena. One specific and fundamental problem is the understanding of the dynamics of a quantum many-body system out of equilibrium.[4,6] In chapter 1 to 9 we investigate a one dimensional system, which is continuously driven out of equilibrium by pumping energy from an external source. Whereas past studies have focused on the long time dynamics in such a system[7,8], our theoretical approach uses the interacting Luttinger Liquid formalism, which as we show breaks due to the permanent number conserving heating after a distinct cutoff in time down.
During this introduction, we discuss in more detail the physical aspects of nonequilibrium dynamics initialized by a so-called quantum quench[9–15], where due to an instantaneous manipulation of the system's parameter, i.e. $H_0 \to H$, a large amount of energy is generated in the system and a time evolution is initialized. The time scale on which the quench needs to happen is smaller than the generic time scale of the system.[9] After quenching the system out of equilibrium, a relaxation process starts, in which generic interactions try to guide the system back to equilibrium. At this stage the time evolution of the system is very complex and the final state is not obvious at all. As an example we consider a Luttinger Liquid[16–20] that describes a one dimensional system in the regime of low energy excitations with a linear dispersion:

$$\hat{H}_\nu = \sum_q \nu |q| \hat{n}_q, \tag{1.1}$$

where $\hat{n}_q$ is the momentum density operator for the generic excitations of the Luttinger Liquid (cf. chapter 2). The initial state of the system is considered to be a pure state of $\hat{H}_\nu$. Now we change suddenly the characteristic velocity of the Luttinger Liquid: $\hat{H}_\nu \to \hat{H}_{\nu'}$. The state of the system is now not any more a superposition of eigenstates with respect to the new Hamiltonian $\hat{H}_{\nu'}$ and therefore the dynamical evolution is not straightforward.
In order to make further progress in understanding the time evolution of the density operator out of equilibrium, we visualize the quench scenario at $t = 0$, where $\hat{H}_\nu \to \hat{H}_{\nu'}$. As a consequence the initial stationary density matrix is shifted out of equilibrium (cf. Fig. 1.1). The state of the system $\hat{\rho}(t = 0)$ does not need to commute with the new Hamiltonian $\hat{H}_{\nu'}$ and the non stationary density operator evolves in time (cf. Fig. 1.1). At an intermediate time interval the density operator can reach a metastable, so-called prethermalized

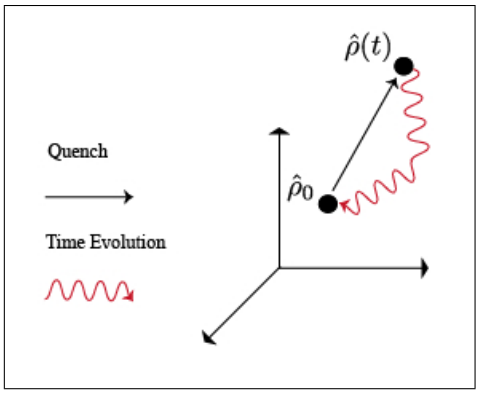

Figure 1.1: *The density operator is quenched out of equilibrium.*

state[21–23] (cf. Fig. 1.2), which we consider as an unstable fixed point. In such a prethermalized state a restricted amount of observables can reach already the final steady state value of a completely thermalized system. Even though the system has yet not completely thermalized, recent works have shown that we can define for instance for a Luttinger Liquid at this stage a generalized Gibb's ensemble[10–12,24]:

$$\hat{\rho} = Z^{-1} e^{-\sum_m \lambda_m \hat{A}_m}, \tag{1.2}$$

where $\left\langle \hat{A}_m \right\rangle$ are the integral of motions and $Z = \mathrm{tr}[e^{-\sum_m \lambda_m \hat{A}_m}]$. λ_m are the Lagrange multipliers, which are explicitely computed maximizing the entropy.
Furthermore, the momentum density operator is at each time step during the dynamics a conserved quantity

$$\partial_t \hat{n}_q = -i[\hat{H}_\nu, \hat{n}_q] \tag{1.3}$$

and thus the system memorizes its initial value at the quench $\langle \hat{n}_q(t=0) \rangle$ for all time. From a classical view the extensive number of integrals of motions restricts the dynamics of the system in phase space and thus the system can not truly thermalize by ergodicity.[25] As a consequence a Luttinger Liquid (Fig 1.3 (a))[26] does not thermalize after a sudden quench, which is experimentally proven (Fig 1.3 (b)).[27,28]
We are interested in the process of thermalization in a one dimensional system of interacting bosons and include thereby to leading order generic scattering terms to generate a possibility for integrability breaking that allows for thermalization.[29–31] Such RG-irrelevant non-linearities do not enter in the static properties of observables, however dominate the dynamics to leading

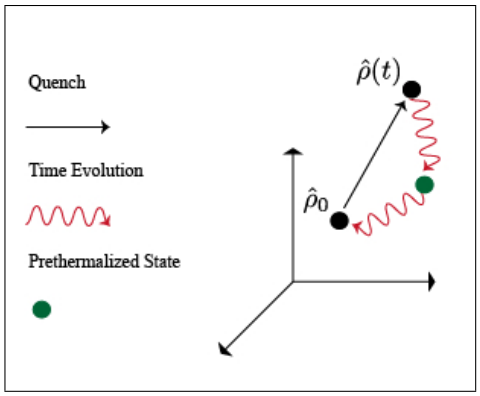

Figure 1.2: *Time evolution of the density operator with a prethermalized intermediate state.*

order and depend on the frequency. The redistribution of energy and momentum due to the interactions between the excitations can cause thermalization.

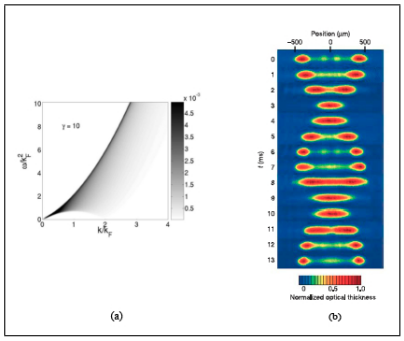

Figure 1.3: *(a) Spectrum of quantum liquid*[26]*, (b) No thermalization in a Luttinger Liquid.*[27]

Thus we extend the bare Luttinger Liquid model by a generic interaction to analyse the dynamics of a one dimensional system during the process of thermalization.
As a starting point of our description we use a microscopic model of interacting bosonic particles in a one dimensional optical lattice.[32] Due to the presence of the laser field, stimulated emission and absorption contribute to the coherent dynamics. Additionally the system undergoes spontaneous processes, which are responsible for the dissipative dynamics in the system. The system is continuously driven out of equilibrium by the presence of a permanent number conserving heating mechanism.
We use the dynamics of the phonon density to determine effective thermal-

ization and determine that the phonon density at each forward time step separates in two regimes: Effective thermalization sets in at large momenta and spreads continuously to lower momenta.[30,31] In contrast universal non-equilibrium linear scaling at low momenta is present. The process of thermalization is at each time step observed in the occupation of the momentum phonon density. Additionally the presence of the interaction renormalizes the lifetime of the phonon excitations. Compared to former work, where the phonon lifetime $\tau_{qp} \propto p^{\alpha}$ scales with $\alpha = \frac{3}{2}$ for $T \neq 0$[31,33–35] and $\alpha = 2$ for $T = 0$[26,31,36,37] due to the presence of the interactions, the characteristic exponent for the universal linear regime is $\alpha = \frac{5}{3}$.[31] This universal scaling behaviour is a direct consequence of the vertex structure and $U(1)$ symmetry. In conclusion, the dynamics is strongly influenced by the presence of the interactions, generate effective thermalization and modify the phonon lifetime. In chapter 10 we consider a completely different setup of two uncoupled wires in a closed quantum system. At $t = 0$ the initial state is prepared in a way that both subsystems are in perfect phase coherence and are thus coupled initially.[58–60] For $t > 0$ the time evolution is that of two uncoupled wires and is described by two independent Hamiltonians of a Luttinger Liquid. We study the time evolution of the important experimental relative phase correlation function and include the case of a Luttinger Liquid with interactions. We observe a new exponential regime in the relative phase correlation function on small relative distances, which indicates a local spreading of the decay of the relative phase correlation function due to the scattering effects. This thesis is organized as follows: The second chapter explains the formalism for the interacting Luttinger Liquid. In the following we start with the quantum master equation (chpater 3), which is mapped to a Keldysh field integral in order to describe the quantum many-body systems out of equilibrium (chapter 4). From this we derive the kinetic equation that describes the time evolution of the phonon density and calculate thereby the self-energies in a diagrammatic approach (cf. chapter 5 and 6). We determine a modification of the quasiparticle lifetime in chapter 7 and specify universality of the system as a consequence of the interaction structure and symmetry. In some limiting cases we conclude from the kinetic equation the scaling regimes of the phonon density and already get a hint on the effective thermalization with respect to the phonon density (cf. chapter 8). Chapter 9 describes the time evolution of the phonon density for a thermal initial state. Finally, we investigate two uncoupled interacting Luttinger Liquids initialized in a state with perfect phase coherence between the liquids (cf. chapter 10).

Chapter 2

Luttinger Liquids

In this chapter the microscopic model of interacting bosonic atoms on a one dimensional lattice is used to derive an effective long wavelength description. We are interested in the low-energy dynamics of a one dimensional system and use the appropriate Luttinger Liquid formalism.[16,19,38] The relations between the microscopic physical parameters and the final effective interacting Luttinger model are estimated at weak coupling[19,20]: For instance the compressibilty of the system κ tunes the Luttinger Liquid parameter ν. Finally in section 2.3 we investigate the leading order scattering processes that drive the dynamics.[29–31]

2.1 Bose-Hubbard Model on a Lattice

We consider a general system of interacting bosons on a one dimensional lattice and conclude the well-known Bose-Hubbard model.[39,40] The corresponding Hamiltonian of N particles that interact via a two-body scattering and confined to an external potential is given by

$$\hat{H} = \underbrace{\sum_i \frac{\hat{p}_i^2}{2m} + V_{\text{ext}}(\hat{x}_i)}_{\hat{H}_0} + \sum_{i,j} V_{\text{int}}(\hat{x}_i - \hat{x}_j), \tag{2.1}$$

where $\hat{p}_i = i\hbar\dfrac{\partial}{\partial x_i}$ and $[\hat{x}_i, \hat{p}_i] = i\hbar$. The full Hamiltonian in second quantization reads

$$\hat{H} = \sum_{i,j} t_{i,j}\hat{b}_i^\dagger\hat{b}_j + \sum_{i,j,k,l} V_{ijkl}\hat{b}_i^\dagger\hat{b}_j^\dagger\hat{b}_k\hat{b}_l, \tag{2.2}$$

where $t_{ij} = \langle i|\, \hat{H}_0\, |j\rangle$ and $V_{ijkl} = \langle ij|\, V_{\text{int}}(\hat{x}_i - \hat{x}_j)\, |kl\rangle$.
Here we choose $\{|i\rangle\}$ to be the Wannier states representing localized atomic orbitals. For a sufficiently deep lattice the free Hamiltonian reduces to a tridiagonal structure

$$\hat{H}_0 = \sum_i [-J(\hat{b}_{i+1}^\dagger\hat{b}_i + \hat{b}_{i+1}\hat{b}_i^\dagger)], \tag{2.3}$$

where the hopping parameter $J = t_{i,i+1}$.
A prominent example for the interaction potential is the contact interaction

$$V_{\text{int}}(\hat{x}_i - \hat{x}_j) = g\delta(\hat{x}_i - \hat{x}_j). \tag{2.4}$$

For instance ultracold dilute quantum gases at low temperatures are well described by such an interaction.[1,2] The parameter g is related to the s-wave

scattering length. Thus the Bose-Hubbard Hamiltonian appears:

$$\hat{H} = \sum_i [-J(\hat{b}_{i+1}^\dagger \hat{b}_i + \hat{b}_{i+1}\hat{b}_i^\dagger) + \frac{U}{2}\sum_i \hat{n}_i(\hat{n}_i - 1)], \tag{2.5}$$

where $\hat{n}_i = \hat{b}_i^\dagger \hat{b}_i$ and $U = g$.
The Bose-Hubbard model is exactly solvable in the two limits $\frac{J}{U} \to \infty$ and $\frac{J}{U} \to 0$.[2,20] The former is equivalent to the Tonks-Girardeau gas (hard core bosons) on a lattice. As a consequence the density operator is constrained to integer values and the Hamiltonian includes only the kinetic term.

2.2 Luttinger Liquid Description of the Bose-Hubbard Hamiltonian

In order to have an effective low-energy model of the system, we start from the discrete Bose-Hubbard Hamiltonian and consider the long-wavelength limit. Such a continuous description is introduced by

$$\hat{b}_i \to a^{\frac{1}{2}} \hat{b}\ (x)|_{x=ia}, \tag{2.6}$$

$$\hat{b}_{i+1}^\dagger \hat{b}_i + \hat{b}_{i+1}\hat{b}_i^\dagger \to (2\hat{n}(x) - 2a^2[\partial_x \hat{b}\ (x)\partial_x \hat{b}^\dagger(x)])a, \tag{2.7}$$

$$\sum_i \to \frac{1}{a}\int dx. \tag{2.8}$$

These definitions are applied to the Hamiltonian of the Bose-Hubbard model (2.5)

$$\begin{aligned}\hat{H} &= \sum_i [-J(\hat{b}_{i+1}^\dagger \hat{b}_i + \hat{b}_{i+1}\hat{b}_i^\dagger) + \frac{1}{2}\sum_i U\hat{n}_i(\hat{n}_i - 1)] \\ &= \int_x J[2a^2(\partial_x \hat{b}\ (x)\partial_x \hat{b}^\dagger(x))] + \frac{U}{2}[\hat{b}^\dagger(x)\hat{b}(x)(\hat{b}^\dagger(x)\hat{b}(x) - 1)].\end{aligned} \tag{2.9}$$

After transforming to the continuum description to arrive at a low energy description, we automatically focus on the minimum of the dispersion relation of the lowest Bloch band (cf. Fig. 2.1).
In one dimension the low-energy theory for interacting bosons is the so-called Luttinger Liquid theory (cf. Appendix A).[16,19,38,41] Its applicability is restricted to the linear regime of the dispersion relation:

$$v_L = \frac{\epsilon(p)}{p}|_{min} \simeq (\frac{p\rho_0}{2m} + \frac{U\rho_0^2}{2p})|_{min} \Rightarrow p_L = \sqrt{U\rho_0 m}. \tag{2.10}$$

In the momentum regime $p < p_L$, the hydrodynamic description is due to (2.10) valid. This liquid phase is not equivalent to the superfluid phase occuring for example in three dimensional systems of ultracold quantum gases, where the system has long-range order. In one dimension the density fluc-

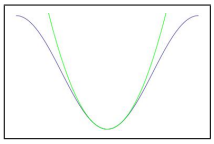

Figure 2.1: *Low-energy description: Minimum of the lowest Bloch band.*

tuations are gapless as well. As a consequence of the reduced dimension the system prefers hydrodynamic collective excitations (cf. Appendix A) and just above the threshold of the Landau criteria the quadratic scaling of the single particle dispersion relation appears.
Within the superfluid phase we represent the complex bosonic operator basis by a real phase $\hat{\theta}(x)$ and density operator $\hat{\phi}(x)$:

$$\hat{b}^{\dagger}(x) = \sqrt{\hat{\rho}(x)}e^{-i\hat{\theta}(x)} = \sqrt{\rho_0 - \frac{1}{\pi}\partial_x\hat{\phi}(x)}e^{-i\hat{\theta}(x)}. \tag{2.11}$$

After this transformation the effective low-energy Hamiltonian (2.9) is

$$\begin{aligned}\hat{H} = \int_x [\frac{U}{2\pi} - \frac{2J}{\pi} + \frac{U\rho_o}{\pi}](\partial_x\hat{\phi}(x)) - [\frac{J}{\pi}](\partial_x^2\hat{\phi}(x) + \partial_x^3\hat{\phi}(x)) \qquad (2.12)\\ + [2J\rho_0](\partial_x\hat{\theta}(x))^2 + [\frac{U}{2\pi^2}](\partial_x\hat{\phi}(x))^2 + [\frac{2J}{\pi}]\partial_x\hat{\phi}(x)(\partial_x\hat{\theta}(x))^2 + [\frac{J}{2\pi^2}](\partial_x^2\hat{\phi}(x))^2.\end{aligned}$$

The first three terms are just a negligeable global shift in energy. Additionally the Hamiltonian consists of terms, which are quadratic in the density and phase field. Furthermore, we determine a cubic vertex.[29,30] Such a scattering term $\hat{H}_{C,1}$ (cf. (2.13)) is irrelevant in the sense of renormalization group, since as we show in the following it scales with the inverse of the distance. In order to see this we rescale

$$x \to x^{'} = xs \tag{2.13}$$

$$t \to t^{'} = ts^z \tag{2.14}$$

and conclude from corresponding quadratic action of the Hamiltonian (2.12) that $z = 1$ for a scale invariant quadratic sector:

$$\begin{aligned}S_Q &= \int dt^{'} \int dx^{'}([\frac{U}{2\pi^2}](\partial_{x^{'}}\phi(x^{'}))^2 + [2J\rho_0](\partial_{x^{'}}\hat{\theta}(x^{'}))^2)\\ &= \int dt \int dx\ s^{z-1}([\frac{U}{2\pi^2}](\partial_x\phi(x))^2 + [2J\rho_0](\partial_x\hat{\theta}(x))^2).\end{aligned} \tag{2.15}$$

On the other hand, the action associated with the non-linearities vanishes if we increase the distance, i.e. $s \gg 1$:

$$\hat{S}_{C,1} = \int dt' \int dx' [\frac{2J}{\pi}] \partial_{x'} \hat{\phi}(x') (\partial_{x'} \hat{\theta}(x'))^2 = \frac{1}{s} \int dt \int dx [\frac{2J}{\pi}] \partial_x \hat{\phi}(x) (\partial_x \hat{\theta}(x))^2. \tag{2.16}$$

In conclusion the cubic scattering term is negligeable on large distances, however is frequency dependent and therefore influences the time evolution of the system.[29–31] Higher order non-linearities, such as the last term in (2.12) $(\partial_x^2 \hat{\phi}(x))^2$, are even less relevant for the dynamics than the cubic vertex. In summary we have now the following effective Hamiltonian:

$$\begin{aligned} \hat{H} &= \int_x [2J\rho_0] (\partial_x \hat{\theta}(x))^2 + [\frac{U}{2\pi^2}] (\partial_x \hat{\phi}(x))^2 + [\frac{2J}{\pi}] \partial_x \hat{\phi}(x) (\partial_x \hat{\theta}(x))^2 \\ &= \underbrace{\frac{1}{2\pi} \int_x [\nu K (\partial_x \hat{\theta}(x))^2 + \frac{\nu}{K} (\partial_x \hat{\phi}(x))^2]}_{\hat{H}_Q} + \underbrace{\frac{1}{2\pi} \int_x [\frac{1}{m}] \partial_x \hat{\phi}(x) (\partial_x \hat{\theta}(x))^2}_{\hat{H}_{C,1}}, \end{aligned} \tag{2.17}$$

where $\nu = \sqrt{\frac{\rho_0 U}{m}}$, $K = \pi \sqrt{\frac{\rho_0}{Um}}$ and the effective mass $\partial_p^2 \epsilon_p = m^{-1} = 4Ja^2$. While transforming to the Luttinger Liquid representation, we automatically enter the low-energy regime. Such a process is normally carried out by continuously integrating out momentum shells of small wavelength in order to arrive at a low-energy action for the physical system. In such a continuous procedure it is possible that new interaction terms are generated that conserve the original symmetries (e.g. Galilean invariance of the original system). Therefore a term proportional to $\hat{\rho}(x)^3$ needs to be included in the low-energy description of (2.17):

$$\hat{H}_{C,2} = \frac{1}{2\pi} \int_x \alpha (\partial_x \hat{\phi}(x))^3. \tag{2.18}$$

Thus the complete low-energy Hamiltonian with the two leading order non-linear terms is:

$$\begin{aligned} \hat{H} = \hat{H}_Q + \hat{H}_{C,1} + \hat{H}_{C,2} &= \frac{1}{2\pi} \int_x [\nu K (\partial_x \hat{\theta}(x))^2 + \frac{\nu}{K} (\partial_x \hat{\phi}(x))^2] \\ &+ \frac{1}{2\pi} \int_x [\frac{1}{m}] (\partial_x \hat{\phi}(x)) (\partial_x \hat{\theta}(x))^2 + \frac{1}{2\pi} \int_x [\alpha] (\partial_x \hat{\phi}(x))^3. \end{aligned} \tag{2.19}$$

2.3 Phonon Eigenbasis

We establish now a relation between the Luttinger fields and the dominant low-energy collective excitations of the quantum system, i.e. phonons.

Therefore we use the canonical Bogoliubov transformation of the Luttinger Liquid fields in bosonic operators[16,19]:

$$\hat{\theta}(x) =(N_R - N_L)\frac{\pi x}{L\sqrt{K}} + \frac{i\pi}{L}\sum_{p\neq 0}\sqrt{(\frac{L|p|}{2\pi K})}\frac{1}{|p|}e^{-\frac{1}{2}a|p|-ipx}(\hat{b}_p^\dagger - \hat{b}_{-p}), \quad (2.20)$$

$$\hat{\phi}(x) = -(N_R + N_L)\frac{\pi x\sqrt{K}}{L} - \frac{i\pi}{L}\sum_{p\neq 0}\sqrt{(\frac{L|p|K}{2\pi})}\frac{1}{p}e^{-\frac{1}{2}a|p|-ipx}(\hat{b}_p^\dagger + \hat{b}_{-p}), \quad (2.21)$$

where a is an ultra-violet cutoff that regularizes the theory and mimics a finite bandwith.
With this definition the quadratic Hamiltonian $\hat{H}_Q$ is straightforwardly rewritten (cf. Appendix A)[16–19]:

$$\hat{H}_Q = \frac{\nu\pi}{L}(N_R^2 + N_L^2) + \sum_{p\neq 0}\nu|p|\hat{b}_p^\dagger\hat{b}_p. \quad (2.22)$$

The linear dispersion $\epsilon(p) = \nu|p|$ is a significant property of a Luttinger Liquid. The first term contributes a finite value to the excitation spectrum in the limit $p \to 0$.
Next the Bogoliubov transformation is used to transform the cubic Hamiltonian $\hat{H}_C$ and investigate the dominant scattering processes in the phonon basis:

$$\begin{aligned}\hat{H}_{C,1} =&\frac{1}{2\pi}\int_x[(\frac{1}{m}\partial_x\hat{\phi}(x))(\partial_x\hat{\theta}(x))^2] \quad (2.23)\\ =&\frac{-1}{16\pi m}\int_{k,p,q}(2\pi)^{\frac{3}{2}}(\frac{1}{KL})^{\frac{1}{2}}\frac{qpk}{\sqrt{|qpk|}}\mathrm{sgn(q)}\delta(q+p+k)\\ &[\hat{b}_q^\dagger\hat{b}_p^\dagger\hat{b}_k^\dagger - \hat{b}_q^\dagger\hat{b}_k^\dagger\hat{b}_{-p} - \hat{b}_q^\dagger\hat{b}_p^\dagger\hat{b}_{-k} + \hat{b}_k^\dagger\hat{b}_p^\dagger\hat{b}_{-q} + h.c.]\\ =&-\sqrt{\frac{\pi\kappa_c^2}{2KL}}\int_{k,p,q}\sqrt{|qpk|}\frac{1}{4}(\frac{qp}{|qp|} + \frac{qk}{|qk|} + \frac{pk}{|pk|})[\delta(k+q-p)\hat{b}_q^\dagger\hat{b}_k^\dagger\hat{b}_p\\ &+ \frac{1}{3}\delta(k+q+p)\hat{b}_q^\dagger\hat{b}_p^\dagger\hat{b}_k^\dagger + h.c.],\end{aligned}$$

$$\begin{aligned}\hat{H}_{C,2} =&\frac{1}{2\pi}\int_x \alpha(\partial_x\hat{\phi}(x))^3 \qquad (2.24)\\ =&\frac{-\alpha}{16\pi}\int_{k,p,q}(2\pi K)^{\frac{3}{2}}(\frac{1}{L})^{\frac{1}{2}}\frac{qpk}{\sqrt{|qpk|}}\mathrm{sgn(q)sgn(p)sgn(k)}\delta(q+p+k)\\ &[\hat{b}_q^\dagger\hat{b}_p^\dagger\hat{b}_k^\dagger+\hat{b}_q^\dagger\hat{b}_k^\dagger\hat{b}_{-p}+\hat{b}_q^\dagger\hat{b}_p^\dagger\hat{b}_{-k}+\hat{b}_k^\dagger\hat{b}_p^\dagger\hat{b}_{-q}+h.c.]\\ =&-\sqrt{\frac{\pi\kappa_c^2}{2KL}}\frac{3\alpha K^2}{4\kappa_c}\int_{k,p,q}\sqrt{|qpk|}[\delta(k+q-p)\hat{b}_q^\dagger\hat{b}_k^\dagger\hat{b}_p\\ &+\frac{1}{3}\delta(k+q+p)\hat{b}_q^\dagger\hat{b}_p^\dagger\hat{b}_k^\dagger+h.c.],\end{aligned}$$

where $\kappa_c = m^{-1}$.
In conclusion the cubic Hamiltonian consists of the following terms:

$$\begin{aligned}\hat{H}_C =&\hat{H}_{C,1}+\hat{H}_{C,2} \qquad (2.25)\\ =&-\frac{1}{\sqrt{L}}\int_{k,p,q}V(q,p,k)[\delta(k+q-p)\hat{b}_q^\dagger\hat{b}_k^\dagger\hat{b}_p+\frac{1}{3}\delta(k+q+p)\hat{b}_q^\dagger\hat{b}_p^\dagger\hat{b}_k^\dagger+h.c.],\end{aligned}$$

where $V(q,p,k)=\sqrt{|qpk|}\sqrt{\frac{\kappa_c^2\pi}{2K}}(\frac{1}{4}(\frac{qp}{|qp|}+\frac{qk}{|qk|}+\frac{pk}{|pk|})+\frac{3\alpha K^2}{4\kappa_c})$.

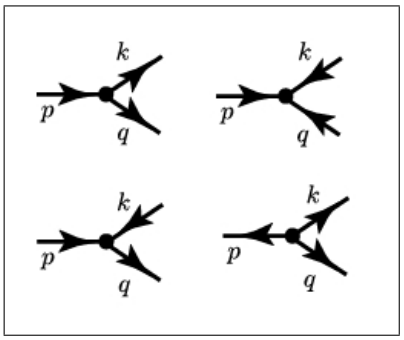

Figure 2.2: *Scattering vertices of the interacting Luttinger Liquid.*

After the canonical Bogoliubov transformation we see that the effective Hamiltonian (2.19) consists of four processes, which are illustrated in Fig. 2.2. The delta distributions $\delta(k+q-p)$ and $\delta(k+q+p)$ implement momentum conservation. Finally we investigate the scaling properties of the vertices by naive power counting and show that it is consistent with the former result (2.16) proportional to q:

$$\int_{\omega,\omega',\omega''}\int_{k,p,q}V(q,p,k)\delta(k+q-p)\hat{b}_q^\dagger(\omega)\hat{b}_k^\dagger(\omega')\hat{b}_p(\omega'')\approx q,$$

where $\hat{b}(q)\propto q^{-\frac{3}{2}}$. The effective mass, α and the Luttinger Liquid parameter K additionally modify the structure of the vertex due to (2.25).

Chapter 3

Master Equation for an Interacting Luttinger Liquid in an Optical Lattice

In the last section we have discussed the scattering processes, which are responsible for redistributing energy and momentum in an interacting Luttinger Liquid. We continue now to consider a specific microscopic model, in which interacting bosons are trapped in an optical lattice. Therefore, we include a bath, which mimics a laser field, i.e. an optical lattice, that interacts with the bosonic system via spontaneous and stimulated emission/absorption.[42] We establish a master equation that describes the time evolution of the interacting bosonic system, trapped in an optical lattice and show that it separates into a coherent and a dissipative part.[32,43,44] In order to point out the properties of the corresponding permanent number conserving heating process we determine the influence of the dissipative part on the time evolution of anomalous and normal occupations.[31,32]

3.1 An Open Quantum System: Single Harmonic Oscillator Coupled to a Thermal Bath

In this section, we explain the derivation of the master equation for the specific example of a harmonic oscillator coupled to a bath.[42–44] The bath has an infinite number of degrees of freedom and is described by a set of harmonic oscillators as well. Subsequently, we use this specific example as a starting point to consider briefly a more general quantum master equation. We consider a system (abbr. s) coupled to a bath (abbr. b) (cf. Fig. 3.1). The bath consists of an infinite number of degrees of freedom embedded in a practically infinite volume and is at thermal equilibrium, i.e. its statistics is described by a thermal ensemble. In the following model the external degrees

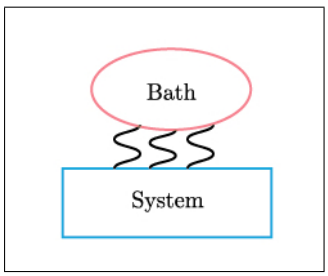

Figure 3.1: *Open quantum system.*

of freedom interact via a coupling parameter with the internal system. The

coupled system is closed and follows the Hamiltonian dynamics:

$$\hat{H} = \hat{H}_s + \hat{H}_b + \hat{H}_{s-b}, \tag{3.1}$$

where $\hat{H}_s = \omega(\hat{a}^\dagger\hat{a} + \frac{1}{2})$, $\hat{H}_b = \sum_k \omega_k(\hat{b}_k^\dagger\hat{b}_k + \frac{1}{2})$ and $\hat{H}_{s-b} = \sum_k c(k)(\hat{b}_k^\dagger\hat{a} + h.c.)$ with $c(k)$ as the coupling parameter between internal system and bath.
Therefore the time evolution of the density operator $\hat{\rho}$ of the coupled system is described by the von Neumann equation ($\hbar = 1$):

$$\partial_t\hat{\rho}(t) = -i[\hat{H}, \hat{\rho}(t)]. \tag{3.2}$$

In the following, we aim to integrate out the external degrees of freedom of the bath in a Born-Markov approximation to reach at an equation that only describes the dynamics of the reduced system.
First we transform into a rotating frame defined by the unitary transformation $\hat{S} = e^{-i(\hat{H}_s+\hat{H}_b)t}$. The time evolution of the density operator in the interaction picture is now due to equation (3.2) (notation: $\tilde{A} = \hat{S}\hat{A}\hat{S}^\dagger$)

$$\partial_t\tilde{\rho}(t) = -i[\tilde{H}_{s-b}(t), \tilde{\rho}(t)] \tag{3.3}$$

with the corresponding integral form:

$$\tilde{\rho}(t) = \tilde{\rho}(0) - i\int_0^t dt'[\tilde{H}_{s-b}(t'), \tilde{\rho}(t')]. \tag{3.4}$$

We substitute this solution into the von Neumann equation (3.3) and find a integro-differential equation for the time evolution of the density operator:

$$\partial_t\tilde{\rho}(t) = -i[\tilde{H}_{s-b}(t),\ \tilde{\rho}(0)] - \int_0^t dt'[\tilde{H}_{s-b}(t), [\tilde{H}_{s-b}(t'), \tilde{\rho}(t')]]. \tag{3.5}$$

Before we trace over the bath in order to have an equation that describes exclusively the time evolution of the reduced system in the presence of interactions with the external bath, we simplify (3.5) on the grounds of various approximation schemes. First we perform a Born approximation based on the assumption of weak coupling between the system and the bath, so that the influence of the internal system on the bath is negligible. According to this the density operator of the coupled system always separates in a density operator of the internal system $\tilde{\rho}_s$ and the bath $\tilde{\rho}_{b,eq}$, which remains in a thermal equilibrium state during the time evolution:

$$\partial_t\tilde{\rho}(t) = -i[\tilde{H}_{s-b}(t),\ \tilde{\rho}_s(0)\otimes\tilde{\rho}_{b,eq}] - \int_0^t dt'[\tilde{H}_{s-b}(t), [\tilde{H}_{s-b}(t'), \tilde{\rho}_s(t')\otimes\tilde{\rho}_{b,eq}]]. \tag{3.6}$$

In order to understand the so-called Markovian approximation, we investigate the time evolution of the density operator for an infinitesimal time step Δt:

$$\tilde{\rho}(t+\Delta t) = \tilde{\rho}(t) + \Delta t \; f[\tilde{\rho}(t^{'})], \tag{3.7}$$

where $f[\tilde{\rho}(t^{'})] = -i[\tilde{H}_{s-b}(t),\ \tilde{\rho}(0)] - \int_0^t dt^{'}[\tilde{H}_{s-b}(t), [\tilde{H}_{s-b}(t^{'}), \tilde{\rho}(t^{'})]]$.
For a Markovian bath the relaxation time of the system τ_r is much larger than the characteristic time scale τ_b of the correlation function of the bath. Therefore, we approximate that the state of the density operator at time $t + \Delta t$ just depends on the state at t, which describes the system at an infinitesimal time step before:

$$f[\tilde{\rho}(t^{'})] \rightarrow f[\tilde{\rho}(t)]. \tag{3.8}$$

According to this, we approximate the density operator $\tilde{\rho}(t^{'}) \simeq \tilde{\rho}(t) = \tilde{\rho}_s(t) \otimes \tilde{\rho}_{b,eq}$ and conclude from (3.6):

$$\begin{aligned} \partial_t \tilde{\rho}(t) = &- i[\tilde{H}_{s-b}(t),\ \tilde{\rho}_s(0) \otimes \tilde{\rho}_{b,eq}] \\ &- \int_0^t dt^{'}[\tilde{H}_{s-b}(t), [\tilde{H}_{s-b}(t^{'}), \tilde{\rho}_s(t) \otimes \tilde{\rho}_{b,eq}]]. \end{aligned} \tag{3.9}$$

The time evolution described by equation (3.9) formally has still the memory of the initial state at $t = 0$ and is therefore not completely Markovian. In order to find a description, which has no memory on the initial state, we substitute $t^{'}$ by $t - t^{'}$ and shift the upper limit of the integral to infinity. This is permissible provided the integrand disappears sufficiently fast for $t^{'} \gg \tau_b$[43]:

$$\begin{aligned} \partial_t \tilde{\rho}(t) = &- i[\tilde{H}_{s-b}(t),\ \tilde{\rho}_s(0) \otimes \tilde{\rho}_{b,eq}] \\ &- \int_0^\infty dt^{'}[\tilde{H}_{s-b}(t), [\tilde{H}_{s-b}(t-t^{'}), \tilde{\rho}_s(t) \otimes \tilde{\rho}_{b,eq}]]. \end{aligned} \tag{3.10}$$

After performing the Born-Markov approximation, we trace over the bath and establish the master equation for the reduced quantum system[42]:

$$\begin{aligned} \partial_t \tilde{\rho}_s(t) &= \mathrm{tr}_b\{\partial_t \tilde{\rho}(t)\} = -\int_0^\infty dt^{'} \mathrm{tr}_b\{[\tilde{H}_{s-b}(t), [\tilde{H}_{s-b}(t-t^{'}), \tilde{\rho}(t)]]\} \\ &= \sum_k \pi\delta(\omega - \omega_k) c(k)^2 [n_B[2\hat{a}^\dagger \tilde{\rho}_s(t)\hat{a} - \hat{a}\hat{a}^\dagger \tilde{\rho}_s(t) - \tilde{\rho}_s(t)\hat{a}\hat{a}^\dagger] \\ &+ (n_B+1)[2\hat{a}\tilde{\rho}_s(t)\hat{a}^\dagger - \hat{a}^\dagger\hat{a}\tilde{\rho}_s(t) - \tilde{\rho}_s(t)\hat{a}^\dagger\hat{a}]], \end{aligned} \tag{3.11}$$

where we assumed

$$\mathrm{tr}_b\{-i[\tilde{H}_{s-b}(t),\ \tilde{\rho}_s(0) \otimes \tilde{\rho}_{b,eq}]\} = 0$$

and use the following notation:

$$\begin{aligned}\tilde{\rho}_s &= \mathrm{tr}_b\{\tilde{\rho}_s \otimes \tilde{\rho}_{b,eq}\} = \tilde{\rho}_s \mathrm{tr}_b\{\tilde{\rho}_{b,eq}\},\\ \mathrm{tr}_b\{\hat{b}_k^\dagger \hat{b}_{k'} \tilde{\rho}(t)\} &= n_B \delta_{k,k'} \tilde{\rho}_s(t),\\ \mathrm{tr}_b\{\hat{b}_k^\dagger \hat{b}_{k'}^\dagger \tilde{\rho}(t)\} &= \mathrm{tr}_b\{\hat{b}_k \hat{b}_{k'} \tilde{\rho}(t)\} = 0.\end{aligned}$$

Finally, we transform back to the Schrödinger picture and determine a master equation that separates in a coherent and a dissipative part:

$$\partial_t \hat{\rho}_s(t) = -i[\hat{H}_s, \hat{\rho}_s] + \hat{J}[\hat{\rho}_s], \tag{3.12}$$

$$\begin{aligned}\hat{J}[\hat{\rho}_s] = \pi\rho(\omega)c(\omega)^2 [n_B[2\hat{a}^\dagger \hat{\rho}_s(t)\hat{a} - \hat{a}\hat{a}^\dagger \hat{\rho}_s(t) - \hat{\rho}_s(t)\hat{a}\hat{a}^\dagger] \\ + (n_B+1)[2\hat{a}\hat{\rho}_s(t)\hat{a}^\dagger - \hat{a}^\dagger\hat{a}\hat{\rho}_s(t) - \hat{\rho}_s(t)\hat{a}^\dagger\hat{a}]],\end{aligned} \tag{3.13}$$

where $\rho(\omega) = \pi \sum_k \delta(\omega - \omega_k)$ is the spectral density of the bath. We assume that the coupling and the thermal distribution depend only on the energy of the reference state: $c_k = c_{\omega_k}$ and $n_B|_{k=\omega_k}$.
The coherent dynamics of the reduced density matrix $\hat{\rho}_s$ is generated by the Hamiltonian of the internal system $\hat{H}_s$. In general the coupling of the system to an external bath could generate terms that contribute to the coherent time evolution of the reduced system. The second term in equation (3.12) mimics the irreversible dissipative part with rates proportional to $\kappa_a \propto \pi\rho(\omega)c(\omega)^2 n_B$ and $\kappa_e \propto \pi\rho(\omega)c(\omega)^2(n_B+1)$.
We close this section with a brief discussion on how to generalize the equation (3.13). We assume an internal system with a large number of spatial degrees of freedom (labeled with a discrete lattice index i) with the dissipation rate κ_i at each lattice point[45,46]:

$$\partial_t \hat{\rho}_s(t) = -i[\hat{H}_s, \hat{\rho}_s] + \sum_i \kappa_i \, (2\hat{L}_i \hat{\rho}_s \hat{L}_i^\dagger - \{\hat{L}_i^\dagger \hat{L}_i, \hat{\rho}_s\}), \tag{3.14}$$

In equation (3.14) a set of so-called Lindblad operators $\{\hat{L}_i, \hat{L}_i^\dagger\}$ reflects the coupling to the bath and is the generator of the dissipative dynamics. Depending on the problem at hand, the Lindblad operators can be more general non-linear operators.

3.2 Master Equation for a One Dimensional System of Interacting Bosons in an Optical Lattice

After the former derivation of the master equation for a single harmonic oscillator coupled to a bath, we are now prepared to establish the quantum master equation for a system of interacting bosons in a one dimensional optical lattice.[7,8,32] The starting point of our description is the corresponding Bloch equation. Finally, we conclude that the reduced system of interacting bosons is heated up by a rate, which scales in the low-energy limit linear in momenta.

3.2.1 Master Equation for a Single Particle in an Optical Lattice

We briefly discuss the derivation of the master equation for a single atom in an optical lattice[32,47]. The starting point is the Bloch equation for a single two-level particle with the internal states $\{|g\rangle, |e\rangle\}$ and mass m:

$$\partial_t \hat{\rho}(t) = -i[\hat{H}, \hat{\rho}(t)] + \Gamma \int d^2\mathbf{u} N(\mathbf{u})(2\hat{L}_{\mathbf{u}}\hat{\rho}(t)\hat{L}_{\mathbf{u}}^\dagger - \{\hat{L}_{\mathbf{u}}^\dagger \hat{L}_{\mathbf{u}}, \hat{\rho}(t)\}). \tag{3.15}$$

The coherent dynamics are generated by the following atomic Hamiltonian

$$\hat{H} = \frac{\hat{p}^2}{2m} - \Delta |e\rangle\langle e| - (|g\rangle\langle e| \frac{\Omega(\hat{\mathbf{x}})}{2} + h.c.), \tag{3.16}$$

where Δ is the detuning of the laser frequency, $\Omega(\hat{\mathbf{x}})$ is the Rabi frequency and we include the free motion of the particle.
The Lindblad operator $\hat{L}_{\mathbf{u}} = e^{-i\mathbf{k}_{eg}\mathbf{u}} |g\rangle\langle e|$ describes the process in which the atom returns to its ground state and emits spontaneously a photon in the direction $\mathbf{u}$. Thereby the atom gets a recoil kick with a rate Γ. The wavenumber $\mathbf{k}_{eg}$ corresponds to the internal transition of the atom and $N(\mathbf{u})$ is the distribution of directions for the emitted photons.
Next we eliminate adiabatically the excited state in the limit of small saturation and large detuning $\Omega, \Gamma \ll |\Delta|$ to obtain a master equation for the reduced density operator that describes exclusively the time evolution of the external degrees of freedom[32,47]:

$$\partial_t \hat{\rho}(t) = -i(\hat{H}_{\text{eff}}\hat{\rho}(t) - \hat{\rho}(t)\hat{H}_{\text{eff}}^\dagger) + \hat{\mathcal{D}}[\hat{\rho}(t)] \tag{3.17}$$

with the effective Hamiltonian

$$\hat{H}_{\text{eff}} = \frac{\hat{p}^2}{2m} + V_{opt}(\hat{\mathbf{x}}) - i\frac{1}{2}\gamma(\hat{\mathbf{x}}), \tag{3.18}$$

which includes the optical lattice potential $V_{opt}(\hat{\mathbf{x}}) = \frac{|\Omega(\hat{\mathbf{x}})|^2}{4\Delta}$ and the rate of light scattering $\gamma(\hat{\mathbf{x}})$.
The last term in equation (3.17) describes the dissipative interaction of the laser field with the atom and is

$$\hat{\mathcal{D}}[\hat{\rho}(t)] = \Gamma \int d^2\mathbf{u} N(\mathbf{u}) 2\hat{l}_{\mathbf{u}}\hat{\rho}(t)\hat{l}_{\mathbf{u}}^{\dagger}, \tag{3.19}$$

where $\hat{l}_{\mathbf{u}}(\hat{\mathbf{x}}) = e^{-i\mathbf{k}_{eg}\mathbf{u}}\ \frac{\Omega(\hat{\mathbf{x}})}{2\Delta}$ is the Lindblad operator.
We represent the effective Hamiltonian in an appropriate basis set for an optical lattice and use localized Wannier states $\hat{\Psi}(\mathbf{x}) = \sum_{i,\mathbf{n}} \omega_{\mathbf{n},i}(\mathbf{x})\hat{b}_{i,\mathbf{n}}$ with lattice site index i and Bloch band $\mathbf{n}$:

$$\hat{H}_{\text{eff}} = -\sum_{\mathbf{n},\langle i,j\rangle} J_{\mathbf{n},i,j}\hat{b}_{i,\mathbf{n}}^{\dagger}\hat{b}_{j,\mathbf{n}} + \sum_{\mathbf{n},i}\epsilon_{\mathbf{n}}\hat{b}_{i,\mathbf{n}}^{\dagger}\hat{b}_{i,\mathbf{n}} - \frac{i}{2}\sum_{\mathbf{n},\mathbf{m},i}\gamma_{\mathbf{n},\mathbf{m}}\hat{b}_{i,\mathbf{n}}^{\dagger}\hat{b}_{i,\mathbf{m}}, \tag{3.20}$$

where

$$J_{\mathbf{n},i,j} = -\int_{\mathbf{x}} \omega_{\mathbf{n},i}(\mathbf{x})[\frac{\hat{p}^2}{2m} + V_{opt}(\hat{\mathbf{x}})]\omega_{\mathbf{n},j}(\mathbf{x}) \text{ is the hopping rate,} \tag{3.21}$$

$$\epsilon_{\mathbf{n}} = \int_{\mathbf{x}} \omega_{\mathbf{n},i}(\mathbf{x})[\frac{\hat{p}^2}{2m} + V_{opt}(\hat{\mathbf{x}})]\omega_{\mathbf{n},i}(\mathbf{x}) \text{ is the on-site energy,} \tag{3.22}$$

$$\gamma_{\mathbf{n},\mathbf{m}} = \int_{\mathbf{x}} \omega_{\mathbf{n},i}(\mathbf{x})\gamma(\mathbf{x})\omega_{\mathbf{m},i}(\mathbf{x}) \text{ is the rate of light scattering.} \tag{3.23}$$

The dissipator consists of the following Lindblad operator

$$\hat{l}_{\mathbf{u}}(\hat{\mathbf{x}}) = \sum_{\mathbf{n},\mathbf{m},i}\int_{\mathbf{x}} \omega_{\mathbf{n},i}(\mathbf{x})e^{-i\mathbf{k}_{eg}\mathbf{u}}\ \frac{\Omega(\hat{\mathbf{x}})}{2\Delta}\omega_{\mathbf{m},i}(\mathbf{x})\hat{b}_{i,\mathbf{n}}^{\dagger}\hat{b}_{i,\mathbf{m}}. \tag{3.24}$$

Due to the localization of the Wannier states, we neglect processes, where the atom jumps between neighbouring lattice sites associated with a spontaneous emission (cf. equation (3.23)).
This example of a single boson in an optical lattice is used in the following subsection to motivate the approach for the case of N interacting particles and gives us a first impression of an optical quantum master equation (3.17) based on a specific microscopic model.

3.2.2 Extension of the Master Equation to N Interacting Bosons in an Optical Lattice

We extend the former microscopic model for one particle in an optical lattice to the case of N bosonic particles.[32] The effective Hamiltonian (3.20) consists of terms associated with nearest neighbour hopping and an energy-shift. In the presence of N particles in an optical lattice we need to consider additionally on-site and dipole-dipole interactions between the particles and the optical field:

$$\hat{H}_{int} = \frac{1}{2} \sum_{i,\mathbf{k},\mathbf{l},\mathbf{m},\mathbf{n}} U_{\mathbf{k},\mathbf{l},\mathbf{m},\mathbf{n}} \hat{b}^\dagger_{i,\mathbf{k}} \hat{b}^\dagger_{i,\mathbf{l}} \hat{b}_{i,\mathbf{m}} \hat{b}_{i,\mathbf{n}}, \tag{3.25}$$

where $U_{\mathbf{k},\mathbf{l},\mathbf{m},\mathbf{n}}$ depends on microscopic parameters[32].
In conclusion, the coherent dynamics of the master equation

$$\partial_t \hat{\rho}(t) = -i[\hat{H}, \hat{\rho}(t)] + \hat{\mathcal{D}}[\hat{\rho}(t)] \tag{3.26}$$

separates in a term describing nearest neighbour hopping, an on-site energy shift and the interaction term:

$$\hat{H} = -\sum_{\mathbf{n},\langle i,j\rangle} J_{\mathbf{n},i,j} \hat{b}^\dagger_{i,\mathbf{n}} \hat{b}_{j,\mathbf{n}} + \sum_{\mathbf{n},i} \epsilon_{\mathbf{n}} \hat{b}^\dagger_{i,\mathbf{n}} \hat{b}_{i,\mathbf{n}} + \frac{1}{2} \sum_{i,\mathbf{k},\mathbf{l},\mathbf{m},\mathbf{n}} U_{\mathbf{k},\mathbf{l},\mathbf{m},\mathbf{n}} \hat{b}^\dagger_{i,\mathbf{k}} \hat{b}^\dagger_{i,\mathbf{l}} \hat{b}_{i,\mathbf{m}} \hat{b}_{i,\mathbf{n}}. \tag{3.27}$$

The dissipator shows a similar structure to the generalized Markovian master equation (3.12) with the Lindblad operator $\hat{L}_i = \hat{b}^\dagger_{i,\mathbf{n}} \hat{b}_{i,\mathbf{m}}$ and dissipation rate $\gamma_{i,\mathbf{k},\mathbf{l},\mathbf{m},\mathbf{n}}$:

$$\hat{\mathcal{D}}[\hat{\rho}(t)] = -\frac{1}{2} \sum_{i,\mathbf{k},\mathbf{l},\mathbf{m},\mathbf{n}} \gamma_{i,\mathbf{k},\mathbf{l},\mathbf{m},\mathbf{n}} [\hat{b}^\dagger_{i,\mathbf{k}} \hat{b}_{i,\mathbf{l}}, [\hat{b}^\dagger_{i,\mathbf{m}} \hat{b}_{i,\mathbf{n}}, \hat{\rho}(t)]], \tag{3.28}$$

where the scattering rate is again restricted to processes on the same lattice site.
The master equation (3.28) describes the dissipative effects generated by stimulated emission/absorption and spontaneous emission of N interacting bosons in the presence of a laser field.[32]

3.2.3 Red-Detuned Laser and Single-Band Hubbard Model

We now distinguish between a red- and blue-detuned optical lattice in order to determine that for the former case the scattering rate in the Lamb-Dicke

limit is dominated by processes including the same Bloch band.[32] According to this, a single boson, which is initially in the lowest Bloch band, returns with leading probability back to its position after light scattering with a red-detuned laser. As a consequence we can simplify equation (3.27) to a single-band Hubbard model.
We first consider the case of a single atom trapped in an optical lattice, where the scattering rate is due to (3.23):

$$\gamma_{\mathbf{n},\mathbf{m}} = \int_{\mathbf{x}} \omega_{\mathbf{n},i}(\mathbf{x})\gamma(\mathbf{x})\omega_{\mathbf{m},i}(\mathbf{x}) \tag{3.29}$$

with $\{\mathbf{m},\mathbf{n}\}$ labeling the Bloch bands.
The sign of the optical lattice $V_{opt}(\hat{\mathbf{x}}) = \frac{|\Omega(\hat{\mathbf{x}})|^2}{4\Delta}$ changes for red- ($\Delta < 0$) and blue-detuned ($\Delta > 0$) laser light. We further assume a periodic optical lattice:

$$\Omega(\hat{\mathbf{x}}) = \Omega_0 \cos(k_L x) \text{ for } \Delta < 0, \tag{3.30}$$
$$\Omega(\hat{\mathbf{x}}) = \Omega_0 \sin(k_L x) \text{ for } \Delta > 0. \tag{3.31}$$

Therefore, a minimum of the field intensity for a red-detuned laser corresponds to a maximum of the field at this position. The opposite is valid for a blue-detuned laser, where at the minimum of an optical lattice the field intensity is minimal. In conclusion, a single atom at the minimum of a blue-detuned optical lattice feels a reduced field intensity and thus has a reduced scattering rate compared to the case of a red-detuned laser. We refer to the corrsponding literature[32] for explicit calculations of the scattering rates in the Lamb-Dicke limit $\eta = \frac{V}{E_R} \ll 1$, where V is a deep lattice potential and $E_R = k_L^2/2m$ is the recoil energy. Figure 3.3 shows a microscopic band model of bosons in an optical lattice and the corresponding scattering rates for red-, respectively blue-detuned laser.[32] According to this an atom that is

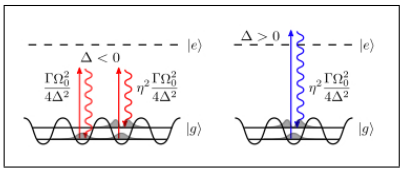

Figure 3.2: *Absorption and emission processes for red- and blue detuned laser in a one dimensional optical lattice.*[32]

initially in the lowest Bloch band returns after absorption/emission of light with high probability back to the same position in momentum space if the laser is red-detuned.

We use this to reduce the multi-band quantum master equation (3.26)-(3.28) to a single-band Hubbard model and consider thereby a red-detuned optical lattice[32]:

$$\begin{aligned}\partial_t\hat{\rho}(t) =& -i[\hat{H}_{\mathrm{BHM}},\hat{\rho}(t)] + \sum_i \gamma[\hat{n}_i,[\hat{n}_i,\hat{\rho}(t)]] \\ =& -i[\hat{H}_{\mathrm{BHM}},\hat{\rho}(t)] + \sum_i \gamma(2\hat{n}_i\hat{\rho}(t)\hat{n}_i - \{\hat{n}_i\hat{n}_i,\hat{\rho}(t)\})\end{aligned} \tag{3.32}$$

with an effective pumping rate γ.
The coherent dynamics of the density operator is due to (3.32) generated by the micoscopic Bose-Hubbard model of chapter 2. We have already discussed, that in the low-energy regime this model includes scattering processes, which redistribute energy and momentum in the system. Additionally, the dissipative part of the final quantum master equation (3.32) includes a so-called effective pumping rate γ, which is directly related to the parameters of the underlying microscopic model.[32] The laser light scatters with the bosonic particles of the system locally and linear in time at a pumping rate γ. The dissipator includes again an anticommutator, that preserves the norm of the density operator. Furthermore, if the intial density operator describes a coherent superposition of particles over many lattice sides, the first term

$$\hat{n}_i\hat{\rho}(t)\hat{n}_i \tag{3.33}$$

continuously eliminates off-diagonal terms in the density operator and generates a state of localized particles. The stationary state of the quantum master equation (3.32) is the unit matrix $\rho_{ss} = \mathbb{1}_N$.[7] In the next section, we focus in more detail on the dissipative part in the low-energy limit and discuss the equation of motion for the diagonal and off-diagonal phonon distribution in the system.

3.3 The Dissipator: Heating Dynamics in the Low-Energy Regime

We are interested in the low-energy dynamics for a one dimensional system of interacting bosons. Therefore, we project the dissipator of the last section to the long wavelength limit by using the following relations

$$\hat{b}_i^\dagger\hat{b}_i \to a\ \hat{n}(x)|_{x=ia}, \tag{3.34}$$

$$\sum_i \to \frac{1}{a}\int dx, \tag{3.35}$$

$$\gamma \to a\gamma, \tag{3.36}$$

and conclude from (3.32):

$$\hat{\mathcal{D}}[\hat{\rho}(t)] = \int_x \gamma(2\hat{n}(x)\rho(t)\hat{n}(x) - \{\hat{n}(x)\hat{n}(x), \rho(t)\}), \tag{3.37}$$

where $\hat{n}(x) = \hat{b}^\dagger(x)\hat{b}(x)$.
We represent the complex annihilation and creation operator by the real Luttinger Liquid phase and density fields (cf. equation (2.11)):

$$\hat{\mathcal{D}}[\hat{\rho}(t)] = \int_x \gamma[2\partial_x\hat{\phi}(x)\rho(t)\partial_x\hat{\phi}(x) - \{(\partial_x\hat{\phi}(x))^2, \rho(t)\}]. \tag{3.38}$$

We use the Bogoliubov transformation of the Luttinger Liquid fields in the bosonic operators (2.20 - 2.21). After this transformation the dissipator is[31]:

$$\hat{\mathcal{D}}[\hat{\rho}(t)] = \int_{p\neq 0} h(p)[2(\hat{b}_p^\dagger + \hat{b}_{-p})\hat{\rho}(t)(\hat{b}_{-p}^\dagger + \hat{b}_p) - \{(\hat{b}_p^\dagger + \hat{b}_{-p})(\hat{b}_{-p}^\dagger + \hat{b}_p), \hat{\rho}(t)\}], \tag{3.39}$$

where $h(p) = \dfrac{\gamma K|p|}{2\pi}$.
Thus, the scaling of the dissipative dynamics in the low-energy regime is proportional to p. The heating process generates phonon modes in the one dimensional chain of atoms and increases thereby continuously the energy of the system.

3.3.1 Dynamics of the Occupation Distribution

The scattering of the laser light from the bosonic particles is expected to generate excitations in form of phonons in the system and is described by the dissipator (3.39). We calculate the equation of motion for the average occupation of phonons in the system to analyze this process in more detail and conclude that the system is constantly heated up.
The equation of motion for the average diagonal density $\hat{n}_p$ including the coherent dynamics of the Luttinger Liquid model (cf. chapter 2) is:

$$\begin{aligned}
\partial_t \langle \hat{n}_p \rangle &= \partial_t \mathrm{Tr}[\hat{n}_p\hat{\rho}(t)] = -i\left\langle [\hat{n}_p, \hat{H}_Q] \right\rangle + \mathrm{Tr}[\hat{n}_p\hat{\mathcal{D}}[\hat{\rho}(t)]] \\
&= \int_{q\neq 0} h(p)\mathrm{Tr}[\hat{n}_p 2\hat{B}_q\hat{\rho}(t)\hat{B}_q^\dagger - \hat{n}_p\{\hat{B}_q\hat{B}_q^\dagger, \hat{\rho}(t)\}] \\
&= \frac{\gamma K|p|}{2\pi}\{\mathrm{Tr}[\hat{n}_p 2\hat{B}_p\hat{\rho}(t)\hat{B}_p^\dagger - \hat{n}_p\{\hat{B}_p\hat{B}_p^\dagger, \hat{\rho}(t)\}] \\
&\quad -\mathrm{Tr}[\hat{n}_p 2\hat{B}_{-p}\hat{\rho}(t)\hat{B}_{-p}^\dagger - \hat{n}_p\{\hat{B}_{-p}\hat{B}_{-p}^\dagger, \hat{\rho}(t)\}]\} \\
&= \frac{\gamma K|p|}{\pi},
\end{aligned} \tag{3.40}$$

where $\hat{B}_q = \hat{b}_q^\dagger + \hat{b}_{-q}$ and we assume without loss of generality $p > 0$. Thus, the diagonal occupation increases linear in time by a rate $\gamma K|p|\pi^{-1}$:

$$\langle \hat{n}_p \rangle (t) = \frac{\gamma K|p|}{\pi} t + \langle \hat{n}_p \rangle (0). \tag{3.41}$$

During the time evolution, the number of phonons in the system increases as a consequence of the scattering of laser light with the atoms. The low-energy description automatically breaks down if the number of phonons passes a distinct threshold. The average energy of the interacting Luttinger Liquid increases as follows[31,32,48]:

$$\partial_t E = \partial_t \langle H_Q \rangle = \sum_{p \neq 0} \nu |p| \partial_t \langle \hat{n}_p \rangle = \sum_{p \neq 0} \frac{\nu \gamma K p^2}{\pi}, \tag{3.42}$$

$$E(t) = (\sum_{p \neq 0} \frac{\nu \gamma K p^2}{\pi}) t + E(t = 0). \tag{3.43}$$

The total energy in the system thus continuously increases by an effective rate $\gamma_E = (\sum_{p \neq 0} \frac{\nu \gamma K p^2}{\pi})$. In order to not pump an infinte amount of energy at each time step in the system, we need to consider a UV-cutoff p_c. The original microscopic model of a single-band Hubbard model includes already an upper cut-off based on the finite lattice length a and the corresponding Brillouin zone. Thus, the continuum master equation has an implicit UV-cutoff. The theory must in general be independent of the exact value of this cutoff as long p_c is large enough. We therefore restrict the summation in (3.43):

$$\gamma_E = (\sum_{p \leq p_c} \frac{\nu \gamma K p^2}{\pi}). \tag{3.44}$$

Furthermore, the effective pumping rate also sets a time scale at which the low-energy approximation is not valid any more and the Luttinger Liquid formalism breaks down. The hydrodynamic description is restricted in momentum space by the Landau criteria of superfluidity (cf. chapter 2):

$$p_L = \sqrt{U \rho_0 m}. \tag{3.45}$$

The continuous pump of energy in the system leads to an increase of excitations above this threshold. If the population of excitations outside the superfluid regime becomes too large, the hydrodynamic description is no longer valid ($k_B = 1$):

$$n_B(p_L) \approx \frac{T(t)}{\nu |p_L|} \geq 1. \tag{3.46}$$

The temperature of the system increases linear in time and we approximate the following upper bound in time for the low-energy description:

$$E(t) = \gamma_E t + E(t=0) = T(t), \tag{3.47}$$

$$\Rightarrow \tau_c = \frac{(\nu|p_L| - E(t=0))}{\gamma_E}. \tag{3.48}$$

In the limit of zero pumping rate, τ_c is shifted to infinity as expected and the low-energy description is thus valid for all times. The upper bound can be explicitly calculated for a set of microscopic parameters (3.48).
The population of the anomalous occupation is also influenced due to the permanent scattering of the laser light with the atoms. In order to determine the dynamical behaviour of the anomalous occupation, we calculate its equation of motion including the coherent dynamics of the Luttinger Liquid model (cf. chapter 2) and consider thereby without loss of generality $p > 0$:

$$\begin{aligned}
\partial_t \langle \hat{m}_p \rangle &= \partial_t \mathrm{Tr}[\hat{m}_p \hat{\rho}(t)] = -i \left\langle [\hat{m}_p, \hat{H}_Q] \right\rangle + \mathrm{Tr}[\hat{m}_p \hat{\mathcal{D}}[\hat{\rho}(t)]] \\
&= -2i\nu|p| \langle \hat{m}_p \rangle \\
&+ \frac{\gamma K|p|}{2\pi} \{ \mathrm{Tr}[\hat{m}_p 2\hat{B}_p \hat{\rho}(t) \hat{B}_p^\dagger - \hat{m}_p \{\hat{B}_p \hat{B}_p^\dagger, \hat{\rho}(t)\}] \\
&- \mathrm{Tr}[\hat{m}_p 2\hat{B}_{-p} \hat{\rho}(t) \hat{B}_{-p}^\dagger - \hat{m}_p \{\hat{B}_{-p} \hat{B}_{-p}^\dagger, \hat{\rho}(t)\}] \} \\
&= -2i\nu|p| \langle \hat{m}_p \rangle - \frac{\gamma K|p|}{\pi},
\end{aligned} \tag{3.49}$$

where $\hat{B}_p = \hat{b}_p^\dagger + \hat{b}_{-p}$.
According to this equation of motion, the anomalous occupation oscillates by a frequency $\omega(p) = 2\epsilon(p)$ in time[31]:

$$\langle \hat{m}_p \rangle (t) = \tfrac{i\gamma K}{2\pi\nu} (e^{-2i\nu|p|t} - 1) + e^{-2i\nu|p|t} \langle \hat{m}_p \rangle (0). \tag{3.50}$$

Due to the accumulation of the phase factor generated by the coherent dynamics at each time step, the long time average of the anomalous occupation remains constant:

$$\langle\langle \hat{m}_p \rangle\rangle_t = \lim_{T\to\infty} \int_0^T \langle \hat{m}_p \rangle (t) dt = \tfrac{\kappa\pi}{\nu K}. \tag{3.51}$$

We conclude at large times the anomalous occupation dephase and thus are negligeable. However, in the following sections we include the full coherent dynamics of an interacting Luttinger Liquid with scattering terms that generate interactions between the anomalous and normal occupation. As a consequence, the dynamics of both occupations are not decoupled any more and the dynamics of the anomalous occupation needs to be considered in order to capture the full time evolution of the diagonal occupation.

Chapter 4

Keldysh Action of an Interacting Luttinger Liquid in an Optical Lattice

We aim to determine the time evolution of the normal and anomalous occupation for a driven interacting Luttinger Liquid in order to find signature of effective thermalization. We use the master equation to calculate the dynamics of a general observable $\hat{O}$:

$$\left\langle \hat{O}(t) \right\rangle = \mathrm{Tr}[\hat{O}\hat{\rho}(t)]. \tag{4.1}$$

In order to determine the time evolution according to equation (4.1), we define the Keldysh partition function, which is the generating function for observables:

$$\mathcal{Z}(t) = \mathrm{Tr}[\hat{\rho}(t)]. \tag{4.2}$$

We start the calculation of the Keldysh partition function (4.2) with the general solution

$$\hat{\rho}(t) = e^{\hat{\mathcal{L}}t}\hat{\rho}(t_0) \tag{4.3}$$

of the master equation for a many-body system out of equilibrium and consider thereby:

$$\partial_t \hat{\rho}(t) = \hat{\mathcal{L}}[\hat{\rho}(t)] = -i[\hat{H}, \hat{\rho}(t)] + \hat{\mathcal{D}}[\hat{\rho}(t)]. \tag{4.4}$$

Subsequently, we continue to map the partition function onto a field integral and establish a field integral representation.[49,50] With this, we can make use of mathematical tools as diagrammatic and perturbation theory, which are commonly used in the field of condensed matter or high energy theory.
On a technical level, we realize this transformation by separating the time line in single slices and introduce at each time step a unitary operator from an appropriate basis set for a many-body problem.[42] According to chapter 3, we separate the time evolution in a forward and backward time line and insert unitary operators on both contours. There are in total 4 two-point correlation functions in the corresponding $\pm$-basis, which show some redundancy. Thus, we rotate from the $\pm$-basis into the so-called Keldysh basis.[42,51,52]

4.1 From the Master Equation to the Keldysh Action

As motivated in the introduction of this section, the central object of interest is the generating function (4.2):

$$\mathcal{Z}(t) = \mathrm{Tr}[e^{\hat{\mathcal{L}}t}\hat{\rho}(t_0)]. \tag{4.5}$$

We assume that the system is described at initial time $t = t_0$ by a density operator in an equilibrium state $\hat{\rho}(t_0) = \hat{\rho}_{eq}$. During the time evolution, the system is not restricted to stay at equilibrium and the density operator evolves in time, according to the dissipative and coherent dynamics of the system (cf. Fig. 1.1 and 1.2).
In order to determine a field integral representation of the master equation[49,50,53], we split the time period $[t_0, t]$ in N equivalent time steps of length $\delta_t = \frac{t}{N}$ and then use the series expansion of the exponential function:

$$\begin{aligned} \mathcal{Z}(t) = \mathrm{Tr}[e^{\hat{\mathcal{L}}t}\hat{\rho}(0)] = \mathrm{Tr}[(e^{\hat{\mathcal{L}}\delta_t})^N\hat{\rho}(0)] = \mathrm{Tr}[(e^{\hat{\mathcal{L}}\delta_t})^N\hat{\rho}(0)] \\ = \lim_{N\to\infty} \mathrm{Tr}[(1+\hat{\mathcal{L}}\delta_t^{(N)})...(1+\hat{\mathcal{L}}\delta_t^{(1)})\hat{\rho}(0)], \end{aligned} \tag{4.6}$$

where $\delta_t^{(l)}$ indicates the time step δ_t at time $t = \frac{lt}{N}$ on the timeline, respectively the contours.
Next, we choose an appropriate basis set to represent the operator $\hat{\mathcal{L}}$. The operator $\hat{\mathcal{L}}$ is commonly represented in the second quantization formalism with annihilation and creation operators. The eigenstates of an annihilation operator $\hat{a}$ are coherent states $\{|\phi\rangle, |\theta\rangle\}$ with the following properties[42]:

$$\hat{a}\,|\phi\rangle = \phi\,|\phi\rangle \;\text{ and }\; \langle\phi|\,\hat{a}^\dagger = \langle\phi|\,\bar{\phi}, \tag{4.7}$$

$$|\phi\rangle = e^{\phi\hat{a}^\dagger}\,|0\rangle\,, \tag{4.8}$$

$$\langle\theta|\,|\phi\rangle = e^{\bar{\theta}\phi}, \tag{4.9}$$

Since the coherent states from a complete set of states in the many-body Hilbert space, we can, due to the completeness relation, define an operator:

$$\mathbb{1} = \int \mathscr{D}\{\phi,\bar{\phi}\}e^{-\bar{\phi}\phi}\,|\phi\rangle\,\langle\phi| = \int \frac{d\bar{\phi}d\phi}{\pi}e^{-\bar{\phi}\phi}\,|\phi\rangle\,\langle\phi|\,. \tag{4.10}$$

Furthermore, we see that a normal ordered operator $\hat{O}(\hat{a}^\dagger,\hat{a})$ has, due to the relations (4.7 − 4.9), the following field representation:

$$\langle\phi|\,\hat{O}(\hat{a}^\dagger,\hat{a})\,|\phi\rangle = O(\bar{\phi},\phi). \tag{4.11}$$

We consider in the following a normal ordered Liouiville operator with the structure[45,46]:

$$\hat{\mathcal{L}}[\hat{\rho}(t)] = -i[\hat{H},\hat{\rho}(t)] + 2\hat{L}\hat{\rho}(t)\hat{L}^\dagger - \hat{L}\hat{L}^\dagger\hat{\rho}(t) - \hat{\rho}(t)\hat{L}\hat{L}^\dagger, \tag{4.12}$$

where the Lindblad operator $\hat{L}$ is non-linear (cf. chapter 3).
We continue to transform the partition function into a field integral by using

a coherent state basis set. At each point in time, the unitary operator (4.10) is introduced in the expansion (4.6) of the partition sum:

$$\mathcal{Z} = \lim_{N\to\infty} \mathrm{Tr}[\mathbb{1}_N^+(1+\delta_t^{(N)}\hat{\mathcal{L}})\mathbb{1}_{N-1}^+ ... [\mathbb{1}_1^+(1+\delta_t^{(1)}\hat{\mathcal{L}})[\mathbb{1}_0^+\hat{\rho}(0)\mathbb{1}_0^-]...\mathbb{1}_N^-]], \quad (4.13)$$

where $\pm$ labels the contour.
We use the following notation for fields ϕ_l^α, which appear at time step $0 \leq l \leq N$ on contour $\alpha \in \{+,-\}$, according to the left or right hand side of the density operator. Furthermore, we restrict ourselves to the computation of the l-th time step and make explicit use of the normal ordering of the Liouville operator (4.12):

$$\begin{aligned}
&[\mathbb{1}_l^+(1+\delta_t^{(l)}\hat{\mathcal{L}})\mathbb{1}_{l-1}^+[...]\mathbb{1}_{l-1}^-]\mathbb{1}_l^-]] \qquad (4.14)\\
&= \int \mathscr{D}\{\phi,\bar{\phi}\} \\
&\left|\phi_l^+\right\rangle\left\langle\phi_l^+\right|\left|\phi_{l-1}^+\right\rangle\left\langle\phi_{l-1}^+\right|[...]\left|\phi_{l-1}^-\right\rangle\left\langle\phi_{l-1}^-\right|\left|\phi_l^-\right\rangle\left\langle\phi_l^-\right|[1+\delta_t^{(l)}\mathcal{L}[\bar{\phi}_l^+,\phi_{l-1}^+,\bar{\phi}_{l-1}^-,\phi_l^-]]
\end{aligned}$$

with

$$\begin{aligned}
\mathscr{D}\{\phi,\bar{\phi}\} = \qquad (4.15)\\
&\mathscr{D}\{\phi_l^-,\bar{\phi}_l^-\}e^{-\bar{\phi}_l^-\phi_l^-}\mathscr{D}\{\phi_{l-1}^-,\bar{\phi}_{l-1}^-\}e^{-\bar{\phi}_{l-1}^-\phi_{l-1}^-}\\
&\mathscr{D}\{\phi_l^+,\bar{\phi}_l^+\}e^{-\bar{\phi}_l^+\phi_l^+}\mathscr{D}\{\phi_{l-1}^+,\bar{\phi}_{l-1}^+\}e^{-\bar{\phi}_{l-1}^+\phi_{l-1}^+}
\end{aligned}$$

and

$$\begin{aligned}
\mathcal{L}[\bar{\phi}_l^+,\phi_{l-1}^+,\bar{\phi}_{l-1}^-,\phi_l^-] &= -iH(\bar{\phi}_l^+,\phi_{l-1}^+) + iH(\bar{\phi}_{l-1}^-,\phi_l^-)\\
&+ 2L(\bar{\phi}_l^+,\phi_{l-1}^+)L^\dagger(\bar{\phi}_{l-1}^-,\phi_l^-) - L(\bar{\phi}_l^+,\phi_{l-1}^+)L^\dagger(\bar{\phi}_l^+,\phi_{l-1}^+)\\
&- L(\bar{\phi}_{l-1}^-,\phi_l^-)L^\dagger(\bar{\phi}_{l-1}^-,\phi_l^-). \qquad (4.16)
\end{aligned}$$

The field representation of the partition function (4.13) is thus[53]

$$\begin{aligned}
\mathcal{Z}(t) &= \lim_{N\to\infty}\{\Pi_{l=0}^N \int \mathscr{D}\{\bar{\phi}_l^-,\phi_l^-,\bar{\phi}_l^+,\phi_l^+\}e^{-\bar{\phi}_l^-\phi_l^-}e^{-\bar{\phi}_l^+\phi_l^+} \qquad (4.17)\\
&\Pi_{k=1}^N e^{\delta_t^{(k)}\mathcal{L}[\bar{\phi}_k^+,\phi_{k-1}^+,\bar{\phi}_{k-1}^-,\phi_k^-]}\ \mathrm{Tr}[\left|\phi_N^+\right\rangle\left\langle\phi_N^+\right|\left|\phi_{N-1}^+\right\rangle\left\langle\phi_{N-1}^+\right|[...]\left|\phi_{N-1}^-\right\rangle\left\langle\phi_{N-1}^-\right|\left|\phi_N^-\right\rangle\left\langle\phi_N^-\right|]\}\\
&\approx \lim_{N\to\infty}\{\Pi_{l=0}^N \int \mathscr{D}\{\bar{\phi}_l^-,\phi_l^-,\bar{\phi}_l^+,\phi_l^+\}\ e^{\sum_{l=1}^N[\bar{\phi}_l^+(\phi_{l-1}^+-\phi_l^+)+\phi_l^-(\bar{\phi}_{l-1}^--\bar{\phi}_l^-)+\delta_t^{(l)}\mathcal{L}[\bar{\phi}_l^+,\phi_{l-1}^+,\bar{\phi}_{l-1}^-,\phi_l^-]]}\},
\end{aligned}$$

where in the last step we neglected the two finite regularizations $e^{\ln\left\langle\phi_0^+\right|\hat{\rho}(t_0)\left|\phi_0^-\right\rangle}$ and $e^{-\bar{\phi}_N^+\phi_N^-}$, which connect both time contours at $t=t_0$ and $t=N$.[51] We will implement this regularization on the basis of the Green's functions.

Finally, we transform the discrete representation in time to a continuum description and use the following relations:

$$\sum \delta_t \to \int_t, \tag{4.18}$$

$$\frac{\bar{\phi}_l^+(\phi_l^+ - \phi_{l-1}^+)}{\delta_t} \to \bar{\phi}^+ \partial_t \phi^+ \text{ and } \frac{\phi_l^-(\bar{\phi}_{l-1}^- - \bar{\phi}_l^-)}{\delta_t} \to \phi^- \partial_t \bar{\phi}^-, \tag{4.19}$$

$$\mathcal{L}[\bar{\phi}_l^+, \phi_{l-1}^+, \bar{\phi}_{l-1}^-, \phi_l^-] \to \mathcal{L}[\bar{\phi}^+, \phi^+, \bar{\phi}^-, \phi^-], \tag{4.20}$$

$$\Pi_{l=0}^N \mathscr{D}\{\bar{\phi}_l^-, \phi_l^-, \bar{\phi}_l^+, \phi_l^+\} \to \mathscr{D}\{\bar{\phi}^-, \phi^-, \bar{\phi}^+, \phi\}. \tag{4.21}$$

Thus, in the continuum limit, the partition sum (4.17) is an integral over all possible field configurations $\{\bar{\phi}^-, \phi^-, \bar{\phi}^+, \phi^+\}$, weighted by a statistical factor $e^{iS[\bar{\phi}^+, \phi^+, \bar{\phi}^-, \phi^-]}$:

$$\begin{aligned} \mathcal{Z}(t) &= \int \mathscr{D}\{\bar{\phi}^-, \phi^-, \bar{\phi}^+, \phi^+\} e^{i \int_t [i\bar{\phi}^+ \partial_t \phi^+ - i\bar{\phi}^- \partial_t \phi^- - i\,\mathcal{L}[\bar{\phi}^+, \phi^+, \bar{\phi}^-, \phi^-]} \\ &= \int \mathscr{D}\{\bar{\phi}^-, \phi^-, \bar{\phi}^+, \phi^+\} e^{iS[\bar{\phi}^+, \phi^+, \bar{\phi}^-, \phi^-]}, \end{aligned} \tag{4.22}$$

with the following action on the $\pm$-contour:

$$S[\bar{\phi}^+, \phi^+, \bar{\phi}^-, \phi^-] = \int_t [i\bar{\phi}^+ \partial_t \phi^+ - i\bar{\phi}^- \partial_t \phi^- - i\,\mathcal{L}[\bar{\phi}^+, \phi^+, \bar{\phi}^-, \phi^-]]. \tag{4.23}$$

With this, we determined a field integral representation for the many-body master equation (4.4). In the following sections, we apply this field integral representation to describe the dynamics of a one dimensional system of N interacting bosons in an optical lattice.

4.1.1 The Bare Green's Function

We follow the last section in order to determine the field integral representation of the master equation for an interacting bosonic system in a red-detuned optical lattice. This master equation reads (cf. equation (3.44)):

$$\begin{aligned} \partial_t \hat{\rho}(t) &= -i[\hat{H}_{\text{BHM}}, \hat{\rho}(t)] + \sum_i \gamma[\hat{n}_i, [\hat{n}_i, \hat{\rho}(t)]] \\ &= -i[\hat{H}_{\text{BHM}}, \hat{\rho}(t)] + \sum_i \gamma(2\hat{n}_i \hat{\rho}(t) \hat{n}_i - \{\hat{n}_i \hat{n}_i, \hat{\rho}(t)\}). \end{aligned} \tag{4.24}$$

We start with the coherent dynamics, generated by the microscopic Bose-Hubbard model. According to the calculations in section 2, the microscopic Bose-Hubbard model in the low-energy regime consists of a quadratic and

cubic part. First we determine the action for the normal ordered quadratic Hamiltonian of the interacting Luttinger Liquid[19,20]:

$$\hat{H}_Q = \sum_{p\neq 0} \nu|p|\hat{b}_p^\dagger \hat{b}_p = \sum_{p\neq 0} \epsilon(p)\hat{b}_p^\dagger \hat{b}_p, \tag{4.25}$$

where $\{\hat{b}_p^\dagger,\ \hat{b}_p\}$ is the phonon basis.
Due to the underlying one dimensional lattice in the microscopic model, the coherent states $\{|\phi(t,p)\rangle\}$ come along with an additional space coordinate (respectively momentum) and according to this, the action (4.23) in the continuum limit contains integrals over time and space. The quadratic action is due to equation (4.25):

$$\begin{aligned} S_Q[\bar{\phi}^+,\phi^+,\bar{\phi}^-,\phi^-] = \int_t \sum_{p\neq 0} [\bar{\phi}^+(p,t)(i\partial_t - \epsilon(p))\phi^+(p,t) \\ - \bar{\phi}^-(p,t)(i\partial_t - \epsilon(p))\phi^-(p,t)]. \end{aligned} \tag{4.26}$$

At first glance, the action S_Q does not show explicit correlations of fields from two distinct time lines, which is however not correct, since they are coupled at $t = t_0$ and $t = N$. In order to show the coupling of the contours, we define the single particle Green's functions (or propagators) as the correlations between fields from equal or different time lines:

$$\left\langle \bar{\phi}^\alpha(p,t)\phi^\beta(p,t')\right\rangle = \int \mathscr{D}\{\bar{\phi}^-,\phi^-,\bar{\phi}^+,\phi^+\}\bar{\phi}^\alpha(p,t)\phi^\beta(p,t')e^{iS[\bar{\phi}^-,\phi^-,\bar{\phi}^+,\phi^+]}, \tag{4.27}$$

where $\alpha,\beta \in \{\pm\}$.
The calculations of the propagators (4.27) for the quadratic action S_Q show the following results for the correlations of fields from equal and distinct time contours[51]:

$$iG_> = \langle \bar{\phi}^+(x,t)\phi^-(x',t')\rangle = n_B(\omega)e^{-i\epsilon(p)(t-t')}, \tag{4.28}$$

$$iG_< = \langle \bar{\phi}^-(x,t)\phi^+(x',t')\rangle = (n_B(\omega)+1)e^{-i\epsilon(p)(t-t')}, \tag{4.29}$$

$$\begin{aligned} iG_+ &= \langle \bar{\phi}_+(x,t)\phi_+(x',t')\rangle \\ &= \Theta(t-t')\,\langle \hat{b}^\dagger(x,t)\hat{b}(x',t')\rangle + \Theta(t'-t)\,\langle \hat{b}(x',t')\hat{b}^\dagger(x,t)\rangle \\ &= \Theta(t-t')iG_> + \Theta(t'-t)iG_<, \end{aligned} \tag{4.30}$$

$$iG_- = \langle \bar{\phi}^-(x,t)\phi^-(x',t')\rangle = \Theta(t'-t)iG_> + \Theta(t-t')iG_<, \tag{4.31}$$

where $n_B(\omega)$ is the bosonic occupation number. The system's dynamics is initialized at $t = t_0$ with a density operator at thermal equilibrium and

evolves according to the bare theory of a Luttinger Liquid. The correlations of fields from different contours (4.28 − 4.29) is due to the coupling of the contours at time $t = t_0$.
In the following we transform from the ±-basis into the Keldysh basis and explain in the subsequent paragraphs the advantage and motivation of this transformation. The Keldysh framework is the common basis used to describe many-body systems out of equilibrium.[42,49–52]
The transformation of fields in the Keldysh basis $\{\bar{\phi}_{cl}, \bar{\phi}_q, \phi_{cl}, \phi_q\}$ into fields in the ±-basis is defined by:

$$\begin{aligned}\begin{pmatrix}\phi_+(p,t)\\ \phi_-(p,t)\end{pmatrix} &= \frac{1}{\sqrt{2}}\begin{pmatrix}1 & 1\\ 1 & -1\end{pmatrix}\begin{pmatrix}\phi_{cl}(p,t)\\ \phi_q(p,t)\end{pmatrix},\\ \begin{pmatrix}\bar{\phi}_+(p,t)\\ \bar{\phi}_-(p,t)\end{pmatrix} &= \frac{1}{\sqrt{2}}\begin{pmatrix}1 & 1\\ 1 & -1\end{pmatrix}\begin{pmatrix}\bar{\phi}_{cl}(p,t)\\ \bar{\phi}_q(p,t)\end{pmatrix}.\end{aligned} \tag{4.32}$$

According to this unitary transformation, we conclude from equation (4.26) the Keldysh action for the quadratic Hamiltonian of the interacting Luttinger Liquid[30,31]:

$$S_Q = \int_t \int_{t'} \sum_{p\neq 0} \left(\bar{\phi}_{cl}(p,t), \bar{\phi}_q(p,t)\right) \underbrace{\begin{pmatrix}0 & \tilde{P}_A(p,t,t')\\ \tilde{P}_R(p,t,t') & \tilde{P}_K(p,t,t')\end{pmatrix}}_{\tilde{G}^{-1}(p,t,t')} \begin{pmatrix}\phi_{cl}(p,t')\\ \phi_q(p,t')\end{pmatrix}, \tag{4.33}$$

with the following bare propagators:

1. Retarded/advanced propagator of the inverse Green's function:

$$\tilde{P}_{R/A}(p,t,t') = [\tilde{G}^{-1}(p,t,t')]_{R/A} = \delta(t-t')[(i\partial_t - \epsilon(p) \pm i\eta)],$$

2. Keldysh propagator of the inverse Green's function:

$$\tilde{P}_K(p,t,t') = [\tilde{G}^{-1}(p,t,t')]_K = 2i\eta\ (2n_B(\omega)+1)e^{-i\epsilon(p)(t-t')},$$

where η is an infinitesimal small regularization in order to obtain a convergent integral (4.33). After the transformation into the Keldysh basis, the amount of propagators is due to (4.33) reduced to two distinct ones.
Retarded and advanced Green's function contain the information of the spectrum of the Luttinger Liquid with the dispersion relation $\omega = \epsilon(p)$. On the other hand, the bare Keldysh Green's function is related to the Bose-Einstein distribution n_B of the system. In conclusion, we see that important physical properties are directly related to the Green's functions in the Keldysh formalism. Via the Keldysh rotation we obviously separated the information

on the spectrum of the system from its occupation.
In the following section, we also map the dissipative and cubic part of the master equation in a field integral representation to reach the complete partition sum for an interacting Luttinger Liquid in a far red-detuned laser field. We showed that the Keldysh description is well suited to describe dynamics of a many-body system out of equilibrium.

4.1.2 Heating Dynamics

In this section, we focus on the dissipative part of a one dimensional interacting Luttinger Liquid out of equilibrium. The presence of the optical lattice induces a finite noise to the system, that replaces the infinitesimal regularization in the Keldysh sector. The heating process generates a time dependent population of normal and anomalous occupation (cf. chapter 3). Thus, we use the Nambu space representation in order to represent the dissipative action in a block-diagonal form.
The dissipative part of the quantum master equation for a driven interacting Luttinger Liquid is:

$$\hat{\mathcal{D}}[\hat{\rho}(t)] = \sum_p h(p)(2(\hat{b}_p^\dagger + \hat{b}_{-p})\hat{\rho}(t)(\hat{b}_{-p}^\dagger + \hat{b}_p) - \{(\hat{b}_p^\dagger + \hat{b}_{-p})(\hat{b}_{-p}^\dagger + \hat{b}_p), \hat{\rho}(t)\}), \tag{4.34}$$

where $h(p) = \frac{\gamma K|p|}{2\pi}$.
We apply relation (4.23) to compute the corresponding action in the $\pm$-basis:

$$\begin{aligned} &S_D[\bar{\phi}^+, \phi^+, \bar{\phi}^-, \phi^-] \\ &= \int_t \sum_p [i\bar{\phi}^+(p,t)\partial_t\phi^+(p,t) - i\bar{\phi}^-(p,t)\partial_t\phi^-(p,t) \\ &-ih(p)\{(2(\bar{\phi}^+(p,t) + \phi^+(-p,t))(\bar{\phi}^-(-p,t) + \phi^-(p,t)) \\ &-(\bar{\phi}^+(p,t) + \phi^+(-p,t))(\bar{\phi}^+(-p,t) + \phi^+(p,t)) \\ &-(\bar{\phi}^-(p,t) + \phi^-(-p,t))(\bar{\phi}^-(-p,t) + \phi^-(p,t))\}]. \end{aligned} \tag{4.35}$$

We recognize from (4.35), that the dissipative action couples fields from both time contours and consists of terms with opposite momenta.
We continue to transform this action into the Keldysh basis in order to analyse the influence of the heating on the occupation and the spectrum of the system. The dissipative Keldysh action is due to the unitary transformation

of the last section:

$$
\begin{aligned}
&S_D[\bar{\phi}_{cl}, \phi_{cl}, \bar{\phi}_q, \phi_q] \qquad (4.36)\\
&= \int_t \sum_p [i\bar{\phi}_{cl}(p,t)\partial_t\phi_q(p,t) + i\bar{\phi}_q(p,t)\partial_t\phi_{cl}(p,t)\\
&- ih(p)[-2(\phi_q(-p,t)\phi_q(p,t) + \bar{\phi}_q(-p,t)\phi_q(-p,t) + \bar{\phi}_q(p,t)\phi_q(p,t)\\
&+\bar{\phi}_q(-p,t)\bar{\phi}_q(p,t)) + \phi_{cl}(p,t)\phi_q(-p,t) + \bar{\phi}_{cl}(-p,t)\phi_q(-p,t)\\
&-\phi_{cl}(-p,t)\phi_q(p,t) - \bar{\phi}_{cl}(p,t)\phi_q(p,t) - \phi_{cl}(-p,t)\bar{\phi}_q(-p,t)\\
&-\bar{\phi}_{cl}(p,t)\bar{\phi}_q(-p,t) + \bar{\phi}_{cl}(-p,t)\bar{\phi}_q(p,t) + \phi_{cl}(p,t)\bar{\phi}_q(p,t)]]\\
&= \int_t \sum_p [i\bar{\phi}_{cl}(p,t)\partial_t\phi_q(p,t) + i\bar{\phi}_q(p,t)\partial_t\phi_{cl}(p,t)\\
&-ih(p)[-2(\phi_q(-p,t)(\phi_q(p,t) + \bar{\phi}_q(-p,t)) + \bar{\phi}_q(p,t)(\phi_q(p,t) + \bar{\phi}_q(-p,t))].
\end{aligned}
$$

Since the Keldysh action has anomalous terms and is invariant for $p \to -p$, we define the Nambu space representation[42]

$$
\Big(\Phi_{cl}(p,t), \Phi_q(p,t)\Big)^T = \Big(\phi_{cl}(p,t), \bar{\phi}_{cl}(-p,t), \phi_q(p,t), \bar{\phi}_q(-p,t)\Big)^T . \qquad (4.37)
$$

The dissipative Keldysh action (4.36) has the following block-diagonal form in the Nambu basis:

$$
\begin{aligned}
&S_D[\bar{\phi}_{cl}, \phi_{cl}, \bar{\phi}_q, \phi_q] \qquad (4.38)\\
&= \int_t \int_{t'} \sum_p \Big(\bar{\Phi}_{cl}(p,t), \bar{\Phi}_q(p,t)\Big) [\delta(t-t') \begin{pmatrix} 0 & i\partial_t - i\eta\sigma_3 \\ i\partial_t + i\eta\sigma_3 & ih(p)(\mathbb{1} + \sigma_1) \end{pmatrix}] \begin{pmatrix} \Phi_{cl}(p,t') \\ \Phi_q(p,t') \end{pmatrix},
\end{aligned}
$$

where $\{\sigma_i\}_{i\in\{1,2,3\}}$ are the Pauli matrices.
The continuous pump of energy with a rate $h(p)$ causes fluctuations in the phonon occupation, which appear in the Keldysh sector. The fluctuations are generated by the spontaneous emission of photons from the bosonic particles.
The retarded and advanced blocks show that the spectrum has a peak centered around $\omega = 0$. If we include the quadratic part of the interacting Luttinger Liquid, we automatically shift this peak to $\omega = \epsilon(p)$. Thus, the spectrum of the quadratic model is not modified in the presence of the interaction between the one dimensional system of interacting bosons and the laser field.
In order to have a compact form for the bare and dissipative action, we transform the quadratic action of the interacting Luttinger Liquid into the

Nambu basis:

$$S_Q = \int_t \int_{t'} \sum_{p\neq 0} \left(\bar{\Phi}_{cl}(p,t), \bar{\Phi}_q(p,t)\right) \begin{pmatrix} 0 & P_A(p,t,t') \\ P_R(p,t,t') & P_K(p,t,t') \end{pmatrix} \begin{pmatrix} \Phi_{cl}(p,t') \\ \Phi_q(p,t') \end{pmatrix}, \tag{4.39}$$

where $P_{R/A}(p,t,t')$ are the retarded and advanced propagators of the inverse Green's function. Due to the Nambu space representation, we have the following 2×2 structure for the propagators:

$$P_{R/A}(p,t,t') = \delta(t-t')[(i\partial_t - \epsilon(p))\mathbb{1} \pm i\eta\sigma_3], \tag{4.40}$$

$$P_K(p,t,t') = 2i\eta\sigma_3(2n_B(\omega)+1)e^{-i\epsilon(p)(t-t')}. \tag{4.41}$$

Thus, the total bare and dissipative action S_{Q+D} in Nambu Space representation is[30,31]:

$$\begin{aligned} &S_{Q+D}[\bar{\Phi}_{cl}, \Phi_{cl}, \bar{\Phi}_q, \Phi_q] \\ &= \int_t \int_{t'} \sum_{p\neq 0} \left(\bar{\Phi}_{cl}(p,t), \bar{\Phi}_q(p,t)\right) [\delta(t-t') \begin{pmatrix} 0 & P_A(p,t,t') \\ P_R(p,t,t') & ih(p)(\mathbb{1}+\sigma_1) \end{pmatrix}] \begin{pmatrix} \Phi_{cl}(p,t') \\ \Phi_q(p,t') \end{pmatrix}. \end{aligned} \tag{4.42}$$

We first of all conclude from (4.42), that the infinitesimal Keldysh component of the quadratic sector is replaced by the finite heating rate of the dissipative Keldysh action. Furthermore, the excitation spectrum is not influenced by the heating dynamics.

4.1.3 Fluctuation-Dissipation Theorem

Linear response theory is used to determine the so-called fluctuation-dissipation theorem for a system at thermal equilibrium.[42,54] We analyse this relation in the Keldysh framework in order to determine if a system is out of equilibrium.
For instance, we consider a system at equilibrium, which is described by the bare quadratic action S_Q of the Luttinger Liquid. In this case, we have the following Keldysh Green's functions:

1. Retarded/advanced Green's function:

   $\tilde{P}_{R/A}(p,\omega) = (\omega - \epsilon(p) \pm i\eta)$,

2. Keldysh propagator of the inverse Green's function:

   $\tilde{P}_K(p, \omega = \epsilon(p)) = 2i\eta(2n_B(p)+1)$.

We see from these relations that the inverse Keldysh Green's function at equilbrium is related to its spectral density function by[42,51]:

$$\tilde{P}_K(p,\omega) = F(p,\omega)[\tilde{P}_R(p,\omega) - \tilde{P}_A(p,\omega)]|_{\omega=\epsilon(p)} \tag{4.43}$$

with the distribution $F(p,\omega = \epsilon(p)) = (2n_B(p)+1) = \coth(\beta\epsilon(p))$ for a bosonic system at equilibrium.
Indeed, we determined the fluctuation-dissipation theorem in the Keldysh framework. We now show, that, if we include dissipative heating, the fluctuation-dissipation theorem is not valid any more. We take the dissipative and quadratic Keldysh action S_{Q+H} with the pumping rate $h(p)$:

$$\tilde{P}_K(p,\omega) = ih(p)(\mathbb{1} + \sigma_1).$$

Obviously relation (4.43) is not true. Indeed, the Luttinger Liquid is, due to the presence of spontaneous emission, continuously driven out of equilibirum and thus the fluctuation-dissipation theorem breaks down.
We have pointed out the importance of the fluctuation-dissipation theorem to analyse if a system is at thermal equilibirum. In the following section, we determine a relation in the Keldysh framework, which in the limit of a thermal state is equivalent to the fluctuation-dissipation theorem. We use this relation to derive a kinetic equation for the occupation of the interacting Luttinger Liquid in an optical lattice.

4.1.4 Scattering Vertex

The interacting Luttinger Liquid includes scattering processes that are described by the following effective cubic Hamiltonian:

$$\begin{aligned}\hat{H}_C =& \hat{H}_{C,1} + \hat{H}_{C,2} \\ =& \frac{1}{\sqrt{2L}} \int_{q,p,k} V(q,p,k)[\delta(k+q-p)\hat{b}_q^\dagger \hat{b}_k^\dagger \hat{b}_p + \frac{1}{3}\delta(k+q+p)\hat{b}_q^\dagger \hat{b}_p^\dagger \hat{b}_k^\dagger + h.c.].\end{aligned} \tag{4.44}$$

We will now determine the corresponding Keldysh field integral representation in order to derive the full partition function for an interacting Luttinger Liquid in a laser field and analyse in more detail the structure of the cubic Keldysh action.
The cubic Keldysh action is, according to equation (4.23), and after rotation

into the Keldysh basis:

$$
\begin{aligned}
&S_C[\bar{\phi}_{cl}, \phi_{cl}, \bar{\phi}_q, \phi_q] \qquad (4.45)\\
&=\frac{1}{\sqrt{2L}} \int_t \int_{q,p,k} V(q,p,k)[\delta(k+q-p)[\bar{\phi}_q(q,t)\bar{\phi}_q(k,t)\phi_q(p,t)\\
&+\bar{\phi}_q(q,t)\bar{\phi}_{cl}(k,t)\phi_{cl}(p,t) + \bar{\phi}_{cl}(q,t)\bar{\phi}_{cl}(k,t)\phi_q(p,t) + \bar{\phi}_{cl}(q,t)\bar{\phi}_q(k,t)\phi_{cl}(p,t)]\\
&+\frac{1}{3}\delta(k+q+p)[\bar{\phi}_q(q,t)\bar{\phi}_q(k)\bar{\phi}_q(p,t) + \bar{\phi}_q(q,t)\bar{\phi}_{cl}(k)\bar{\phi}_{cl}(p,t)\\
&+\bar{\phi}_{cl}(q,t)\bar{\phi}_q(k)\bar{\phi}_{cl}(p,t) + \bar{\phi}_{cl}(q,t)\bar{\phi}_{cl}(k)\bar{\phi}_q(p,t)] + h.c.],
\end{aligned}
$$

where we omitted the two terms including the partial time derivations.
The cubic action S_C consists of vertices with an odd number of quantum fields. Therefore, the action vanishes if the fields are equal on the forward and backward time line, i.e. $\bar{\phi}_+ = \bar{\phi}_-$ and $\phi_+ = \phi_-$ (cf. definition of $\{\bar{\phi}_q, \phi_q\}$). According to the following definition, we split the cubic action in two parts[30,31]:

$$
\begin{aligned}
&S_{C,1}[\bar{\phi}_{cl}, \phi_{cl}, \bar{\phi}_q, \phi_q] \qquad (4.46)\\
&=\frac{1}{\sqrt{2L}} \int_t \int_{q,p,k} V(q,p,k)[\delta(k+q-p)[\bar{\phi}_q(q,t)\bar{\phi}_q(k,t)\phi_q(p,t)\\
&+\bar{\phi}_q(q,t)\bar{\phi}_{cl}(k,t)\phi_{cl}(p,t) + \bar{\phi}_{cl}(q,t)\bar{\phi}_{cl}(k,t)\phi_q(p,t) + \bar{\phi}_{cl}(q,t)\bar{\phi}_q(k,t)\phi_{cl}(p,t)],
\end{aligned}
$$

$$
\begin{aligned}
&S_{C,2}[\bar{\phi}_{cl}, \phi_{cl}, \bar{\phi}_q, \phi_q] \qquad (4.47)\\
&=\frac{1}{3}\delta(k+q+p)[\bar{\phi}_q(q,t)\bar{\phi}_q(k)\bar{\phi}_q(p,t) + \bar{\phi}_q(q,t)\bar{\phi}_{cl}(k)\bar{\phi}_{cl}(p,t)\\
&+\bar{\phi}_{cl}(q,t)\bar{\phi}_q(k)\bar{\phi}_{cl}(p,t) + \bar{\phi}_{cl}(q,t)\bar{\phi}_{cl}(k)\bar{\phi}_q(p,t)] + h.c.],
\end{aligned}
$$

The first part of equation (4.46) describes a process, where a phonon splits into two phonons. If all three phonons travel in the same direction, such a process is able to fullfill energy and momentum conservation in one dimension. The second equation (4.47) consists of processes, where three fields are created/annihilated with the momentum conservation $\delta(k+q+p)$. In order to show explictely the non-resonant character of such terms with respect to the quadratic theory, we transform into a rotating frame:

$$\phi_\alpha(x,t) \to e^{-i\epsilon(p)t}\phi_\alpha(x,t), \qquad (4.48)$$

$$\bar{\phi}_\alpha(x,t) \to e^{i\epsilon(p)t}\bar{\phi}_\alpha(x,t), \qquad (4.49)$$

where $\alpha \in \{q, cl\}$.
The cubic action in the interaction picture is:

$$\begin{aligned}
&S_C[\bar{\phi}_{cl}, \phi_{cl}, \bar{\phi}_q, \phi_q] \qquad (4.50)\\
&=\frac{1}{\sqrt{2L}} \int_t \int_{q,p,k} V(q,p,k)[e^{-i[\epsilon(p)-\epsilon(q)-\epsilon(k)]t}\delta(k+q-p)[\bar{\phi}_q(q,t)\bar{\phi}_q(k,t)\phi_q(p,t)\\
&+\bar{\phi}_q(q,t)\bar{\phi}_{cl}(k,t)\phi_{cl}(p,t) + \bar{\phi}_{cl}(q,t)\bar{\phi}_{cl}(k,t)\phi_q(p,t) + \bar{\phi}_{cl}(q,t)\bar{\phi}_q(k,t)\phi_{cl}(p,t)]\\
&+\frac{1}{3}e^{i[\epsilon(p)+\epsilon(q)+\epsilon(k)]t}\delta(k+q+p)[\bar{\phi}_q(q,t)\bar{\phi}_q(k)\bar{\phi}_q(p,t) + \bar{\phi}_q(q,t)\bar{\phi}_{cl}(k)\bar{\phi}_{cl}(p,t)\\
&+\bar{\phi}_{cl}(q,t)\bar{\phi}_q(k)\bar{\phi}_{cl}(p,t) + \bar{\phi}_{cl}(q,t)\bar{\phi}_{cl}(k)\bar{\phi}_q(p,t)] + h.c.].
\end{aligned}$$

The action describes virtual processes for distinct momenta $\{k, q, p\}$ with

$$\epsilon(p) - \epsilon(q) - \epsilon(k) \neq 0, \qquad (4.51)$$
$$\epsilon(p) + \epsilon(q) + \epsilon(k) \neq 0, \qquad (4.52)$$

where a time dependent phase is picked up. Virtual processes violate due to (4.51 - 4.52) energy conservation and the corresponding excitations are metastable. As a consequence, the contribution of such processes to the dynamics of the system is subleading. On the other hand, resonant processes, which fullfill the relations

$$\epsilon(p) - \epsilon(q) - \epsilon(k) = 0 \text{ and } k + q - p = 0, \qquad (4.53)$$
$$\epsilon(p) + \epsilon(q) + \epsilon(k) = 0 \text{ and } k + q + p = 0, \qquad (4.54)$$

will dominantly influence the system's dynamics. The second condition (4.54) has no solution for $\epsilon(p) = \nu|p|$. However, (4.53) is fullfilled for all momenta $\{k, q, p\}$ with equal sign. Therefore, the processes with three annihilated, respectively created fields are non-resonant processes with respect to the quadratic theory and thus do not influence the dynamics of the system to leading order. In conclusion, we use in the following subsections a reduced effective cubic action, which includes just the resonant part[30,31]:

$$\begin{aligned}
&S_C[\bar{\phi}_{cl}, \phi_{cl}, \bar{\phi}_q, \phi_q]\\
&=\frac{1}{\sqrt{2L}} \int_t \int_{q,p,k} V(q,p,k)\delta(k+q-p)\\
&\quad[\bar{\phi}_q(q,t)\bar{\phi}_q(k,t)\phi_q(p,t) + \bar{\phi}_q(q,t)\bar{\phi}_{cl}(k,t)\phi_{cl}(p,t)\\
&\quad + \bar{\phi}_{cl}(q,t)\bar{\phi}_{cl}(k,t)\phi_q(p,t) + \bar{\phi}_{cl}(q,t)\bar{\phi}_q(k,t)\phi_{cl}(p,t) + h.c.]. \qquad (4.55)
\end{aligned}$$

In summary, we have determined the following Keldysh action of an interacting Luttinger Liquid in a laser field:

$$S = S_Q + S_C + S_D, \qquad (4.56)$$

where

$$S_{Q+D} \tag{4.57}$$
$$= \int_t \int_{t'} \sum_p \left(\bar{\Phi}_{cl}(p,t), \bar{\Phi}_q(p,t)\right) [\delta(t-t') \begin{pmatrix} 0 & P_A(p,t,t') \\ P_R(p,t,t') & ih(p)(\mathbb{1}+\sigma_1) \end{pmatrix}] \begin{pmatrix} \Phi_{cl}(p,t') \\ \Phi_q(p,t') \end{pmatrix}.$$

Furthermore, we derived the fluctuation-dissipation theorem in the Keldysh formalism, which is a tool to determine if a system is at thermal equilibrium.

Chapter 5

The Kinetic Equation for a Driven Interacting Luttinger Liquid

We are interested in the dynamics of an interacting Luttinger Liquid in an optical lattice. The time evolution is generated by the interplay of interaction and dissipation as discussed in the previous section. In this section, we determine the corresponding kinetic equation in the Keldysh framework, which describes the time evolution of the phonon density. We start with a short paragraph on examples of kinetic equations from different physical fields in order to outline their importance and to describe their structure.[55,56] Subsequently, the Dyson equation and the fluctuation-dissipation theorem are used to compute a kinetic equation for the occupation distribution of interacting bosons in a red-detuned laser field.[30,31] The kinetic equation is transformed in Wigner coordinates and simplified by scale separation, which allows for the Wigner approximation.[51]

5.1 Examples of Kinetic Equations in Physics

In general, the kinetic equation in classical physics is a first order differential equation, which describes the time evolution of the distribution function $f(\vec{x}, \vec{v}, t)$ in a many-particle phase space $\{\vec{x}, \vec{v}\}$:

$$(\partial_t + \vec{v}\nabla_{\vec{x}} + \frac{\vec{F}}{m}\nabla_{\vec{v}})f(\vec{x}, \vec{v}, t) = \frac{\partial f}{\partial t}|_{\text{coll}}. \tag{5.1}$$

The probability density function $f(\vec{x}, \vec{v}, t)$ contains the information of number of particles per phase space point at time t. The collision term on the right hand side of equation (5.1) is based on the dominant scattering processes in the system.
We consider for example a classical system of many particles, which is initially at $t = t_0$ described by a Maxwell-Boltzmann distribution. If the system is driven at $t > t_0$ out of equilibrium, the distribution function evolves due to the kinetic equation (5.1) in time. The exchange of energy and momentum among particles due to generic interactions can generate a mechanism for thermalization. The time evolution of this relaxation process is described by equation (5.1) and is normally very complex.
For instance, we consider a neutral two component gas (labeled: a and b), which interacts via local scattering with outgoing velocities $\vec{v}_a'$ and $\vec{v}_b'$. The collision term is assumed to consist of two terms: The first term describes the increase of particles in the velocity element $d\vec{v}_b$ and competes with a second term, which is responsible for the loss of particles in the velocity element $d\vec{v}_b$. This is the famous approach of L. Boltzmann to describe the dynamics of a

neutral gas of two species[55,56]:

$$\frac{\partial f_a}{\partial t}|_{\text{coll}} = \int \left(f_a(\vec{v}_a')f_b(\vec{v}_b') - f_a(\vec{v}_a)f_b(\vec{v}_b)\right) |\vec{v}_a - \vec{v}_b| \; \sigma_{ab} \; d\vec{v}_b \tag{5.2}$$

with the distribution functions f_a and f_b, and the scattering cross section σ_{ab} between particles of both species.
Since both particle species are indistinguishable, the collision term is symmetric under $a \leftrightarrow b$ ($\sigma_{ab} = \sigma_{ba}$).
Furthermore, the stationary solutions of f_a and f_b, for which the collision term vanishes, fullfill:

$$f_a(\vec{v}_a')f_b(\vec{v}_b') - f_a(\vec{v}_a)f_b(\vec{v}_b) = 0. \tag{5.3}$$

The number of incoming particles equals the flow of particles out of the velocity element $d\vec{v}_b$.
The second example we consider is a cloud of ions, which is injected in a thermal plasma. The ions are due to the interactions with the plasma continuously slowed down. The distribution function is a superposition of $f_0(\vec{x}, \vec{v})$ for the thermal plasma and the distribution function $f_1(\vec{x}, \vec{v}, t)$ for the ions[56]:

$$(\partial_t + \vec{v}\nabla_{\vec{x}} + \frac{q}{m}(\vec{E} + \vec{v} \times \vec{B})\nabla_{\vec{v}})f_1(\vec{x}, \vec{v}, t) = \frac{\partial f_1}{\partial t}|_{\text{coll}} \tag{5.4}$$

with the Lorentz force $\vec{F} = q(\vec{E} + \vec{v} \times \vec{B})$, where $\vec{E}$ and $\vec{B}$ describe the magnetic and electric field at the position of the charged particles. The dynamics of such a system is well described by the so-called Fokker-Planck collision term[56]:

$$\frac{\partial f_1}{\partial t}|_{\text{coll}} = \gamma \; f_1(\vec{v}, t) + \gamma \; \vec{v} \; \nabla_{\vec{v}} \; f_1(\vec{v}, t) + \frac{T}{\alpha}\nabla_{\vec{v}}^2 \; f_1(\vec{v}, t), \tag{5.5}$$

where γ is the deceleration time of the ions in the background, T the temperature of the plasma and α the coefficient of friction.
The collision term consists of two processes, which generate the dynamics of the system: The ions decelerate due to the first two terms in equation (5.5) in the plasma background. Therefore, the distribution function f_1 is continuously shifted from its initial average velocity v_0 in phase space closer to the average velocity of the plasma. Simultaneously, the distribution function of the ions spreads continuously in phase space, which is described by an additional diffusion term $\frac{T}{\alpha}\nabla_{\vec{v}}^2 \; f_1(\vec{v}, t)$. The Fokker-Planck collision term vanishes for the thermal Maxwell-Boltzmann distribution.
In conclusion, kinetic equations are present in many different fields of physics and are used to describe the dynamics of a many-body system. The collision term is based on the generic processes in the system and needs to be established for the model under consideration.

5.2 The Kinetic Equation in the Keldysh Framework

In the following, we aim to find a quantum Boltzmann equation with a collision term for an interacting Luttinger Liquid in an optical lattice, which describes the dynamics of the system out of equilibrium and helps us to understand the interplay between the interactions and dissipation.
The definition of the Green's function in the Keldysh formalism reads[42,51]:

$$\left\langle \bar{\phi}_\alpha(x)\phi_\beta(x^{'})\right\rangle = \int \mathscr{D}\{\bar{\phi}_q,\phi_q,\bar{\phi}_{cl},\phi_{cl}\}\bar{\phi}_\alpha(x)\phi_\beta(x^{'})e^{iS[\bar{\phi}_{cl},\phi_{cl},\bar{\phi}_q,\phi_q]}, \tag{5.6}$$

where $\alpha,\beta \in \{q,cl\}$ and $x=(\vec{x},t)$.
According to this, the dressed Green's function has a 2×2 structure with zero entry in the $q-q$ sector:

$$G(x,x^{'}) = \begin{pmatrix} G^K(x,x^{'}) & G^R(x,x^{'}) \\ G^A(x,x^{'}) & 0 \end{pmatrix}. \tag{5.7}$$

The dressed Green's function is the propagator of the full theory: $S = S_0 + S_{\text{int}}$. We expand the dressed Green's functions in S_{int}:

$$\left\langle \bar{\phi}^\alpha(x)\phi^\beta(x^{'})\right\rangle = \int \mathscr{D}\{\bar{\phi}^q,\phi^q,\bar{\phi}^{cl},\phi^{cl}\}\bar{\phi}^\alpha(p,t)\phi^\beta(p,t^{'})e^{iS_0[\bar{\phi}^-,\phi^-,\bar{\phi}^+,\phi^+]}\sum_{n=0}^{\infty}\frac{(iS_{\text{int}})^n}{n!}. \tag{5.8}$$

The bare propagator of the theory is the zero order term of (5.8). Furthermore, higher order terms consist of complex correlations averaged with respect to the free theory, which are computed by the use of Wick's theorem.[42,54]
Depending on the specific example, we perform different approximation schemes to simplify the series (5.8) in an appropriate manner. For instance, if the interaction strength is very small, we can restrict the series expansion (5.8) to a finite number of terms.
Next, we define a well known object in the many-body theory, the so-called self-energy Σ, which has all the information on the renormalization of the free theory due to the presence of interactions in the system (for more details[42,54]).
The full Green's function is expressed in terms of the self-energy in the so-called Dyson equation:

$$G^\alpha(x,x^{'}) = \tilde{G}^\alpha(x,x^{'}) + \tilde{G}^\alpha(x,y^{'})\Sigma^\alpha(y^{'},y)G^\alpha(y,x^{'}), \tag{5.9}$$

$$(G^\alpha)^{-1}(x,x^{'}) = (\tilde{G}^\alpha)^{-1}(x,x^{'}) - \Sigma^\alpha(x,x^{'}), \tag{5.10}$$

where α is a label for retarded, advanced or Keldysh.
The inverse Green's function reads as:

$$G^{-1}(x,x^{'}) = \begin{pmatrix} 0 & P^A(x,x^{'}) \\ P^R(x,x^{'}) & P^K(x,x^{'}) \end{pmatrix}. \tag{5.11}$$

The inverse Green's function is due to causality zero in the $q-q$ sector. If the fields on both time contours are equivalent, i.e. $\phi_q = 0$ and $\bar{\phi}_q = 0$, the action needs to vanish. Moreover, we conclude from equation (5.10) and the structure of the inverse Green's function, that the self-energy has the same causality structure:

$$\Sigma(x,x^{'}) = \begin{pmatrix} 0 & \Sigma^A(x,x^{'}) \\ \Sigma^R(x,x^{'}) & \Sigma^K(x,x^{'}) \end{pmatrix}. \tag{5.12}$$

In order to determine the relation between the inverse dressed and the dressed Green's functions, we consider the following equation in the Keldysh formalism:

$$\int_{x^{''}} G^{-1}(x,x^{''}) \circ G(x^{''},x^{'}) = \delta(x-x^{'}). \tag{5.13}$$

An alternative approach is to straightforward invert equation (5.7). In both cases, we find:

$$\begin{aligned} G(x,x^{'}) &= \begin{pmatrix} -(P^R(x,x^{'}))^{-1} \circ P^K(x,x^{'}) \circ (P^A(x,x^{'}))^{-1} & (P^R(x,x^{'}))^{-1} \\ (P^A(x,x^{'}))^{-1} & 0 \end{pmatrix} \\ &= \begin{pmatrix} G^K(x,x^{'}) & G^R(x,x^{'}) \\ G^A(x,x^{'}) & 0 \end{pmatrix}. \end{aligned} \tag{5.14}$$

The convolution operation in equation (5.13) is for two two-point functions $A(x_1,x^{'})$ and $B(x^{'},x_2)$ defined by an integration over an intermediate coordinate $x^{'}$[42,51]:

$$A(x_1,x^{'}) \circ B(x^{'},x_2) = \int_{x^{'}} A(x_1,x^{'}) B(x^{'},x_2). \tag{5.15}$$

The Keldysh Green's function is by definition (5.6) and (5.7) antihermitian:

$$G^K(p,t,t^{'}) = -i \left\langle \bar{\phi}_{cl}(p,t), \phi_{cl}(p,t^{'}) \right\rangle, \tag{5.16}$$

$$[G^K]^{\dagger} = -G^K. \tag{5.17}$$

Retarded and advanced Green's functions are hermitian conjugate:

$$[G^R]^{\dagger} = G^A. \tag{5.18}$$

We use these properties to define the following equation with the hermitian distribution function F:

$$G^K(x,x^{'}) = G^R(x,y) \circ F(y,x^{'}) - F(x,y) \circ G^A(y,x^{'}). \tag{5.19}$$

A system at equilibrium is time and space translation invariant and therefore the two-point functions in equation (5.19) just depend on the relative space and time coordinates. Thus, the convolution integral in Fourier space equals the product of the Fourier transformed two-point functions:

$$\begin{aligned} &A(x_1,x^{'}) \circ B(x^{'},x_2) = \int_{x^{'}} A(x_1 - x^{'})B(x^{'} - x_2) = \int_{x^{''}} A((x_1 - x_2) - x^{''})B(x^{''}) \\ &\Rightarrow \mathcal{FT}[A \circ B](p,\omega) = A(p,\omega)B(p,\omega) \end{aligned} \tag{5.20}$$

For a thermal system equation (5.19) equals the fluctuation-dissipation theorem, which connects the spectral density and the Keldysh Green's function via the occupation:

$$G^K(\omega,p) = \mathcal{B}(\omega,p)F(\omega,p) = \mathcal{B}(\omega,p)(2n_{B/F}+1), \tag{5.21}$$

where $\mathcal{B}(\omega,p) = [G^R(\omega,p) - G^A(\omega,p)]$.
According to (5.10), we split the dressed Green's functions in equation (5.19) into a superposition of self-energy and bare Green's function:

$$(\tilde{G}^R)^{-1}(x,y) \circ F(y,x^{'}) - F(x,y) \circ (\tilde{G}^A)^{-1}(y,x^{'}) = I_{\text{coll}}(x,x^{'}) \tag{5.22}$$

with the following collision integral[51]

$$I_{\text{coll}}(x,x^{'}) = \Sigma^K(x,x^{'}) - [\Sigma^R(x,y) \circ F(y,x^{'}) - F(x,y) \circ \Sigma^A(y,x^{'})]. \tag{5.23}$$

In order to compute the convolution integrals in equations (5.22) and (5.23), we represent the two point functions in relative, respectively absolute coordinates and apply the so-called Wigner approximation to the collision integral. We consider again the two point function $A(x_1,x_2)$. The Wigner transformation is defined as follows:

$$A(x,p) = \int_{x^{'}} e^{-ipx^{'}} A(x = \frac{x_1+x_2}{2}, x^{'} = x_1 - x_2) = WT\{A(x_1,x_2)\}, \tag{5.24}$$

where p is the momentum, which corresponds to the relative coordinate $x^{'}$. In many physical systems such a two point function is a slow function of the absolute coordinate $x = \frac{1}{2}(x_1+x_2)$ compared to fast variations in the relative coordinate $x^{'} = x_1 - x_2$. For instance, at equilibrium the distribution function $F(x_1,x_2)$ is translation invariant in space and time and therefore

depends only on the relative coordinate. If such scale separation into slow and fast variations is appropriate, we can simplify the complex structure of the collision integral.
According to its definition, the Wigner transformation of $C(x_1, x_2) = A(x_1, x_3) \circ B(x_3, x_2)$ is[51]:

$$C(x,p) = A(x,p) e^{\frac{i}{2}(\overleftarrow{\partial}_x \overrightarrow{\partial}_p - \overleftarrow{\partial}_p \overrightarrow{\partial}_x)} B(x,p), \tag{5.25}$$

where $A(x,p) = WT\{A(x_1,x_2)\}$ and $B(x,p) = WT\{B(x_1,x_2)\}$. The arrows on top of the partial derivations point to the functions on which they operate. We expand (5.25) in a series:

$$C(x,p) = A(x,p)(\sum_{n=0}^{\infty} \frac{1}{n!}[\frac{i}{2}(\overleftarrow{\partial}_x \overrightarrow{\partial}_p - \overleftarrow{\partial}_p \overrightarrow{\partial}_x))]^n) B(x,p). \tag{5.26}$$

If the variables can be decomposed into slowly and fastly varying ones, we find[51]

$$\partial_{p/x} A(x,p) \partial_{x/p} B(x,p) \ll A(x,p) B(x,p) \tag{5.27}$$

and (5.26) can be approximated by a first order expansion:

$$\begin{aligned} &C(x,p) \approx \\ &A(x,p)B(x,p) + \frac{i}{2}(\partial_x A(x,p) \partial_p B(x,p) - \partial_p A(x,p) \partial_x B(x,p)). \end{aligned} \tag{5.28}$$

We recognize that for translation invariant two point functions, where $\partial_x A(x,p) = 0$ and $\partial_x B(x,p) = 0$, equation (5.28) reduces to $C(x,p) = A(x,p)B(x,p)$.
We now perform the Wigner transformation of the kinetic equation (5.22) for a translation invariant system in space and conclude with the following result for the left hand side:

$$\begin{aligned} &[(\tilde{G}^R)^{-1}(x,p) - (\tilde{G}^A)^{-1}(x,p)] F(x,p) \\ &+ \frac{i}{2}(\partial_x (\tilde{G}^R)^{-1} \partial_p F(x,p) - \partial_p (\tilde{G}^R)^{-1} \partial_x F(x,p)) \\ &+ \frac{i}{2}(\partial_x (\tilde{G}^A)^{-1} \partial_p F(x,p) - \partial_p (\tilde{G}^A)^{-1} \partial_x F(x,p)) \\ &= 2i\eta F(\tau,\omega,p) + i\partial_\tau F(\tau,\omega,p) \overset{\eta \to 0}{=} i\partial_\tau F(\tau,\omega,p), \end{aligned} \tag{5.29}$$

where we used in the last step $(x,p) = (\tau, \vec{r}, \omega, p)$.
Since the phonon density and the self-energies are translation invariant in space, i.e.

$$F(\tau,\vec{r},\omega,p) = F(\tau,\omega,p), \tag{5.30}$$

$$\Sigma^{K/R/A}(\tau,\vec{r},\omega,p) = \Sigma^{K/R/A}(\tau,\omega,p), \tag{5.31}$$

the partial derivation with respect to the absolute space coordinate vanishes:

$$\partial_{\bar{r}} F = 0, \tag{5.32}$$

$$\partial_{\bar{r}} \Sigma^{K/R/A} = 0. \tag{5.33}$$

Next, the collision integral is represented in Wigner coordinates. We assume, that the system evolves slowly in forward time τ compared to the fast evolution of the relative time t'. Thus, the dynamics of the system is approximately resolved by computing independently for each point in forward time τ the self-energy as a function of frequency. This so-called Wigner approximation is summarized in the following inequality:

$$\frac{\partial_\omega \Sigma^{R/A}(\tau,\omega,p)\partial_\tau F(\tau,\omega,p)}{\Sigma^{R/A}(\tau,\omega,p)F(\tau,\omega,p)} \ll 1 \tag{5.34}$$

As a consequence of Wigner approximation, the collision integral (5.23) is approximated in a zero order expansion:

$$I_{\text{coll}}[F(\tau,\omega,p)] \approx \Sigma^K(\tau,\omega,p) - F(\tau,\omega,p)[\Sigma^R(\tau,\omega,p) - \Sigma^A(\tau,\omega,p)]. \tag{5.35}$$

In summary, the kinetic equation in absolute and relative coordinates is approximated to zero order due to constraint (5.34)[30,31]:

$$\begin{aligned} -i\partial_\tau F(\tau,\omega,p) &= I_{\text{coll}}(\omega,p) \\ &= \Sigma^K(\tau,\omega,p) - F(\tau,\omega,p)[\Sigma^R(\tau,\omega,p) - \Sigma^A(\tau,\omega,p)]. \end{aligned} \tag{5.36}$$

The truncation of the series expansion due to scale separation needs to be justified for the specific physical model under considerations. Thus, in the following section, we first compute the self-energies and the occupation distribution for the interacting Luttinger Liquid in an optical lattice. A posteriori the constraint (5.34) is valid and the Wigner approximation was applicable to approximate the collision integral to zero order.
We briefly continue to analyse the structure of (5.36) in Nambu space representation. In the former section, we saw that the dissipative action is invariant under $p \to -p$ and may contain anomalous terms. Therefore, the Nambu space representation was used to determine a block diagonal form of the dissipative action. We conclude from equation (5.36) and its 2×2 structure in the Nambu space representation, that the time evolution of anomalous and normal occupations is coupled.[30,31]
In order to simplify the complex structure of the kinetic equation in Nambu space representation, we evaluate the self-energy on-shell, i.e. the poles of G^R are assumed to be sharp and close to the real axis. According to this,

the external frequency ω is pinned on the dispersion relation of the system by integrating equation (5.36) over the following spectral function:

$$\mathcal{A}(\omega, p) = \frac{i}{2\pi}[\tilde{G}^R(\omega, p) - \tilde{G}^A(\omega, p)]. \tag{5.37}$$

In conclusion, we determine the occupation at $\epsilon(p) = \nu|p|$:

$$F(\tau, \omega = \epsilon(p), p) = \int_\omega \mathcal{A}(\omega, p) F(\tau, \omega, p). \tag{5.38}$$

The distribution function has then the following 2×2-structure in Nambu space:

$$F(\tau, \omega = \epsilon(p), p) = \begin{pmatrix} 2n(\tau, p) + 1 & 2\bar{m}(\tau, p) \\ 2m(\tau, p) & 2n(\tau, -p) + 1 \end{pmatrix}. \tag{5.39}$$

The anomalous occupations in equation (5.39) are also populated by permanent heating. The finite occupation of the anomalous distribution increases the complexity of the dynamics and we can expect from the kinetic equation (5.36) that both occupations interact at each time step.
In the next section, we determine the self-energies and the kinetic equation for the interacting Luttinger Liquid in an optical lattice without including the anomalous occupations. As we point out later, the anomalous occupations are negligible small and influence the dynamics of the normal occupation only subleading.[30,31] Thus, such a simplifaction is already a qualitative good approach.

Chapter 6

The Self-Energy

The retarded self-energy $\Sigma^R(p,\omega)$ is defined by the Dyson equation (cf. equation (5.9)):

$$G^R(p,\omega) = \frac{1}{\omega - \epsilon(p) + i\eta - \Sigma^R(p)}, \tag{6.1}$$

with dispersion relation $\epsilon(p)$. We assume, that the frequency ω is pinned on the dispersion relation $\Sigma^R(p) = \Sigma^R(p,\omega)|_{\omega=\epsilon(p)}$.
The corresponding spectral density is

$$\mathcal{A}(p,\omega) = -2\mathrm{Im}[G^R(p,\omega)] = \frac{-2\mathrm{Im}[\Sigma^R(p)]}{(\omega - \epsilon(p) - \mathrm{Re}[\Sigma^R(p)])^2 + (\mathrm{Im}[\Sigma^R(p)]^2)}, \tag{6.2}$$

where we absorbed the regularization in the imaginary part of the self-energy. Thus, the spectral density is positive for $\mathrm{Im}[\Sigma^R(p)] < 0$ and a Lorentzian curve, which is centered around $\omega = \epsilon(p) + \mathrm{Re}[\Sigma^R(p)]$ with a width $|\mathrm{Im}[\Sigma^R(p,\omega)]|$ and a height $|\mathrm{Im}[\Sigma^R(p)]|^{-1}$. If the imaginary retarded self-energy vanishes, the spectrum has a sharp delta peak at the renormalized dispersion relation $\omega = \epsilon(p) + \mathrm{Re}[\Sigma^R(p)]$.
In order to analyse the meaning of the imaginary part of the self-energy, we represent the retarded Green's function (6.1) in time and momentum space[42,54]:

$$\begin{aligned} G^R(p,t) =& \frac{1}{2\pi}\int_\omega e^{-i\omega t} G^R(p,\omega) = -i\Theta(t) e^{-i(\epsilon(p)+\mathrm{Re}[\Sigma^R(p)])t} e^{-t|\mathrm{Im}[\Sigma^R(p)]|} \\ =& -i\Theta(t) e^{-i(\epsilon(p)+\mathrm{Re}[\Sigma^R(p)])t} e^{-\frac{t}{\tau_{qp}}}, \end{aligned} \tag{6.3}$$

where the Heaviside function appears due to causality.
In conclusion, the imaginary part of the retarded self-energy is associated with the finite lifetime of the quasiparticles $\tau_{qp} = |\mathrm{Im}[\Sigma^R(p)]|^{-1}$ and the real part of retarded self-energy renormalizes the dispersion relation of the bare theory.
In the following section, we determine the self-energy by a diagrammatic approach based on the vertex structure of the interacting Luttinger Liquid in the Keldysh formalism.

6.1 Diagrammatic Approach for the Collision Integral

In this section, the diagonal elements of the retarded, advanced and Keldysh self-energies are computed. The diagrammatic evaluation is performed using

a so-called self-consistent Born-approximation, which we motivate and explain in the following.
Two specific vertices of the effective cubic action (cf. equation (4.55)) of the interacting Luttinger Liquid are shown in Fig. 6.1. These two vertices

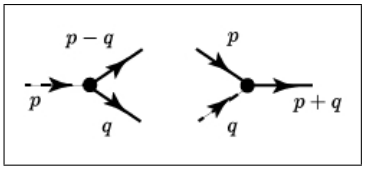

Figure 6.1: *Two resonant vertices of an interacting Luttinger Liquid.*

generate for instance the one loop diagram in Fig. 6.2, which contributes to the correction of the retarded two-point bare propagator. We now perform a scaling analysis of this diagram. The analytic expression of the one loop

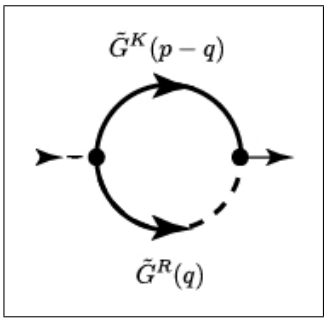

Figure 6.2: *One loop diagram from the vertices in Fig. 6.1 of the interacting Luttinger Liquid.*

diagram in Fig. 6.2 is:

$$\begin{aligned}
&\int_q \int_\nu V^2(q,p,p-q)\tilde{G}^K(p-q,\omega-\nu)\tilde{G}^R(q,\nu) \qquad (6.4)\\
&= \int_q \int_\nu V^2(q,p,p-q)\tilde{\mathcal{B}}(p-q,\omega-\nu)F(p-q,\omega-\nu)\tilde{G}^R(q,\nu)\\
&= \int_q \int_\nu V^2(q,p,p-q)\frac{1}{\omega-\nu-\epsilon(p-q)+i\eta}\frac{1}{\nu-\epsilon(q)+i\eta}F(p-q,\omega-\nu)\\
&= \int_q V^2(q,p,p-q)\frac{-2\pi i}{\omega-\epsilon(q)-\epsilon(p-q)+2i\eta}F(p-q,\omega-\epsilon(q)),
\end{aligned}$$

where $\tilde{\mathcal{B}}(p-q,\omega-\nu) = \tilde{G}^R(p-q,\omega-\nu) - \tilde{G}^A(p-q,\omega-\nu)$.
The quasiparticles are assumed to be well-defined and therefore we can pin

the external frequency ω on the dispersion relation:

$$\int_q \int_\omega V^2(q,p,p-q) \frac{[\tilde{G}^R(\omega,p) - \tilde{G}^A(\omega,p)]}{\omega - \epsilon(q) - \epsilon(p-q) + 2i\eta} F(p-q, \omega - \epsilon(q)) \tag{6.5}$$
$$= \int_q \frac{2\pi}{i} V^2(q,p,p-q) \frac{1}{\epsilon(p) - \epsilon(q) - \epsilon(p-q) + 2i\eta} [2n_B(\epsilon(p) - \epsilon(q)) + 1].$$

The resonance condition requires $\epsilon(p) = \epsilon(q) + \epsilon(p-q)$ and thus expression (6.5) diverges.
In conclusion, the whole retarded self-energy is divergent for a one loop approximation with the bare Green's function.[29] We miss relevant contributions from the full theory and therefore further analysis needs a resummation.
In the following, we select the relevant diagrams of the full theory in two steps: First, the bare propagators in the one loop order diagrams are substituted by the dressed Green's function. We determine the scaling behaviour of such diagrams and discuss the physical meaning of this approach. Second, we compute the scaling behaviour of a higher order loop diagrams, e.g. a second order loop diagram, which is not included in the self-consistent Born approximation, however in the vertex correction, and determine if and how it significantly contributes to the self-energy.

6.1.1 The Self-Consistent Equation for the Self-Energy

In order to lift the divergence of the self-energy for a bare one loop analysis, we replace the bare by the dressed Green's function:

$$G^{R/A}(\omega,p) = \frac{1}{\omega - \epsilon(p) \pm i\sigma^{R/A}(p)}, \tag{6.6}$$

where we assumed, that the frequency of the self-energy is due to the sharply peaked lifetime of the quasiparticles pinned on the dispersion relation, i.e. $\epsilon(p) > \sigma^R(p)$ for low momenta. This is indicated by the following notation:

$$\sigma^{R/A}(p) = \int_\omega \frac{i}{2\pi} [\tilde{G}^R(p,\omega) - \tilde{G}^A(p,\omega)] \sigma^{R/A}(p,\omega). \tag{6.7}$$

Furthermore, the self-energy is purely imaginary and thus $\sigma^R(p) = \sigma^A(p)$, since retarded and advanced self-energy are hermitian conjugate.The self-energy is due to this approach computed in a self-consistent approximation.[29,30] This approximation scheme is visualized in Fig. 6.3, which shows that we actually sum up an infinite series of diagrams, which are generated from itteratively adding up one loop diagrams. The analytic expression for the one

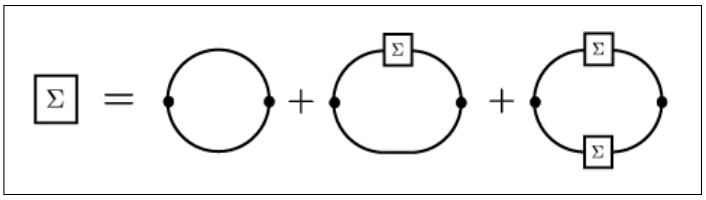

Figure 6.3: *Self-consistent approach*

loop diagram in Fig. 6.2 with the dressed Green's function reads:

$$\begin{aligned} &\int_q \int_\nu V^2(q,p,p-q) G^K(p-q,\omega-\nu) G^R(q,\nu) \qquad (6.8)\\ &= \int_q \int_\nu V^2(q,p,p-q) \mathcal{B}(p-q,\omega-\nu) F(p-q,\omega-\nu) G^R(q,\nu)\\ &= \int_q V^2(q,p,p-q) \frac{-2\pi i}{\omega-\epsilon(q)-\epsilon(p-q)+i\sigma^R(p-q)+i\sigma^R(q)} F(p-q), \end{aligned}$$

where $\mathcal{B}(p-q,\omega-\nu) = G^R(p-q,\omega-\nu) - G^A(p-q,\omega-\nu)$.
After pinning the external frequency on the dispersion relation like in the last section (cf. equation (6.5)) and considering the resonance condition $\epsilon(p) = \epsilon(p-q) + \epsilon(q)$, we approximate equation (6.8):

$$\int_{0<q<p} \frac{2\pi}{i} V^2(q,p,p-q) \frac{1}{\sigma^R(p-q)+\sigma^R(q)} [2n_B(\epsilon(p)-\epsilon(q))+1]. \qquad (6.9)$$

According to equation (6.9), the diagram converges due to the finite lifetime of the quasiparticles and can be computed self-consistently.
In order to analyse the scaling behaviour of the retarded self-energy from equation (6.9), we use for the retarded self-energy a power function: $\sigma^R(k) \approx \alpha k^\gamma$. Thus, equation (6.9) further simplifies to:

$$\begin{aligned} \alpha p^\gamma &\approx \frac{v_0^2 2\pi}{\alpha u} \int_{0<q<p} [pq(p-q) \frac{1}{q^\gamma + (p-q)^\gamma}] (\frac{T}{p-q}) \qquad (6.10)\\ &= \frac{v_0^2 2\pi}{\alpha u} p^{-\gamma+3} \int_{0<q<p} [\frac{q}{p}(1-\frac{q}{p}) \frac{1}{(\frac{q}{p})^\gamma + (1-\frac{q}{p})^\gamma}] (\frac{T}{1-\frac{q}{p}}) = p^{-\gamma+3} I_1, \end{aligned}$$

where we assumed $n_B(\epsilon(p-q)) \approx \frac{T}{u|p-q|}$ and defined $I_1 = \frac{2\pi T v_0^2}{\alpha u} \int_{0<x<1} [\frac{x}{x^\gamma + (1-x)^\gamma}]$ with $x = \frac{q}{p}$.
In conclusion, the self-energy scales with an exponent $\gamma = \frac{3}{2}$.[33–35] It is analysed in a one loop approximation based on the dressed Green's function and we showed that the self-energy can be computed in a self-consistent equation.

6.1.2 Two Loop Diagram

Next, we consider a specific two loop diagram (cf. Fig. 6.4) and analyse its scaling behaviour. As a result, we determine, that the scaling exponent of this two loop diagram at finite temperature is $\gamma = \frac{3}{2}$.

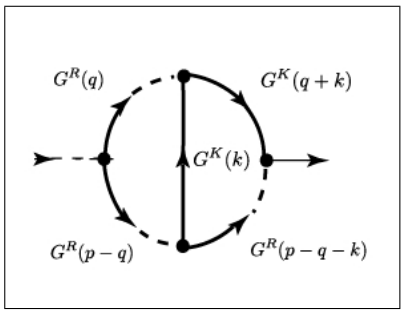

Figure 6.4: *Two loop diagram*

The following notation is used during the computation of the two loop diagram: $\mathbf{p} = (p, \omega)$,$\mathbf{k} = (k, \omega^{'})$ and $\mathbf{q} = (q, \omega^{''})$. We conclude from Fig. 6.4 the following analytic expression:

$$\begin{aligned}
&\int_q \int_k \int_{\omega'} \int_{\omega''} V(q,p,p-q)V(q,k,q+k)V(p-q,k,p-q-k) \qquad (6.11)\\
&V(q+k,p-q-k,p)\; G^R(\mathbf{q})G^K(\mathbf{k})G^K(\mathbf{q}+\mathbf{k})G^R(\mathbf{p}-\mathbf{q})G^R(\mathbf{p}-\mathbf{q}-\mathbf{k})\\
\approx &\int_{0<q<p} \int_{0<k<p-q} V(q,p,p-q)V(q,k,q+k)V(p-q,k,p-q-k)V(q+k,p-q-k,p)\\
&[\frac{-2i\pi}{\sigma^R(q)+\sigma^R(p-q)}\;\frac{1}{\sigma^R(p-q-k)+\sigma^R(q+k)}\;\frac{1}{\sigma^R(k)+\sigma^R(q+k)+\sigma^R(p-q)}\\
&[2n_B(\epsilon(k))+1][2n_B(\epsilon(q+k))+1]\\
&+\frac{2i\pi}{\sigma^R(q)+\sigma^R(p-q)}\;\frac{1}{\sigma^R(p-q-k)+\sigma^R(q)+\sigma^R(k)}\;\frac{1}{\sigma^R(k)+\sigma^R(q+k)+\sigma^R(q)}\\
&[2n_B(\epsilon(k))+1][2n_B(\epsilon(q+k))+1]\\
&-\frac{2i\pi}{\sigma^R(q)+\sigma^R(p-q)}\;\frac{1}{\sigma^R(p-q-k)+\sigma^R(q)+\sigma^R(k)}\;\frac{1}{\sigma^R(q+k)+\sigma^R(p-q-k)}\\
&[2n_B(\epsilon(k-p))+1][2n_B(\epsilon(q+k-p))+1]],
\end{aligned}$$

where we used during the calculations the resonance conditions and that the retarded-self-energy is smaller than the dispersion relation for low momenta: $\epsilon(k) > \sigma^R(k)$.
In order to determine the scaling behaviour of this self-energy contribution, we use the scaling function of the former section and conclude from equation

(6.11):

$$\alpha p^{\gamma} \approx p^{-3\gamma+6} I_2, \tag{6.12}$$

where we assumed $n_B(\epsilon(k)) \approx \frac{T}{u|k|}$ and defined

$$\begin{aligned} I_2 = \frac{2\pi T^2 v_0^4}{\alpha^3 u^2} \int_{0<x<1} \int_{0<y<1-x} & [(1-x)xy(x+y)(1-(x+y))] \\ & \Big[\frac{1}{x^{\gamma}+(1-x)^{\gamma}} \frac{1}{y^{\gamma}+(x+y)^{\gamma}+(1-x)^{\gamma}} \frac{1}{(x+y)^{\gamma}+(1-(x+y))^{\gamma}} \frac{1}{x} \frac{1}{x+y} \\ & - \frac{1}{x^{\gamma}+(1-x)^{\gamma}} \frac{1}{y^{\gamma}+(x+y)^{\gamma}+x^{\gamma}} \frac{1}{(1-(x+y))^{\gamma}+x^{\gamma}+y^{\gamma}} \frac{1}{x} \frac{1}{x+y} \\ & + \frac{1}{x^{\gamma}+(1-x)^{\gamma}} \frac{1}{y^{\gamma}+(1-(x+y))^{\gamma}+x^{\gamma}} \frac{1}{(x+y)^{\gamma}+(1-(x+y))^{\gamma}} \frac{1}{x-1} \frac{1}{x+y-1}\Big]. \end{aligned}$$

Thus, the two loop diagram has a scaling exponent $\gamma = \frac{3}{2}$, which is the same as the result for the one loop diagram in a self-consistent Born-approximation and thus does not significantly modify the self-energy. The same is true for the prefactor of the self-energy.[30,31]
This analysis can be continued to diagrams with n loops. For instance, we consider a constant three-point interaction and use only classical fields in order to simplify the following analysis:

$$S_{\text{int}} = \lambda(\phi^2\bar{\phi} + \bar{\phi}^2\phi). \tag{6.13}$$

The n loop correction of the two-point propagator in a perturbative approach is generated by the $2n-$ th order expansion:

$$\Sigma^{(n-o)} \approx \frac{\lambda^{2n}}{4!} \left\langle S_{\text{int}}^{2n} \right\rangle_0, \tag{6.14}$$

where $\Sigma^{(n-o)}$ stands for the part of the self-energy with n loop diagrams.
We conclude, that diagrams with n loops consist of $2n$ vertices and $3n-1$ propagators. In order to analyse the scaling behaviour of a diagram with n loops, we would first derive the analytic expression including n frequency and n momentum integrals. After performing the integrals over the frequencies, a term of n density distributions appear in the self-consistent equation for the self-energy. Then, the self-energy is represented by a power function with exponent γ. Finally, the external momentum is pulled out of the integral and we determine an equation like (6.10) or (6.12). Due to this protocol, the following scaling behaviour is determined for a n loop diagram with the

corresponding exponent γ_n of the self-energy:

$$\underbrace{2n \cdot \frac{3}{2}}_{\text{Vertices}} + \underbrace{n}_{\text{Momentum Integrals}} - \underbrace{n}_{\text{Density Distribution}} - \underbrace{\gamma \cdot (2n-1)}_{\text{No. of propagators minus no. of frequency integrals}}$$
$$\rightarrow 3n - \gamma \cdot (2n-1) = \gamma_n. \tag{6.15}$$

If the diagrams with less than n loops scale with an exponent $\gamma = \frac{3}{2}$, we determine that the self-energy including the n loop diagram scales due to equation (6.15) with $\gamma_n = \frac{3}{2}$. Thus, a self-energy including n loops scales in momentum space with an exponent $\gamma_n = \frac{3}{2}$. The scaling behaviour of higher order loop diagrams is equivalent to the one loop evaluation in a self-consistent Born-approximation and even the prefactor of the self-energy is not significantly modified due to higher order loop diagrams.[30,31]
According to this, the further diagrammatic analysis for the interacting Luttinger Liquid is performed in a self-consistent Born approximation.[30,31]

6.1.3 The Diagrammatic Dictionary

We now again distinguish between classical and quantum fields. The effective interaction of an interacting Luttinger Liquid is due to chapter 2:

$$\begin{aligned} &S_C[\bar{\phi}_{cl}, \phi_{cl}, \bar{\phi}_q, \phi_q] \\ &= \frac{1}{2\pi} \int_t \int_{q,p} V(q,p,p-q) \\ &\quad [\bar{\phi}_q(q,t)\bar{\phi}_q(p-q,t)\phi_q(p,t) + \bar{\phi}_q(q,t)\bar{\phi}_{cl}(p-q,t)\phi_{cl}(p,t) \\ &\quad + \bar{\phi}_{cl}(q,t)\bar{\phi}_{cl}(p-q,t)\phi_q(p,t) + \bar{\phi}_{cl}(q,t)\bar{\phi}_q(p-q,t)\phi_{cl}(p,t) + h.c.], \end{aligned} \tag{6.16}$$

where

$$V(q,p,p-q) = \sqrt{|qp(p-q)|}\sqrt{\frac{\kappa_c^2 \pi}{2K}}\left(\frac{1}{4}\left(\frac{qp}{|qp|} + \frac{q(p-q)}{|q(p-q)|} + \frac{p(p-q)}{|p(p-q)|}\right) + \frac{3\alpha K^2}{4\kappa_c}\right).$$

Resonance further requires that $\epsilon(p) = \epsilon(p-q) + \epsilon(q)$ and thus the vertex simplifies:

$$V(q,p,p-q) = \sqrt{|qp(p-q)|}\sqrt{\frac{\kappa_c^2 \pi}{2K}}\left(\frac{3}{4} + \frac{3\alpha K^2}{4\kappa_c}\right) = \sqrt{|qp(p-q)|}v_0. \tag{6.17}$$

The following diagrammatic dictionary is used during the computation of the self-energies:

- The momentum and corresponding frequency are labeled during the computation by one letter, e.g. $(p, \omega) \to \mathbf{p}$ and $(q, \nu) \to \mathbf{q}$.
- Dressed inverse Keldysh Green's function:

$$[(G)^{-1}(k,\omega)]^K = -\Sigma^K(k,\omega) \approx i\sigma^K(k). \tag{6.18}$$

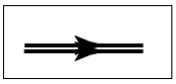

Figure 6.5: *Dressed Keldysh Green's function*

- Dressed inverse retarded Green's function:

$$\begin{aligned}(G^R)^{-1}(k,\omega) &= (\tilde{G}^R)^{-1}(k,\omega) - \Sigma^R(k,\omega) \\ &\approx \omega - \epsilon(k) + i\sigma^R(k).\end{aligned} \tag{6.19}$$

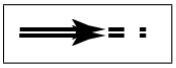

Figure 6.6: *Dressed retarded Green's function*

- Dressed inverse advanced Green's function:

$$\begin{aligned}(G^A)^{-1}(k,\omega) &= (\tilde{G}^A)^{-1}(k,\omega) - \Sigma^A(k,\omega) \\ &\approx \omega - \epsilon(k) - i\sigma^A(k).\end{aligned} \tag{6.20}$$

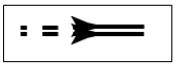

Figure 6.7: *Dressed advanced Green's function*

Since the lifetime of the quasiparticles is finite due to the resonant scattering processes, well-defined and sharply centered at $\omega = \epsilon(k)$, the frequencies of the self-energies are in the so-called on-shell approximation pinned on the dispersion relation (cf. chapter 5):

$$\sigma^{R/K/A}(k) = \int_\omega \frac{i}{2\pi}[\tilde{G}^R(k,\omega) - \tilde{G}^A(k,\omega)]\sigma^{R/K/A}(k,\omega). \tag{6.21}$$

During the computations we use the notation $|_{\omega=\epsilon(k)}$ in order to indicate the on-shell approximation defined due to equation (6.29).
Retarded and advanced Green's functions are hermitian conjugate, so that due to equations $(6.19 - 6.20)$ $\sigma^R(k)$ and $\sigma^A(k)$ are equivalent. Be aware that the Keldysh Green's function is by definiton (6.18) antihermitian, i.e. $(\Sigma^K)^\dagger = -\Sigma^K$.

6.2 The Keldysh Self-Energy

The full Keldysh self-energy is derived from the effective cubic interaction, which consists only of the resonance scattering terms (cf. equation (4.55)). Thus, we compute all one loop diagrams with two outgoing quantum legs, which are generated by the scattering vertices (6.16).
In summary, six one loop diagrams (cf. Fig. 6.8) contribute to the Keldysh self-energy. Subsequently, the diagrams are expressed in a corresponding analytic equation from general diagrammatic rules[42,54]:

$$\begin{aligned}
&-\sigma^K(p) \qquad\qquad (6.22)\\
&\quad = \frac{1}{4\pi^2}\int_{\mathbf{q}} (G^K(\mathbf{p}-\mathbf{q})G^K(\mathbf{q})V^2(p,q,p-q) + 2G^K(\mathbf{p}+\mathbf{q})G^K(\mathbf{q})V^2(p,q,p+q)\\
&\quad + G^R(\mathbf{p}-\mathbf{q})G^R(\mathbf{q})V^2(p,q,p-q) + G^A(\mathbf{p}-\mathbf{q})G^A(\mathbf{q})V^2(p,q,p-q)\\
&\quad + 2G^A(\mathbf{p}+\mathbf{q})G^R(\mathbf{q})V^2(p,q,p+q) + 2G^R(\mathbf{p}+\mathbf{q})G^A(\mathbf{q})V^2(p,q,p+q))|_{\omega=\epsilon(p)}.
\end{aligned}$$

Some of the diagrams are due to combinatorial factors counted twice: We

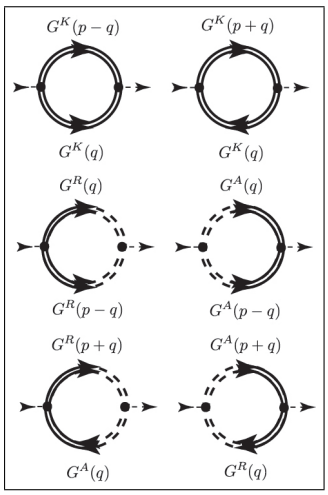

Figure 6.8: *Diagrams for the Keldysh self-energy*

have in the last two diagrams the freedom to rotate the legs at one of the

vertices by holding at the same time the other vertex fixed.
Since retarded and advanced Green's function $G^{R/A}(\mathbf{q})$ have their poles on the lower and upper half of the complex plane, the integral $\int_q G^R(\mathbf{q})G^A(-\mathbf{q})$ vanishes by closing the contour in the upper complex plane.
Thus, the Keldysh self-energy in equation (6.22) reads:

$$\begin{aligned}-\sigma^K(p) \\ =&\frac{1}{4\pi^2}\int_{\mathbf{q}}(G^K(\mathbf{p}-\mathbf{q})G^K(\mathbf{q})V^2(p,q,p-q)+2G^K(\mathbf{p}+\mathbf{q})G^K(\mathbf{q})V^2(p,q,p+q)\\ &+[G^R(\mathbf{p}-\mathbf{q})-G^A(\mathbf{p}-\mathbf{q})][G^R(\mathbf{q})-G^A(\mathbf{q})]V^2(p,q,p-q)\\ &-2[G^R(\mathbf{p}+\mathbf{q})-G^A(\mathbf{p}+\mathbf{q})][G^R(\mathbf{q})-G^A(\mathbf{q})]V^2(p,q,p+q))|_{\omega=\epsilon(p)}.\end{aligned} \tag{6.23}$$

In order to express the Keldysh self-energy as a function of phonon density $F(\mathbf{k})$ and spectral density, we use the relation (cf. equation (5.19))

$$G^K(\mathbf{k}) = [G^R(\mathbf{k}) - G^A(\mathbf{k})]F(\mathbf{k}). \tag{6.24}$$

According to this, we have the following analytic equation for the Keldysh self-energy:

$$\begin{aligned}-\sigma^K(p) \\ =&\frac{1}{4\pi^2}\int_{\mathbf{q}}([F(\mathbf{p}-\mathbf{q})F(\mathbf{q})+1]\mathcal{B}(\mathbf{p}-\mathbf{q})\mathcal{B}(\mathbf{q})|qp(p-q)|v_0^2\\ &+2[F(\mathbf{p}+\mathbf{q})F(\mathbf{q})-1]\mathcal{B}(\mathbf{p}+\mathbf{q})\mathcal{B}(\mathbf{q})|qp(p+q)|v_0^2)|_{\omega=\epsilon(p)},\end{aligned} \tag{6.25}$$

where $\mathcal{B}(\mathbf{k}) = G^R(\mathbf{k}) - G^A(\mathbf{k}) = \frac{-2i\sigma^R(k)}{(\omega-\epsilon(k))^2+(\sigma^R(k))^2}$.
In the next section, the same approach is used to compute retarded and advanced self-energy.

6.3 Advanced and Retarded Self-Energy

The advanced Green's function $G^A(\mathbf{p}) = i\langle\bar{\phi}_q(\mathbf{p})\phi_{cl}(\mathbf{p})\rangle$ consists of the bare propagator and the advanced self-energy $\Sigma^A(\mathbf{p})$. The self-energy is computed from the three diagrams in Fig. 6.9.
According to this, we derive an analytic expression for the advanced self-

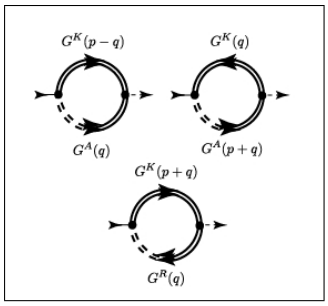

Figure 6.9: *Diagrams for the advanced self-energy*

energy:

$$\begin{aligned}
&\sigma^A(p) \qquad (6.26)\\
&=\frac{1}{4\pi^2}\int_{\mathbf{q}}(2G^A(\mathbf{q})G^K(\mathbf{p}-\mathbf{q})V^2(p,q,p-q)+2G^A(\mathbf{p}+\mathbf{q})G^K(\mathbf{q})V^2(p,q,p+q)\\
&+2G^K(\mathbf{p}+\mathbf{q})G^R(\mathbf{q})V^2(p,q,p+q))|_{\omega=\epsilon(p)}\\
&=\frac{1}{4\pi^2}\int_{\mathbf{q}}(G^A(\mathbf{q})G^K(\mathbf{p}-\mathbf{q})|qp(p-q)|v_0^2+G^A(\mathbf{p}-\mathbf{q})G^K(\mathbf{q})|qp(p-q)|v_0^2\\
&+2G^A(\mathbf{p}+\mathbf{q})G^K(\mathbf{q})|qp(p+q)|v_0^2+2G^K(\mathbf{p}+\mathbf{q})G^R(\mathbf{q})|qp(p+q)|v_0^2)|_{\omega=\epsilon(p)}.
\end{aligned}$$

Since $[G^R]^\dagger = G^A$, the retarded self-energy is the hermitian conjugate of the advanced self-energy. On the other hand, the retarded self-energy is also determined from the corresponding three diagrams in Fig. 6.10.

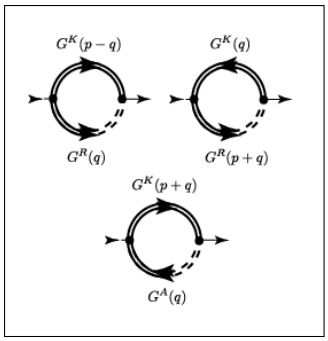

Figure 6.10: *Diagrams for the retarded self-energy*

Both approaches result in the same analytic equation for the retarded self-

energy:

$$
\begin{aligned}
&-\sigma^R(p) \qquad (6.27)\\
&=\frac{1}{4\pi^2}\int_{\mathbf{q}}(2G^R(\mathbf{q})G^K(\mathbf{p}-\mathbf{q})V^2(p,q,p-q)+2G^R(\mathbf{p}+\mathbf{q})G^K(\mathbf{q})V^2(p,q,p+q)\\
&+2G^K(\mathbf{p}+\mathbf{q})G^A(\mathbf{q})V^2(p,q,p+q))|_{\omega=\epsilon(p)}\\
&=\frac{1}{4\pi^2}\int_{\mathbf{q}}(G^R(\mathbf{q})G^K(\mathbf{p}-\mathbf{q})|qp(p-q)|v_0^2+G^R(\mathbf{p}-\mathbf{q})G^K(\mathbf{q})|qp(p-q)|v_0^2\\
&+2G^R(\mathbf{p}+\mathbf{q})G^K(\mathbf{q})|qp(p+q)|v_0^2+2G^K(\mathbf{p}+\mathbf{q})G^A(\mathbf{q})|qp(p+q)|v_0^2)|_{\omega=\epsilon(p)}.
\end{aligned}
$$

We compute the difference of retarded and advanced self-energy and use again relation (6.24) to represent it as a function of the phonon density and $\mathcal{B}$:

$$
\begin{aligned}
&(\Sigma^R(p)-\Sigma^A(p)) \qquad (6.28)\\
&\quad=\frac{i}{4\pi^2}\int_{\mathbf{q}}([G^R(\mathbf{q})-G^A(\mathbf{q})]G^K(\mathbf{p}-\mathbf{q})|qp(p-q)|v_0^2\\
&\quad+[G^R(\mathbf{p}-\mathbf{q})-G^A(\mathbf{p}-\mathbf{q})]G^K(\mathbf{q})|qp(p-q)|v_0^2\\
&\quad+2[G^R(\mathbf{p}+\mathbf{q})-G^A(\mathbf{p}+\mathbf{q})]G^K(\mathbf{q})|qp(p+q)|v_0^2\\
&\quad+2[G^A(\mathbf{q})-G^R(\mathbf{q})]G^K(\mathbf{p}+\mathbf{q})|qp(p+q)|v_0^2)|_{\omega=\epsilon(p)}\\
&\quad=\frac{i}{4\pi^2}\int_{\mathbf{q}}(\mathcal{B}(\mathbf{q})\mathcal{B}(\mathbf{p}-\mathbf{q})|qp(p-q)|v_0^2[F(\mathbf{p}-\mathbf{q})+F(\mathbf{q})]\\
&\quad+2\mathcal{B}(\mathbf{q})\mathcal{B}(\mathbf{p}+\mathbf{q})|qp(p+q)|v_0^2[F(\mathbf{q})-F(\mathbf{p}+\mathbf{q})])|_{\omega=\epsilon(p)}.
\end{aligned}
$$

After computing the self-energies in a diagrammatic approach, we continue to derive the collision integral of the kinetic equation for an interacting Luttinger Liquid in an optical lattice.

6.4 Kinetic Equation for an Interacting Luttinger Liquid

The time evolution of the phonon density is described by the kinetic equation with an appopriate collision integral based on the self-energies of the interacting Luttinger Liquid.
The collision term of the one dimensional system of interacting bosons in the low-energy regime reads due to equation (5.36) and the results of the last

section:

$$\begin{aligned} I_{\text{coll}} =&\Sigma^K(\mathbf{p}) - F(\mathbf{p})[\Sigma^R(\mathbf{p}) - \Sigma^A(\mathbf{p})] \\ =&h(p) \\ &+\frac{1}{4\pi^2}\int_{\mathbf{q}}([F(\mathbf{p}-\mathbf{q})F(\mathbf{q}) + 1 - F(\mathbf{p})(F(\mathbf{p}-\mathbf{q}) + F(\mathbf{q}))]\mathcal{B}(\mathbf{p}-\mathbf{q})\mathcal{B}(\mathbf{q})V^2(p,q,p-q) \\ &+2[F(\mathbf{p}+\mathbf{q})F(\mathbf{q}) - 1 - F(\mathbf{p})(F(\mathbf{q}) - F(\mathbf{p}+\mathbf{q}))]\mathcal{B}(\mathbf{p}+\mathbf{q})\mathcal{B}(\mathbf{q})V^2(p,q,p+q))|_{\omega=\epsilon(p)}, \end{aligned} \tag{6.29}$$

where we now also included the permanent heating $h(p)$.
We perform the frequency integral on the right hand side of equation (6.29) and use thereby the residue theorem. The term $\mathcal{B}(\mathbf{p}\pm\mathbf{q})\mathcal{B}(\mathbf{q})$ (cf. e.g. (6.25)) has in total 4 poles, two on each side of the complex plane (cf. Fig. 6.11 and Fig. 6.12). We choose to close the contour on the upper complex plane, so that the singularities are enclosed counter-clockwise.

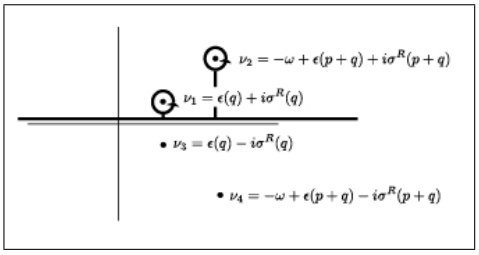

Figure 6.11: *Pole structure of* $\mathcal{B}(\mathbf{p}+\mathbf{q})\mathcal{B}(\mathbf{q})$.

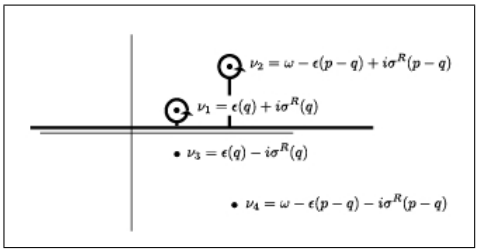

Figure 6.12: *Pole structure of* $\mathcal{B}(\mathbf{p}-\mathbf{q})\mathcal{B}(\mathbf{q})$.

Additionally, the external frequency is pinned on the singularity $\omega = \epsilon(p) \pm i\sigma^R(p)|_{\omega=\epsilon(p)}$ of $\mathcal{B}(\mathbf{p})$ as follows:

$$\int_\omega \frac{i}{2\pi}\mathcal{B}(\mathbf{p})F(\mathbf{p}) = F(\mathbf{p})|_{\omega=\epsilon(p)+i\sigma^R(p)} = 2n_p + 1. \tag{6.30}$$

In conclusion, the non-linear differential kinetic equation for the phonon density is[30,31]:

$$\begin{aligned}\partial_\tau n_p(\tau) &\\ =&h(p)\\ &+\frac{1}{2\pi}\int_{0<q<p}\left(\frac{qp(p-q)v_0^2}{\sigma^R(p)+\sigma^R(q)+\sigma^R(p-q)}[n_{p-q}n_q-n_p(n_{p-q}+n_q+1)]\right)\\ &+\frac{1}{2\pi}\int_{0<q}\left(\frac{2qp(p+q)v_0^2}{\sigma^R(p)+\sigma^R(q)+\sigma^R(p+q)}[n_{p+q}+n_{p+q}n_q+n_{p+q}n_p-n_qn_p]\right),\end{aligned} \tag{6.31}$$

where we use the notation $n(k) = n_k$.
The kinetic equation (6.31) consists of the heating term with rate $h(p)$, which was analysed in section three, and two additional terms based on the interactions. The decrease of the phonon distribution n_p due to annihilation of a phonon is described in the second row of equation (6.31). In this case, the integral over the internal momentum q is limited by p, since the created phonons need by momentum and energy conservation to propagate in the same direction with a lower momentum than the annihilated phonon. In a second process, two photons merge into a single one (cf. third row of equation (6.31)).
A quasiparticle with momentum k approximately annihilates with a rate $\tau_{qp}^{-1}(k) = \sigma^R(k)$ and thus propagates through the system for an average time $\tau_{qp}(k)$. Considering that the lifetimes of the phonons with different momenta are independent, the total rate for the two resonant processes is:

$$\sigma_1^R(q,p) = \sigma^R(q) + \sigma^R(p-q) + \sigma^R(p), \tag{6.32}$$

$$\sigma_2^R(q,p) = \sigma^R(q) + \sigma^R(p+q) + \sigma^R(p). \tag{6.33}$$

The total lifetimes of the processes 1 and 2 appear in the kinetic equation (6.39):

$$\tau_{1/2}(q,p) = \frac{1}{\sigma_{1/2}^R(q,p)} = \frac{1}{\sigma^R(q)+\sigma^R(p\mp q)+\sigma^R(p)}. \tag{6.34}$$

In conclusion, we have determined the kinetic equation for the normal occupation and briefly summarized its structure. The integrals in equation (6.31) converge due to the finite quasiparticle lifetime $\tau_{qp}(k)$ (cf. section on self-consistent Born approximation).
Next, we focus on the quasiparticle lifetimes and continue to discuss the solution of the kinetic equation.

Chapter 7

The Quasiparticle Lifetime

The finite lifetime $\tau_{qp}(p) \propto \sigma^R(p)^{-1}$ of the excitations is generated by the interactions and lifts the divergence of the bare one loop diagrams. We now determine a self-consistent equation for the retarded self-energy, which depends on the occupation distribution.[29–31] Furthermore, a scaling analysis of the phonon density and the retarded/advanced self-energy is performed.

7.1 The Retarded Self-Energy

In order to analyse the quasiparticle lifetime, we start to compute the retarded self-energy based on the diagrammatic approach of the last section. This equation is then further simplified and studied in more detail.
We use for the computation of the retarded self-energy the diagrammatic approach (cf. equation (6.27)) of the last section:

$$\begin{aligned} -i\sigma^R(p) & \\ =&\frac{1}{4\pi^2}\int_{\mathbf{q}}(2G^R(\mathbf{q})G^K(\mathbf{p}-\mathbf{q})v_0^2|qp(p-q)| + 2G^R(\mathbf{p}+\mathbf{q})G^K(\mathbf{q})v_0^2|qp(p+q)| \\ &+2G^A(\mathbf{q})G^K(\mathbf{p}+\mathbf{q})v_0^2|qp(p+q)|)_{\omega=\epsilon(p)} \end{aligned} \tag{7.1}$$

The Keldysh Green's function is due to causality and the Dyson equation as follows:

$$G^K(\mathbf{k}) = -(P^R(\mathbf{k}))^{-1}P^K(\mathbf{k})(P^A(\mathbf{k}))^{-1} = -iG^R(\mathbf{k})\sigma^K(\mathbf{k})G^A(\mathbf{k}) \tag{7.2}$$

According to this, the retarded self-energy in equation (7.1) reads:

$$\begin{aligned} \sigma^R(p) & \\ =&\frac{v_0^2}{2\pi^2}\int_{\mathbf{q}}(G^R(\mathbf{q})G^R(\mathbf{p}-\mathbf{q})\sigma^K(\mathbf{p}-\mathbf{q})G^A(\mathbf{p}-\mathbf{q})|qp(p-q)| \\ &+G^R(\mathbf{p}+\mathbf{q})G^R(\mathbf{q})\sigma^K(\mathbf{q})G^A(\mathbf{q})|qp(p+q)| \\ &+G^A(\mathbf{q})G^R(\mathbf{p}+\mathbf{q})\sigma^K(\mathbf{p}+\mathbf{q})G^A(\mathbf{p}+\mathbf{q})|qp(p+q)|)_{\omega=\epsilon(p)}. \end{aligned} \tag{7.3}$$

Furthermore, we substitute in the last term the internal momentum $\mathbf{q}$ by $\mathbf{q}-\mathbf{p}$ and and in the first term $\mathbf{p}-\mathbf{q}$ by $\mathbf{q}$ in order to determine a compact equation for the retarded self-energy:

$$\begin{aligned} \sigma^R(p) & \\ =&\frac{v_0^2}{2\pi^2}\int_{\mathbf{q}}(G^R(\mathbf{p}-\mathbf{q})G^R(\mathbf{q})\sigma^K(\mathbf{q})G^A(\mathbf{q})|qp(p-q)| \end{aligned} \tag{7.4}$$

$$+G^R(\mathbf{p}+\mathbf{q})G^R(\mathbf{q})\sigma^K(\mathbf{q})G^A(\mathbf{q})|qp(p+q)|$$
$$+G^A(\mathbf{q}-\mathbf{p})G^R(\mathbf{q})\sigma^K(\mathbf{q})G^A(\mathbf{q})|qp(q-p)|)_{\omega=\epsilon(p)}$$

The pole structure of the integral (7.4) consists for each term of three singularities. We use the residue theorem in order to perform the integral over the internal frequency:

$$\begin{aligned}\sigma^R(p) &\qquad (7.5)\\ =&\frac{v_0^2}{2\pi}\int_q \frac{\sigma^K(q)}{\sigma^R(q)}\\ &[\frac{1}{\omega-\epsilon(q)-\epsilon(p-q)+i(\sigma^R(q)+\sigma^R(p-q))}|qp(p-q)|\\ &+\frac{1}{\omega+\epsilon(q)-\epsilon(p+q)+i(\sigma^R(p+q)+\sigma^R(q))}|qp(p+q)|\\ &+\frac{1}{\epsilon(q)-\omega-\epsilon(q-p)-i(\sigma^R(q-p)+\sigma^R(q))}|qp(q-p)|]|_{\omega=\epsilon(p)}\end{aligned}$$

The dynamics of the system is due to the fourth chapter dominantly generated by the resonant scattering processes with the conditions:

$$\epsilon(p)=\epsilon(q)+\epsilon(p-q), \qquad (7.6)$$
$$\epsilon(p)=\epsilon(p+q)-\epsilon(q), \qquad (7.7)$$
$$\epsilon(p)=\epsilon(q)-\epsilon(q-p). \qquad (7.8)$$

According to this, the dominant contributions to the computation of the integral are based on resonant processes:

$$\begin{aligned}\sigma^R(p) &\qquad (7.9)\\ \approx&v_0^2\int_{0<q<p}\frac{\sigma^K(q)}{\sigma^R(q)}\frac{1}{\sigma^R(q)+\sigma^R(p-q)}qp(p-q)\\ &+v_0^2\int_{0<q}\frac{\sigma^K(q)}{\sigma^R(q)}\frac{1}{\sigma^R(q)+\sigma^R(p+q)}qp(p+q)\\ &+v_0^2\int_{0<p<q}\frac{\sigma^K(q)}{\sigma^R(q)}\frac{1}{\sigma^R(q)+\sigma^R(q-p)}qp(p-q).\end{aligned}$$

Since the self-energy is symmetric by inversion of momentum, i.e. $\sigma^R(k)=\sigma^R(-k)$, equation (7.9) simplifies to:

$$\sigma^R(p)=v_0^2\int_{0<q}\frac{\sigma^K(q)}{\sigma^R(q)}[\frac{qp(p-q)}{\sigma^R(q)+\sigma^R(p-q)}+\frac{qp(p+q)}{\sigma^R(q)+\sigma^R(p+q)}]. \qquad (7.10)$$

The retarded self-energy is due to this equation self-consistently determined as a function of the Keldysh self-energy. However, the latter depends due to equations (5.36) and (6.24) on the occupation distribution and the quasiparticle lifetime:

$$\sigma^K(k) = \partial_\tau 2n_k + (2n_k + 1)2\sigma^R(k). \tag{7.11}$$

According to this, the retarded self-energy is determined by the following self-consistent equation as a function of the phonon density[30,31]:

$$\begin{aligned}\sigma^R(p) =& v_0^2 2 \int_{0<q} \left(\frac{\partial_\tau n_q}{\sigma^R(q)} + (2n_q + 1)\right) \\ & \left[\frac{qp(p-q)}{\sigma^R(q) + \sigma^R(p-q)} + \frac{qp(p+q)}{\sigma^R(q) + \sigma^R(p+q)}\right].\end{aligned} \tag{7.12}$$

The coupled system of non-linear differential equations (7.12) and the kinetic equation (6.31) are numerically solved in chapter 9. Furthermore, we can now start to analyse from equation (7.12) the scaling properties of the quasiparticle lifetime.

7.2 Scaling Solution of the Self-Energy

We assume that the phonon density n_p can be separable in momentum regimes. In each segment the phonon density can be further approximated by a power function of momentum, i.e. $n_p \propto p^{\eta_K}$, with a characteristic exponent η_K. For instance, the Bose-Einstein distribution scales in the low mentum regime as $n_B(p) \approx \frac{T}{u|p|}$.
Since the phonon density relates the self-energies of the system by equation (7.12), we conclude that the self-energies can also be approximated by power functions in each momentum regime:

$$\sigma^{R/A}(p) = \gamma_{R/A}\ p^{\eta_{R/A}} \text{ and } \ \sigma^K(p) = \gamma_K\ p^{\eta_K}. \tag{7.13}$$

We compute the self-consistent equation (7.9) of the retarded self-energy for the functions (7.13) in order to find a relation between the exponents (η_K, η_R):

$$\begin{aligned}&\sigma^R(p) \\ &\quad = v_0^2 \int_{0<q<p} \frac{\sigma^K(q)}{\sigma^R(q)} \frac{1}{\sigma^R(q) + \sigma^R(p-q)} qp(p-q)\end{aligned} \tag{7.14}$$

$$
\begin{aligned}
&+v_0^2 \int_{0<q} \frac{\sigma^K(q)}{\sigma^R(q)} \frac{1}{\sigma^R(q)+\sigma^R(p+q)} qp(p+q) \\
&+v_0^2 \int_{0<p<q} \frac{\sigma^K(q)}{\sigma^R(q)} \frac{1}{\sigma^R(q)+\sigma^R(p-q)} qp(p-q) \\
=&v_0^2 \frac{\gamma_K}{\gamma_R^2} \int_{0<q<p} \frac{q^{\eta_K}}{q^{\eta_R}} \frac{1}{q^{\eta_R}+(p-q)^{\eta_R}} qp(p-q) \\
&+v_0^2 \frac{\gamma_K}{\gamma_R^2} \int_{0<q} \frac{q^{\eta_K}}{q^{\eta_R}} \frac{1}{q^{\eta_R}+(p+q)^{\eta_R}} qp(p+q) \\
&+v_0^2 \frac{\gamma_K}{\gamma_R^2} \int_{0<p<q} \frac{q^{\eta_K}}{q^{\eta_R}} \frac{1}{q^{\eta_R}+(p-q)^{\eta_R}} qp(p-q) \\
=&p^{\eta_K-2\eta_R+4}\ J,
\end{aligned}
$$

where

$$
\begin{aligned}
J =& v_0^2 \frac{\gamma_K}{\gamma_R^2} \int_{\tilde{q}} \frac{\tilde{q}^{\eta_K}}{\tilde{q}^{\eta_R}} \left[\frac{1}{\tilde{q}^{\eta_R}+(1+\tilde{q})^{\eta_R}} \tilde{q}(1+\tilde{q}) + \frac{1}{\tilde{q}^{\eta_R}+(1-\tilde{q})^{\eta_R}} \tilde{q}(1-\tilde{q}) \right] \\
=& v_0^2 \frac{\gamma_K}{\gamma_R^2} \int_{\tilde{q}} I(\tilde{q}, \eta_K, \eta_R)
\end{aligned}
\tag{7.15}
$$

with $\tilde{q} = \frac{q}{p}$.
The scaling exponents of the Keldysh and retarded self-energies (η_K, η_R) must due to equation (7.15) satisfy the following relation[30,31]:

$$
\eta_R = \frac{\eta_K + 4}{3}. \tag{7.16}
$$

On the other hand, the Keldysh self-energy depends on the phonon density n_k according to:

$$
\sigma^K(k) = \partial_\tau 2n_k + (2n_k+1) 2\sigma^R(k). \tag{7.17}
$$

In the following subsection, we investigate the scaling behaviour of the self-energies via the coupled equations (7.11 - 7.12). We analyse the scaling exponents for different phonon distributions and compute the corresponding integral J (cf. equation (7.15)).

7.3 Thermal Phonon Distribution

We assume that the phonon density is described by a stationary Bose-Einstein distribution with a finite temperature $T > 0$. In this case $(2n_k + 1) = \coth(\beta\epsilon(k)) \overset{k\to 0}{=} \frac{T}{u|k|}$:

$$
\begin{aligned}
\gamma_K k^{\eta_K} &= (2k^{-1}+1) 2\gamma_R k^{\eta_R} \overset{k\to 0}{=} 4k^{-1+\eta_R}\gamma_R \\
&\to \eta_K = \eta_R - 1.
\end{aligned}
\tag{7.18}
$$

According to this, the retarded self-energy scales as:

$$\eta_R = \frac{\eta_K + 4}{3} = \frac{\eta_R - 1 + 4}{3} = \frac{\eta_R + 3}{3}$$
$$\rightarrow (\eta_K, \eta_R) = (\frac{1}{2}, \frac{3}{2}). \tag{7.19}$$

The phonon lifetime shows a sub-diffusive behaviour $\tau^{qp}_{T>0} = p^{-\frac{3}{2}}$.[31,33–35]

7.4 T=0 Distribution

For a constant phonon density $F(k)$=const., which is reached in the limit of $T \rightarrow 0$, the derivation of the phonon density with respect to the forward time is zero. Therefore the scaling exponents of the retarded and Keldysh self-energy are equal: $\eta_K = \eta_R$.
Due to relation (7.16) the quasipartilce lifetime scales diffusive with $\tau^{qp}_{T=0} = p^{-2}$ at zero temperature. The Keldysh self-energy has the same exponent $\eta_K = 2$.[26,31,36,37]

7.5 Universality

The results of the former section are protected by the vertex structure and do not depend on the UV-cutoff. We verify this by plotting the integrand $I(\tilde{q}) = I(\tilde{q}, \eta_K, \eta_R)$ (with $\tilde{q} = \frac{q}{p}$) for different scaling regimes of the exponents (η_K, η_R) (cf. Fig. 7.1). $I(\tilde{q})$ weights the contribution of different internal momentas q to the retarded self-energy $\sigma^R(p)$ of external momentum p. The

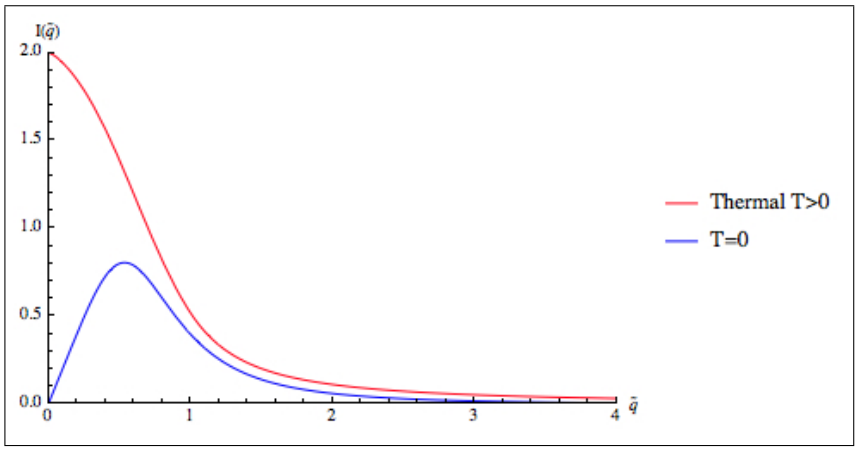

Figure 7.1: *UV-cutoff independent integrand I(q).*

dominant contribution to $\sigma^R(p)$ comes from the momentum $q < p$ manifesting the independence of the results from the explicit UV-cutoff Λ.[30,31] For the thermal and constant phonon distribution the integrand is tending to zero momentum. For instance, if the occupation is described by a Bose-Einstein distribution the dominant modification of the retarded self-energy $\sigma^R(p)$ comes from the regime $q \to 0$, where $n(q) \propto \frac{1}{q}$ is divergent.

Chapter 8

Dynamics of the Interacting Luttinger Liquid for a Low Temperature Initial State

In this chapter, the time evolution of the phonon density for an interacting Luttinger Liquid in an optical lattice is evaluated.[31] We explain the implementation of the kinetic equation and the self-consistent equation for the retarded self-energy. The time evolution of the phonon density is computed for each time step as a function of momentum.
We initialize the numerical evaluation with a low temperature distribution $T \approx 0$, so that the phonon density is approximately constant. The results show, that the phonon density separates at each time step into two characteristic regimes with a crossover momentum, which scales algebraic.
We determine a universal linear scaling regime in the phonon density and a corresponding exponent for the quasiparticle lifetime.

8.1 System of Coupled Differential Equations

In this section, we explain the approach to solve the system of coupled differential equations for the phonon density and the retarded self-energy.
The phonon density evolves at each time step $\delta\tau \ll 1$ approximately with

$$n_p(\tau + \delta\tau) \approx n_p(\tau) + \delta\tau I_{\text{coll}}[n_p(\tau), \sigma^R(p)], \tag{8.1}$$

where the collision integral reads

$$\begin{aligned} &I_{\text{coll}}[n_p(\tau), \sigma^R(p)] \\ &\quad = h(p) \\ &\quad + \frac{1}{2\pi}\int_{0<q<p} \frac{qp(p-q)v_0^2}{\sigma^R(p)+\sigma^R(q)+\sigma^R(p-q)}([n_{p-q}n_q - n_p(n_{p-q}+n_q+1)]) \\ &\quad + \frac{1}{2\pi}\int_{0<q} \frac{2qp(p+q)v_0^2}{\sigma^R(p)+\sigma^R(q)+\sigma^R(p+q)}(2[n_{p+q}+n_{p+q}n_q+n_{p+q}n_p-n_qn_p]). \end{aligned}$$

The finite lifetime is caused by the dressing of the quasiparticle and thus depends on the phonon density:

$$\sigma^R(p) = v_0^2 2\int_q \left(\frac{\partial_\tau n_q}{\sigma^R(q)} + (2n_q+1)\right)\left[\frac{qp(p-q)}{\sigma^R(q)+\sigma^R(p-q)} + \frac{qp(p+q)}{\sigma^R(q)+\sigma^R(p+q)}\right]. \tag{8.2}$$

Equations (8.1) and (8.2) form a system of coupled differential equations, which describe the time evolution of the phonon density in an interacting Luttinger Liquid out of equilbrium. The system of coupled differential equations is solved in an itterative routine with a given initial value $n_p(\tau = 0)$ (cf. Fig. 8.1): We start with the given occupation n_p at forward time τ

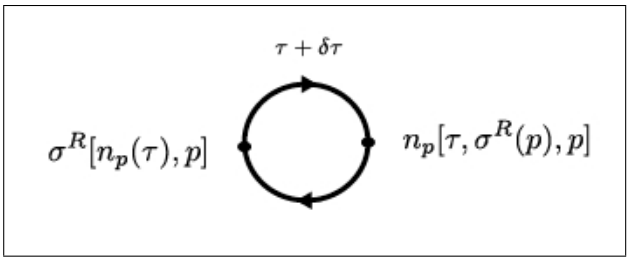

Figure 8.1: *Routine for solving coupled differential equations.*

to calculate the lifetime of the quasiparticles $\tau_{qp} \propto (\sigma^R(p))^{-1}$ according to equation (8.2). In order to determine the fixed-point of equation (8.2), we initialize the retarded self-energy with the appropriate scaling function (cf. chapter 7). Subsequently, we use the solution for the retarded self-energy to compute the phonon density n_p at time $\tau + \delta\tau$ with the kinetic equation (8.1). This routine is repeated until the final forward time τ_f.
In the next section, we describe how to choose an appropriate initial value for the retarded self-energy based on the approach in chapter 7. Moreover, we rescale the kinetic equation and parameters in appropriate units.

8.2 Rescaling Forward Time and the Initial Value of the Retarded Self-Energy

We rescale the forward time and the retarded self-energy in order to derive a kinetic equation, which is independent of microscopic parameters.
If we rescale the forward time $\tau \to \tilde{\tau} = v_0\tau$ and the retarded self-energy $\sigma^R(p) \to \tilde{\sigma}^R(p) = (v_0)^{-1}\sigma^R(p)$, the kinetic equation (8.1 ff.) and the self-consistent equation (8.2) read:

$$\partial_{\tilde{\tau}} n_p(\tilde{\tau}) = I_{\text{coll}}[n_p(\tilde{\tau}), \tilde{\sigma}^R(p)], \tag{8.3}$$

$$\tilde{\sigma}^R(p) = 2\int_q \left(\frac{\partial_{\tilde{\tau}} n_q}{\tilde{\sigma}^R(q)} + (2n_q + 1)\right)\left[\frac{qp(p-q)}{\tilde{\sigma}^R(q) + \tilde{\sigma}^R(p-q)} + \frac{qp(p+q)}{\tilde{\sigma}^R(q) + \tilde{\sigma}^R(p+q)}\right], \tag{8.4}$$

where the paramter v_0 is now absorbed in the forward time and the retarded self-energy.
We continue to compute an appropriate initial retarded self-energy $\tilde{\sigma}^R(p) = \tilde{\gamma_R} p^2$ for $T \approx 0$ (cf. section 7.4). According to equations $(7.14 - 7.17)$, $\tilde{\gamma}_R$ is for an approximately constant phonon density

$$\tilde{\gamma}_R^3 = \tilde{\gamma}_K \int_{\tilde{q}} I(\tilde{q}, \eta_K = 2, \eta_R = 2),$$

$$2\tilde{\gamma}_R = \tilde{\gamma}_K,$$
$$\rightarrow \tilde{\gamma}_R = \sqrt{2\int_{\tilde{q}} I(\tilde{q}, \eta_K = 2, \eta_R = 2)} = \sqrt{2\pi}, \tag{8.5}$$

where the integral $I(\tilde{q}, \eta_K = 2, \eta_R = 2)$ is defined in equation (7.15).
In conclusion, we have determined a rescaled system of coupled differential equations and an appropriate weighting factor $\tilde{\gamma}_R$ of the retarded self-energy in the low temperature limit.

8.3 Numerical Results

The time evolution of the phonon density is evaluated for a constant initial phonon distribution (blue curve in Fig. 8.2). The phonon density $n_p(\tilde{\tau})$ is evaluated at four time steps. We now qualitatively discuss the numerical

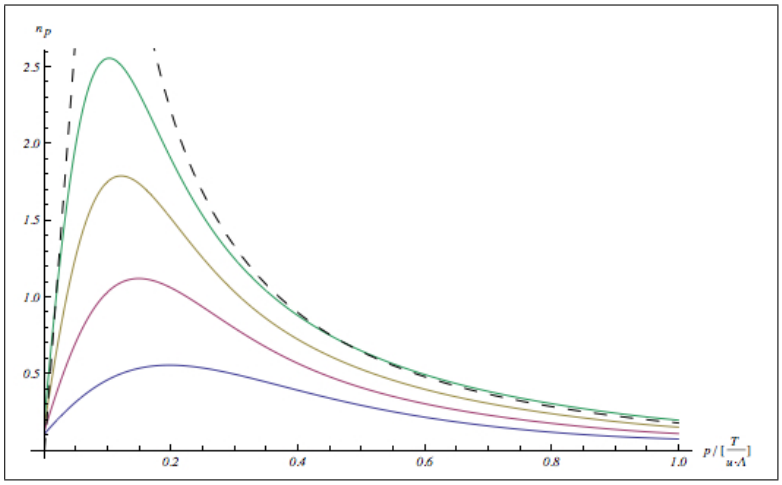

Figure 8.2: *The figure shows the phonon density at* $\tilde{\tau}_0 = 0.5 \cdot \frac{1}{\Lambda}$ *(blue line),* $\tilde{\tau}_1 = 1 \cdot \frac{1}{\Lambda}$ *(red line),* $\tilde{\tau}_2 = 2 \cdot \frac{1}{\Lambda}$ *(yellow line) and* $\tilde{\tau}_3 = 2.5 \cdot \frac{1}{\Lambda}$ *(green line) with* $\gamma = \frac{\pi\ 0.35}{K}$*. The crossover between the linear and the effective thermalized regime scales approximately as* $p_0 \propto \tilde{\tau}^{-0.8}$*. The phonon density scales, as indicated by the dashed fitting curves, in the low momentum regime as* $n_p(\tilde{\tau}) \propto p\tilde{\tau}$ *and in the effective thermalized regime with* $n_p(\tilde{\tau}) \approx n_B(p, T(\tilde{\tau}))$ *(in Fig. 8.2:* $T(\tilde{\tau}_3) = 1.85 \cdot \Lambda$*).*

results based on Fig. 8.2 and supplement them in the next section with analytic calculations:
At each time step, the behaviour of the phonon density separates into two regimes. For low momenta the phonon density increases linear. It is obviously pinned in the limit $p \rightarrow 0$ to a finite value. The slope of the linear

function in this regime increases as a function of forward time.
On the other hand, the phonon density shows an effective thermalization with $n_p(\tilde{\tau}) \propto \frac{T(\tilde{\tau})}{p}$ in the high momentum regime. The scattering rate increases for higher momenta and therefore causes a mechanism for effective thermalization. The regime of the phonon density, where effective thermalization occurs, spreads during the dynamics to lower momenta.
Furthermore, we determine an algebraic crossover momentum scale $p_0(\tilde{\tau}) \propto \tilde{\tau}^{-\alpha}$, which connects the linear and effectively thermalized regime of the phonon density.

8.4 Discussion of the Time Evolution

In this section, the numerical results from the previous section are supplemented by analytic calculations.

8.4.1 Kinetic Equation for Small Incoming Momentum

The kinetic equation, which describes the dynamics of the phonon density, is a non-linear differential equation, first order in time:

$$\begin{aligned}&\partial_\tau n_p(\tau) \\ &\quad = h(p) \\ &\quad + \frac{1}{2\pi}\int_{0<q<p} v_0^2 \frac{qp(p-q)}{\sigma^R(p)+\sigma^R(q)+\sigma^R(p-q)}([n_{p-q}n_q - n_p(n_{p-q}+n_q+1)]) \\ &\quad + \frac{1}{2\pi}\int_{0<q} v_0^2 \frac{2qp(p+q)}{\sigma^R(p)+\sigma^R(q)+\sigma^R(p+q)}([n_{p+q}+n_{p+q}n_q+n_{p+q}n_p-n_qn_p]).\end{aligned} \tag{8.6}$$

We now focus on the determination of the scaling behaviour in the limit of small incoming momentum. If the incoming momentum is small, the first integral in equation (8.6) is limited to a narrow interval and is thus negligible. On the other hand, the sum of incoming and internal momentum can be approximated in this limit by $(p+q) \overset{p\to 0}{=} q$ and the retarded self-energy fullfilles: $\sigma^R(p) \ll \sigma^R(q)$ for $p \ll q$.
According to this, the collision integral simplifies to

$$I_{\text{coll}}[n_q(\tau), \sigma^R(q)] \approx p\int_{0<q} \frac{v_0^2 q^2}{\pi\sigma^R(q)}[n_q(\tau)(1+n_q(\tau))]. \tag{8.7}$$

Thus, the kinetic equation in the limit of small incoming momentum reads:

$$\partial_\tau n_p(\tau) \approx \frac{\kappa K}{2\pi}p + p\int_{0<q} \frac{v_0^2 q^2}{\pi\sigma^R(q)}[n_q(\tau)(1+n_q(\tau))]. \tag{8.8}$$

The phonon density is linear in the low momentum regime and is pinned to the initial value $n_p(\tau = 0)$ at zero incoming momentum:

$$n_p(\tau) = n_p(\tau = 0) + p \int_0^\tau (\frac{\kappa K}{2\pi} + \int_{0<q} \frac{v_0^2 q^2}{\pi \sigma^R(q)} [n_q(\tau')(1 + n_q(\tau'))] d\tau'). \quad (8.9)$$

From equation (8.9) we define the slope

$$a(\tau, I[n_q, \sigma^R(q)]) = \int_0^\tau (\frac{\kappa K}{2\pi} + \int_{0<q} \frac{v_0^2 q^2}{\pi \sigma^R(q)} [n_q(\tau')(1 + n_q(\tau'))] d\tau'), \quad (8.10)$$

which scales due to the numerical results approximately quadratic in the forward time $a(\tau, I[n_q, \sigma^R(q)]) \sim \tau^{2\cdot}$.
In conclusion, the linear slope of the phonon density in the low momentum regime is caused by the vertex structure, which scales $V^2(q, p, q + p) \overset{p\to 0}{\approx} p$. This generic behaviour of the interacting Luttinger Liquid is confirmed by the numerical results. The presence of the permanent heating additionally supports this linear regime (cf. equation (8.8)).[31]

8.4.2 Scaling Exponent of the Quasiparticle's Lifetime

As discussed in the last section, the phonon density scales linear in the low momentum regime, i.e. $n_p(\tilde{\tau}) \overset{p\to 0}{=} n_p(\tilde{\tau} = 0) + a(\tilde{\tau}, I[n_q, \tilde{\sigma}^R(q)])\ p$. We use relation (7.17) in order to determine the scaling exponent η_K of the Keldysh self-energy for a linear phonon density:

$$\tilde{\sigma}^K(p) = 2\ (\partial_{\tilde{\tau}}\ n_p + (2n_p + 1)\ \tilde{\sigma}^R(p)), \quad (8.11)$$

where the right hand side scales for $p \to 0$ linear in momentum and $\eta_R > 0$. As a consequence, $\eta_K = 1$ and thus the exponent of the retarded self-energy reads:

$$\eta_R = \frac{\eta_K + 4}{3} = \frac{5}{3}. \quad (8.12)$$

Thus, the lifetime of the phonons has the following universal scaling behaviour $\tau^{qp}(p) \propto p^{-\frac{5}{3}}$.[31]
We continue to analyse the integrand $I(\tilde{q}, \eta_K, \eta_R)$, which weights the impact of internal momenta $\tilde{q} = \frac{q}{p}$ on the retarded self-energy. The definition of the integrand is due to chapter 7:

$$I(\tilde{q}, \eta_K = 1, \eta_R = \frac{5}{3}) = \frac{\tilde{q}}{\tilde{q}^{\frac{5}{3}}} [\frac{1}{\tilde{q}^{\frac{5}{3}} + (1 + \tilde{q})^{\frac{5}{3}}} \tilde{q}(1 + \tilde{q}) + \frac{1}{\tilde{q}^{\frac{5}{3}} + (1 - \tilde{q})^{\frac{5}{3}}} \tilde{q}(1 - \tilde{q})]. \quad (8.13)$$

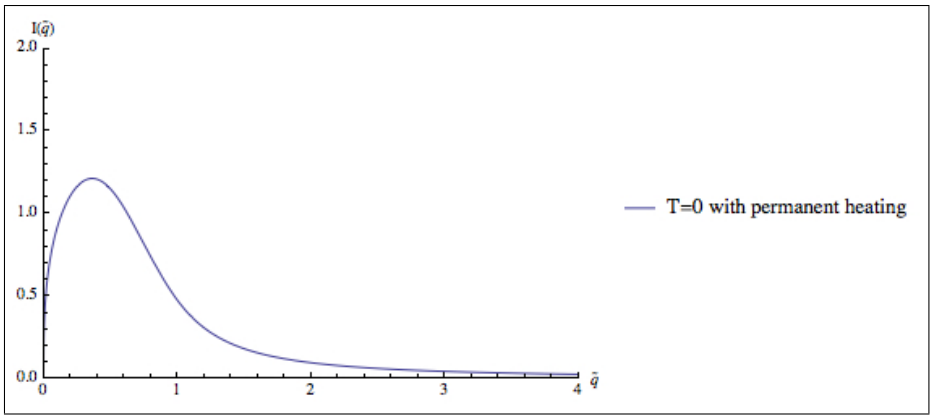

Figure 8.3: *UV - cutoff independent integrand I(q) for universal scaling regime.*

We observe in Fig. 8.3, that the integrand weights for low internal momenta stronger and is obvisiouly independent from the UV-cutoff Λ.
In summary, we determined a universal nonequilibrium scaling exponent $\frac{5}{3}$ for the quasiparticle's lifetime and confirmed the independence of the theory from the UV-cutoff.

8.4.3 Crossover Momentum

The phonon density scales linearly in the low momentum regime and $\eta_R > 0$, so that the following inequality holds for $p \to 0$:

$$(2n_p + 1)\ \tilde{\sigma}^R(p)\ \ll \partial_{\tilde{\tau}}\ n_p. \tag{8.14}$$

On the other hand, in the high momentum regime, where the phonon density is thermal $n_p \propto \frac{1}{p}$, the inequality is reversed:

$$\partial_{\tilde{\tau}}\ n_p \ll\ (2n_p + 1)\ \tilde{\sigma}^R(p). \tag{8.15}$$

Since the Keldysh self-energy is a continuous function (cf. equation 8.11), both regimes are smoothly connected at the crossover momentum:

$$\partial_{\tilde{\tau}}\ n_{p_0} \approx\ (2n_{p_0} + 1)\ \tilde{\sigma}^R(p_0), \tag{8.16}$$

where $p_0(\tau)$ is the crossover momentum between linear and thermal regime. Due to the scaling functions $\tilde{\sigma}^R(p_0) = \tilde{\gamma}_R p_0^{\eta_R}$ and $n_{p_0} \propto p_0^{\beta}$ equation (8.16) can be approximated as follows:

$$p_0(\tilde{\tau}) \propto\ (\tilde{\gamma}_R \tilde{\tau})^{\frac{1}{\eta_R}}. \tag{8.17}$$

We now approach the crossover from the lower momentum regime, where $\eta_R = \frac{5}{3}$ and the phonon density scales due to the numerical results $n_p \propto p\tau^{1.86}$, where the exponent depends on the heating, however stays in a small interval around 2. The prefactor $\tilde{\gamma}_R$ of the retarded self-energy reads (cf. equations (7.14 - 7.17)):

$$\begin{aligned} \tilde{\gamma}_R^3 &= \tilde{\gamma}_K \int_{\tilde{q}} I(\tilde{q}, \eta_K = 2, \eta_R = 2), \\ \partial_{\tilde{\tau}} n_p &\approx \tilde{\gamma}_K, \\ \rightarrow \tilde{\gamma}_R &= (\partial_{\tilde{\tau}} n_p \int_{\tilde{q}} I(\tilde{q}, \eta_K = 1, \eta_R = \frac{5}{3}))^{\frac{1}{3}} \propto (\partial_{\tilde{\tau}} n_p)^{\frac{1}{3}} = (\tau^{0.86})^{\frac{1}{3}}, \end{aligned} \tag{8.18}$$

where the second equation results from (8.11) and (8.14).
According to this, we conclude from equation (8.17) that the crossover momentum scales as a function of the forward time as follows[31]:

$$p_0(\tilde{\tau}) \propto \ (\tilde{\tau})^{0.77}. \tag{8.19}$$

8.4.4 Effective Thermalization

In the high momentum regime the numerical results show due to Fig. 8.2 an effective thermalization, where the phonon density equals approximately the Bose-Einstein distribution $n_p(\tilde{\tau}) \approx n_B(p, T(\tilde{\tau}))$ with an effective temperature $T(\tilde{\tau})$.[31,57]
The vertex scales in this regime $V^2(p, q, p \pm q) \rightarrow p^2$, so that the energy and momentum is redistributed faster and the phonon density approaches a stationary point of the collision integral for zero heating.
The increase of the average phonon density scales in the presence of the permanent heating linear in forward time $\tilde{\tau}$ and therefore causes an effective temperature $T(\tilde{\tau}) \propto \tilde{\tau}$ (cf. Fig. 8.2).
In conclusion, an effective thermalization sets in at high momenta, where the vertex structure causes scattering processes at a higher rate, and spreads during the time evolution to lower momenta. The phonon density is in this regime a Bose-Einstein distribution with an effective temperature, which scales due to the permanent heating linear in forward time $\tilde{\tau}$.

8.5 Verification of the Wigner approximation

In chapter 5 we used the Wigner approximation for the evaluation of the convolution integrals, which is valid if the following inequality holds (cf.

equation 5.34):

$$\frac{\partial_\omega \sigma^R(p) \partial_\tau 2n_p(\tau)}{\sigma^R(p)(2n_p(\tau)+1)} \ll 1. \tag{8.20}$$

Based on the previous results, the Wigner approximation is justified. The scaling approach (7.13) shows that

$$\frac{\partial_\omega \sigma^R(p)}{\sigma^R(p)} = \frac{\eta_R}{\nu|p|}. \tag{8.21}$$

Due to the kinetic equation (6.31) in the thermal region, where $n_p(\tau) = n_B(p, T(\tau)) \approx \frac{T(\tau)}{\nu|p|}$, we conclude that:

$$\frac{\partial_\tau 2n_p(\tau)}{(2n_p(\tau)+1)} = l\tau\gamma \frac{T_0 v_0^2}{\nu^2} p^2, \tag{8.22}$$

where $l = \mathcal{O}(1)$ and $T(\tau) = \tau\gamma T_0$.
According to this, the inequality (8.20) simplifies to:

$$\tau \ll \frac{\nu^2}{c_0 \gamma v_0 T_0 \eta_R}, \tag{8.23}$$

where we used for the momentum the cutoff $\Lambda \approx \frac{\nu}{v_0}$ (cf. equations (2.10) and (2.17)) in order to determine the lower bound above the Wigner approximation breaks down.
The Luttinger Liquid description is due to equation (3.60) valid up to the following point in forward time:

$$\tau \ll \frac{\nu^2}{\gamma v_0 T_0}. \tag{8.24}$$

In conclusion, the Luttinger Liquid description breaks down before the Wigner approximation is invalid.[31]

Chapter 9

Dynamics of the Interacting Luttinger Liquid for a Finite Temperature Initial State

We analyse the time evolution of the phonon density based on the kinetic equation and the self-consistent equation for the retarded self-energy with $n_p(\tau = 0) = n_B(p, T(\tau))$ at finite temperature $T > 0$.[31]
For large enough times the normal occupation shows a local maximum, which is approached from the low momentum regime by a linear slope. Furthermore, the phonon density is during the time evolution divergent for $p \to 0$. We determine with a semi-numerical approach a second crossover as a function of the forward time. Finally, the initial temperature and the heating rate are varied to find an optimally enlarged linear scaling regime.

9.1 Initial Value for the Retarded Self-Energy

In this section, we briefly repeat the determination of the scaling behaviour of the retarded self-energy for a phonon distribution at finite temperature and analyse the prefactor $\tilde{\gamma}_R$.
The phonon density is approximated $n_p(\tilde{\tau} = 0) \approx \frac{T}{\nu|p|}$ in the limit $\frac{\epsilon(p)}{T} \ll 1$.
The Keldysh self-energy is related to the retarded self-energy according to:

$$\tilde{\sigma}^K(p) = 2\ \partial_{\tilde{\tau}}\ n_p + (2n_p + 1)\ 2\ \tilde{\sigma}^R(p). \tag{9.1}$$

The second term on the right hand side of equation (9.1) dominates for $\frac{\epsilon(p)}{T} \ll 1$ and we conclude ($\eta_R > 0$):

$$\tilde{\gamma}_K\ p^{\eta_K} \overset{1 \ll p}{\approx} \frac{4T}{\nu}\ \tilde{\gamma_R}\ p^{\eta_R - 1} \tag{9.2}$$

$$\to \eta_K = \eta_R - 1. \tag{9.3}$$

From equations (7.16) and (9.3), we determine the scaling exponent of the retarded self-energy to be $\eta_R = \frac{3}{2}$. Thus, the quasiparticle lifetime scales $\tau_{qp} \approx \tau^{-\frac{3}{2}}$.[31]
Furthermore, the relation between the prefactor of retarded and Keldysh self-energy reads due to equation (9.2):

$$\tilde{\gamma}_K = \frac{4T}{\nu}\tilde{\gamma}_R. \tag{9.4}$$

According to this, $\tilde{\gamma}_R$ is:

$$\tilde{\gamma}_R^3 = \tilde{\gamma}_K \int_{\tilde{q}} I(\tilde{q}, \eta_K = \frac{1}{2}, \eta_R = \frac{3}{2}),$$

$$\to \tilde{\gamma}_R = \sqrt{\frac{4T}{\nu} \int_{\tilde{q}} I(\tilde{q}, \eta_K = \frac{1}{2}, \eta_R = \frac{3}{2})}, \tag{9.5}$$

where $\tilde{q} = \frac{q}{p}$.
In conclusion, we have determined the prefactor $\tilde{\gamma}_R$ of the retarded self-energy for a phonon density at finite temperature. This result is used to initialize the retarded self-energy for the numerical evaluation.

9.2 Numerical Results

In this section, we analyse the dynamics of the phonon density for a initial distribution at finite temperature (cf. Fig. 9.1). The phonon density is at each time step separated in three regimes. We observe that the distribution is in the high momentum regime thermal with an effective temperature $T(\tilde{\tau})$ (cf. Fig. 9.1, regime III). The phonon density is due to its initial value for all time divergent in the limit $p \to 0$, even though this third regime is continuously repeled by the linear slope. The universal linear scaling behaviour starts below a certain crossover momentum and is present in an intermediate regime (cf. Fig. 9.1, regime II).
We continue the analysis of these results by detailed computations of the second crossover between the linear regime and the divergent part of the phonon density. Furthermore, the universal regime is enlarged by variation of the system's parameters.

9.3 Discussion of the Time Evolution

The time evolution of the phonon density shows due to the initial distribution at finite temperature some new characteristic behaviour (cf. Fig. 9.1). We continue to analyse the single regimes in more detail.

9.3.1 Superposition of Initial Distribution and Bare Time Evolution

We have already observed in equation (8.9) that at low momenta the phonon density is a superposition of the initial phonon density and a linear slope:

$$n_p(\tau) = n_p(\tau = 0) + p \int_0^\tau \left(\frac{\kappa K}{2\pi} + \int_{0<q} \frac{v_0^2 q^2}{\pi \sigma^R(q)} [n_q(\tau')(1 + n_q(\tau'))] d\tau'\right). \quad (9.6)$$

The time evolution of the phonon density $\Delta n_p(\tau) = n_p(\tau) - n_p(\tau = 0)$ is due to Fig. 9.2 qualitatively equivalent for a initial phonon density at zero temperature.

We observe two regimes, an effectively thermal regime at high momenta and universal linear scaling. Both are separated by a crossover momentum.

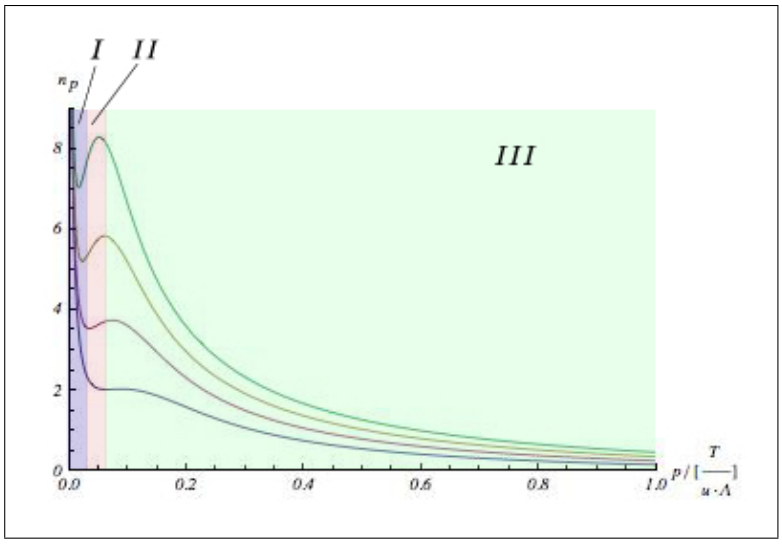

Figure 9.1: *The figure shows the phonon density at* $\tilde{\tau}_0 = 2\cdot\frac{1}{\Lambda}$ *(blue line),* $\tilde{\tau}_1 = 3\cdot\frac{1}{\Lambda}$ *(red line),* $\tilde{\tau}_2 = 4\cdot\frac{1}{\Lambda}$ *(yellow line) and* $\tilde{\tau}_3 = 5\cdot\frac{1}{\Lambda}$ *(green line) with* $\gamma = \frac{\pi\ 0.35}{K}$*. The phonon density separates at each time step in three regimes: The phonon density is thermal in the low momentum regime (regime I),* $n_p(\tilde{\tau}) \propto p\tilde{\tau}$ *in regime II and in the effective thermalized regime* $n_p(\tilde{\tau}) \approx n_B(p, T(\tilde{\tau}))$ *(in Fig. 8.2, regime III:* $T(\tilde{\tau}_3) = 1.85\cdot\Lambda$*).*

9.3.2 Determination of the Second Crossover

In this section, we determine in a semi-numerical analysis the scaling behaviour of the second crossover $q_1(\tau)$ between the linear regime and the divergent slope of the phonon density for low momenta (cf. Fig. 9.1). The phonon density scales due to the numerical results $\Delta n_p(\tau) = mp\tau^{1.86}$, where m is a proportionality factor, and the exponent varies around 2. for different heating regimes. According to this, we conclude the following relation for the phonon density:

$$n_p(\tau) = n_p(\tau = 0) + mp\tau^{1.86} = n_B(T_0, p) + mp\tau^{1.86}. \tag{9.7}$$

The second crossover is the minimum of the phonon density in the low momentum regime:

$$\begin{aligned} \frac{dn_p(\tau)}{dp} &\approx -\frac{T_0}{p^2} + m\tau^{1.86} = 0. \\ \rightarrow p_1(\tau) &= \sqrt{\frac{T_0}{m}}\tau^{-0.93}. \end{aligned} \tag{9.8}$$

In conclusion, we have analysed the algebraic decay of the second crossover

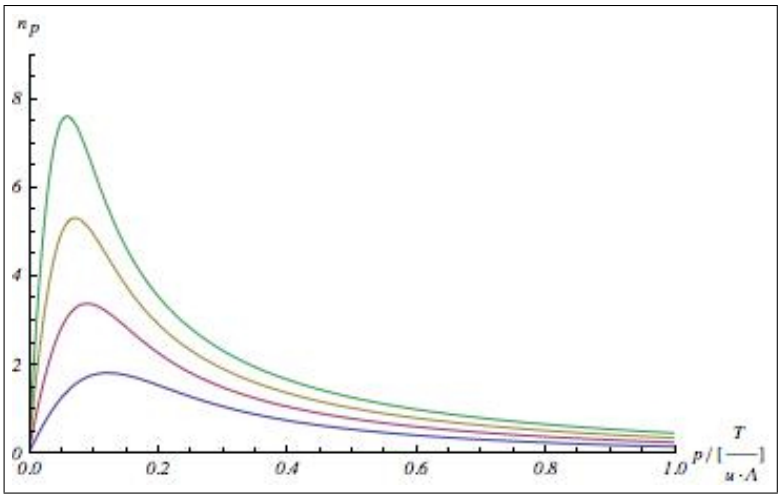

Figure 9.2: *Time evolution of* $\Delta n_p(\tilde{\tau}) = n_p(\tilde{\tau}) - n_p(\tilde{\tau}=0)$ *at* $\tilde{\tau}_0 = 2 \cdot \frac{1}{\Lambda}$ *(blue line),* $\tilde{\tau}_1 = 3 \cdot \frac{1}{\Lambda}$ *(red line),* $\tilde{\tau}_2 = 4 \cdot \frac{1}{\Lambda}$ *(yellow line) and* $\tilde{\tau}_3 = 5 \cdot \frac{1}{\Lambda}$ *(green line) with* $\gamma = \frac{\pi\ 0.35}{K}$.

and determined its scaling exponent in equation (9.8) as a function of the forward time.

Chapter 10

Two Uncoupled One Dimensional Condensates

10.1 Introduction: Summary of Experimental and Theoretical Works

Recent experimental works have shown that a one dimensional condensate at equilibrium can be coherenty split, producing two uncoupled one dimensional condensates with perfect phase coherence (cf. Fig. 10.1, first column).[58–60] As a consequence, the relative phase $\hat{\theta}_R(z) := \hat{\theta}_1(z) - \hat{\theta}_2(z)$ is approximately zero after the splitting. Such a global sate, where both one dimensional systems share approximately the same longitudinal phase profile, is out of equilibrium, since two independently created one dimensional condensates would have totally uncorrelated phase profiles. The following relative-phase coherence function (RPC) is defined in the literature in order to determine the relative phase coherence between the two condensates[58–60]:

$$C(z,z',t) = \frac{\left\langle \hat{\Psi}_1(z)\hat{\Psi}_2^\dagger(z)\hat{\Psi}_1^\dagger(z')\hat{\Psi}_2(z')\right\rangle}{\left\langle |\hat{\Psi}_1(z)|^2\right\rangle \left\langle |\hat{\Psi}_2(z')|^2\right\rangle} = e^{-\frac{1}{2}\left\langle (\hat{\theta}_R(z)-\hat{\theta}_R(z'))^2\right\rangle}, \tag{10.1}$$

where the state is transformed in a density-phase representation $\hat{\Psi}_j(z) = \sqrt{\hat{\rho}_\alpha(z)}e^{i\hat{\theta}_\alpha(z)}$ with the label α for the condensate.
After the splitting, the relative phase correlation length λ_{θ_R}, defined via

$$C(z,z',t_e=0) \propto e^{-\frac{z-z'}{\lambda_{\theta_R}}}, \tag{10.2}$$

is infinite (cf. Fig. 10.1, row b).
In this part we consider a completely different setup of two uncoupled wires in a closed quantum system. At $t = 0$ the initial state is prepared in a way that both subsystems are in perfect phase coherence and are thus coupled initially. For $t > 0$ the time evolution is that of two uncoupled wires and is described by two independent Hamiltonians of a Luttinger Liquid. We study the time evolution of the important experimental observable RPC (10.1) and include, unlike previous works, the case of a Luttinger Liquid with interactions. We observe a new exponential regime in the RPC on small relative distances, which indicates a local spreading of the decay of the RPC due to the scattering effects.
The dynamics of the phase coherence is studied in an experiment by a matter-wave interference, in which the interference patterns are obtained by overlapping the two gases in a time-of-flight after different evolution times.[58–60] Thus, we determine the loss of memory on the correlation between the two phase profiles. This scenario is indicated in the second and third column of Fig. 10.1, where the relative phase correlation continuously decays for $t_e > 0$

ms and thus the corresponding correlation length reaches $\lambda_{\theta_R} \approx \lambda_T$ ($\lambda_T :=$ relative-phase correlation length for a thermal system).[59]

We consider now that the dynamics after the splitting is due to the former

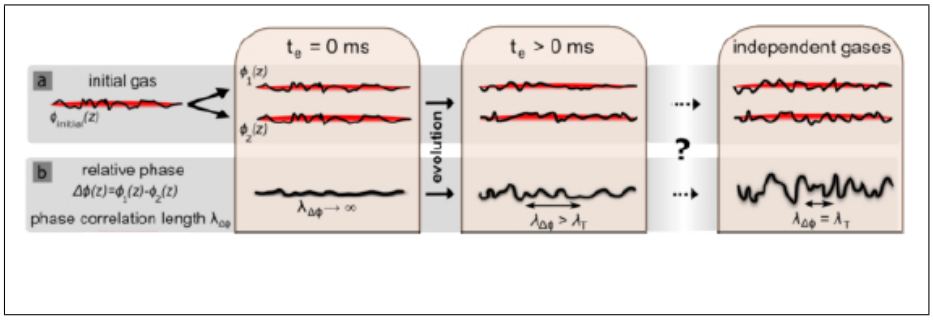

Figure 10.1: *Relaxation of two initially coupled one dimensional condensates.*[59]

theoretical work generated by the sum of two independent Luttinger Liquids without interactions and no hopping between the two wires[28,58–64]:

$$\begin{aligned}\hat{H} =& \hat{H}_{1,\mathrm{LL}} + \hat{H}_{2,\mathrm{LL}} \\ =& \sum_{\alpha=1,2} \frac{1}{2\pi} \int_x [\nu K (\partial_x \hat{\theta}_\alpha(x))^2 + \frac{\nu}{K} (\partial_x \hat{\phi}_\alpha(x))^2].\end{aligned} \tag{10.3}$$

Since we are interested in the relative phase evolution, the Hamiltonian is now represented in a relative and absolute density-phase basis:

$$\hat{\theta}_{A/R}(z) = \frac{\hat{\theta}_1(z) \pm \hat{\theta}_2(z)}{\sqrt{2}}, \;\; \hat{\phi}_{A/R}(z) = \frac{\hat{\phi}_1(z) \pm \hat{\phi}_2(z)}{\sqrt{2}}. \tag{10.4}$$

After the transformation, the Hamiltonian splits for equal average density in both subsystems into a relative and absolute component:

$$\hat{H} = \hat{H}_{R,\mathrm{LL}} + \hat{H}_{A,\mathrm{LL}} \tag{10.5}$$

$$= \sum_{\alpha=R,A} \frac{1}{2\pi} \int_x [\nu K (\partial_x \hat{\theta}_\alpha(x))^2 + \frac{\nu}{K} (\partial_x \hat{\phi}_\alpha(x))^2]. \tag{10.6}$$

The absolute component of the Hamiltonian $\hat{H}_{A,\mathrm{LL}}$ is neglected in the further analysis, since we are interested in the dynamics of the relative phase. Thus, we only consider the relative Luttinger Liquid fields and thus drop the index. Furthermore, we transform the relative Hamiltonian in the Fourier space:

$$\hat{H}_{R,\mathrm{LL}} \approx \sum_{p \neq 0} [K \nu p^2 \hat{\theta}_p^\dagger \hat{\theta}_p + \frac{\nu}{K} \hat{\phi}_p^\dagger \hat{\phi}_p], \tag{10.7}$$

where

$$\hat{\theta}(x) = \frac{1}{L}\sum_{p\neq 0} e^{ipx}\hat{\theta}_p,$$
$$\hat{\phi}(x) = \frac{1}{L}\sum_{p\neq 0} e^{ipx}\hat{\phi}_p.$$

and we neglected the zero momentum contribution in equation (10.7).
The initial state after the splitting is described by the following phenomenological initial conditions in the literature[28,58–60]:

$$\langle\hat{\rho}_p\hat{\rho}_{-p}\rangle\,(t=0) = \frac{\rho_0}{2}, \tag{10.8}$$
$$\left\langle\hat{\theta}_p^\dagger\hat{\theta}_p\right\rangle(t=0) = \frac{1}{2\rho_0}, \tag{10.9}$$

where ρ_0 is the mean density in one wire. In the limit of large density the initial relative phase correlation becomes very small.
The equations of motions for the relative phase $\hat{\theta}_p$ and the density $\hat{\phi}_p$ read[60]:

$$i\frac{d}{dt}\hat{\theta}_p = [\hat{\theta}_p, \hat{H}_{LL,R}] = \frac{\nu}{K}(-2i)\hat{\phi}_p, \tag{10.10}$$
$$i\frac{d}{dt}\hat{\phi}_p = [\hat{\phi}_p, \hat{H}_{LL,R}] = \nu K p^2(2i)\hat{\theta}_p. \tag{10.11}$$

These are the equations of motions of a harmonic oscillator with a momentum dependent frequency. The phononic excitations oscillate between the density and phase quadratures.
We use the following Bogoliubov transformation in order to diagonalize $\hat{H}_{LL,R}$:

$$\hat{\theta}_p = i\sqrt{(\frac{\pi}{2|p|LK})}e^{-\frac{1}{2}a|p|}(\hat{b}_p^\dagger - \hat{b}_{-p}), \tag{10.12}$$
$$\hat{\phi}_p = i\sqrt{(\frac{|p|K}{2\pi L})}e^{-\frac{1}{2}a|p|}(\hat{b}_p^\dagger + \hat{b}_{-p}), \tag{10.13}$$

where a is an ultra-violet cutoff that regularizes the theory and mimics a finite bandwith.
The relative Hamiltonian reads in the phonon eigenbasis:

$$\hat{H}_{LL,R} \approx \sum_{p\neq 0}[K\nu p^2\hat{\theta}_p^\dagger\hat{\theta}_p + \frac{\nu}{K}\hat{\phi}_p^\dagger\hat{\phi}_p] = \sum_{p\neq 0}\nu|p|\hat{b}_p^\dagger\hat{b}_p. \tag{10.14}$$

The phonon operators evolve in the interaction picture according to equation (10.14) in time as follows: $\hat{b}_p^\dagger(t) = \hat{b}_p^\dagger e^{-i\epsilon(p)t}$ and $\hat{b}_p(t) = \hat{b}_p e^{i\epsilon(p)t}$. Thus, the

average off-diagonal occupation vanishes after a long evolution time:

$$\int_0^T \left\langle \hat{b}_p^\dagger(t)\hat{b}_p^\dagger(t)\right\rangle dt = \int_0^T \left\langle \hat{b}_p^\dagger\hat{b}_p^\dagger\right\rangle e^{-2i\epsilon(p)t}dt = 0. \tag{10.15}$$

The decay of the anomalous occupations is caused by dephasing. The diagonal occupations stay unaffected.
We can represent the RPC due to definitions (2.20 - 2.21) in terms of the normal and anomalous relative occupations in order to explain the influence of the dephasing in more detail:

$$C(z,z',t) \propto e^{-\frac{1}{2}\left\langle[\hat{\theta}(\bar{z},t)-\hat{\theta}(0,t)]^2\right\rangle}, \tag{10.16}$$

where $\bar{z} = z - z'$ and

$$\begin{aligned}&\left\langle[\hat{\theta}(\bar{z},t)-\hat{\theta}(0,t)]^2\right\rangle\\ &= \int_p \frac{1}{2Kp}e^{-ap}[1-\cos(p\bar{z})](2n_p(t)+1-m_p(t)-m_p^\dagger(t))\end{aligned}$$

with $n_p(t) = \left\langle \hat{b}_p^\dagger(t)\hat{b}_p(t)\right\rangle$ and $m_p^\dagger(t) = \left\langle \hat{b}_p(t)\hat{b}_{-p}(t)\right\rangle$.
According to this, the RPC decreases due to the dephasing in time. The point z_c, above which the relative phase correlation stays constant, is continuously shifted to longer relative distances $\bar{z} = z - z'$ (cf. Fig. 10.2).[58–60] The

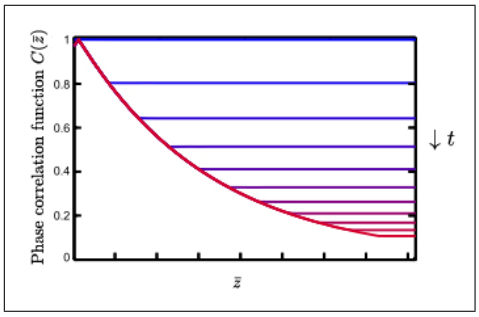

Figure 10.2: *RPC as a function of relative distance.*[60]

point z_c increases linear as a function of time (cf. Fig. 10.3)[28,60]: $z_c(t) = 2\nu t$, where ν is the characteristic Luttinger Liquid velocity. This so-called light-cone propagation is characteristic for the decay of the initial relative phase correlation in a Luttinger Liquid and indicates the local spreading of dephasing in the system.

We are motivated by these experimental and theoretical results to analyse the interplay of dephasing and interaction in two uncoupled interacting Luttinger Liquids. According to the former chapters, we have observed that due

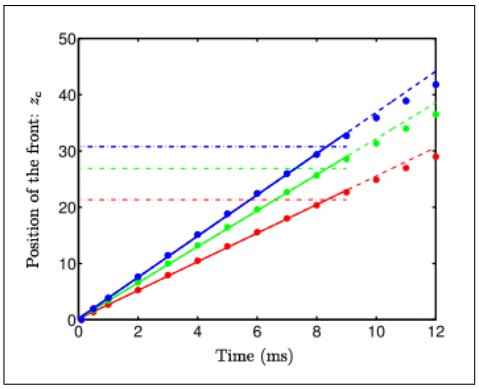

Figure 10.3: *Light-cone propagation in a Luttinger Liquid for different number of atoms (Red: 3000, Green: 6000, Blue: 9000). The horizontal dashed lines indicate half the Thomas-Fermi radius.*[60]

to the presence of interactions the system effectively thermalizes. Thus, the diagonal occupations $n_p(t)$ do not dephase and decay only in time due to phonon-phonon scattering. On the other hand, the dynamics of the anomalous occupations $m_p^\dagger$, m_p is influenced by the interplay of dephasing and interaction. Since dephasing happens on much faster time scales, the decay of the off-diagonal occupations is dominated by the dephasing process. In conclusion, we can expect to observe a signature of thermalization in the time evolution of the RPC based on the decay of the normal relative phonon density caused by the scattering processes in two uncoupled interacting Luttinger Liquids.
Moreover, we show in the main section that the initial relative mode occupation $n_p(t = 0)$ separates due to the phenomenological values (10.8 - 10.9) in two regimes: For low momenta the relative phonon density is thermal. Above a certain threshold it increases approximately linear in momentum. Former works have neglected the higher mode occupations by a high density limit.[28,58–64] However, the scattering processes in an interacting Luttinger Liquid can generate a mechanism to redistribute occupations from higher to lower momenta. Thus, we are interested in the influence of the redistriution of higher mode occupations on the time evolution of the RPC.
In the following sections we determine the kinetic equations for the system of initially coupled interacting Luttinger Liquids and compute numerically the RPC for the phenomenological inital values in the high and low mean density limit.

10.2 Green's Functions of Two Uncoupled Luttinger Liquids

10.2.1 Bare Green's Functions in Nambu Space Representation

In this section, we analyse the Green's function of a single condensate in the Nambu space representation and transform them into a rotating frame. We use these results in the following to describe two uncoupled, but interacting Luttinger Liquids.
The bare Keldysh Green's function in the Nambu space representation reads:

$$i\tilde{G}^K(p,\tau,\Delta t) = \begin{pmatrix} (2n_p+1)e^{-i2\epsilon(p)\Delta t} & 2m_p e^{-i2\epsilon(p)\tau} \\ 2m_p^\dagger e^{i2\epsilon(p)\tau} & (2n_p+1)e^{i2\epsilon(p)\Delta t} \end{pmatrix}, \tag{10.17}$$

where we used the anomalous occupation m_p and switched into a frame of relative and forward time: $\{t,t'\} \to \{\tau = \frac{t+t'}{2}, \Delta t = t-t'\}$ (cf. chapter 3).
The off-diagonal elements oscillate for a non zero anomalous occupation on a fast time scale with frequency $\omega_p = 2\epsilon(p)$. This forbids the application of the Wigner approximation, which holds in the case of a single condensate with only diagonal occupation for the inequality (5.34).[30]
For further analysis, we transform into the interaction picture:

$$\hat{b}^\dagger(t) \to \hat{b}^\dagger e^{i\epsilon(p)t}, \tag{10.18}$$

$$\hat{b}(t) \to \hat{b}\ e^{-i\epsilon(p)t}. \tag{10.19}$$

In the rotating frame, the Keldysh Green's function simplifies to:

$$i\tilde{G}^K(p,\omega) = \delta(\omega)\begin{pmatrix} (2n_p+1) & 2m_p \\ 2m_p^\dagger & (2n_p+1) \end{pmatrix}. \tag{10.20}$$

Furthermore, the retarded Green's function in the interaction picture reads:

$$\tilde{G}^R(p,\omega) = \begin{pmatrix} (\omega+i\eta)^{-1} & 0 \\ 0 & (-\omega-i\eta)^{-1} \end{pmatrix} = (\omega+i\eta)^{-1}\sigma_z, \tag{10.21}$$

where we use the Pauli matrix σ_z.
The retarded self-energy (10.21) shows that the transformation into the rotating frame shifts the two peaks centered around the dispersion relation at $\pm\epsilon(p)$ in the spectrum to zero.
Since the advanced and retarded Green's function are hermitian conjugate to

each other, which is a property independet of the specific basis, we conclude from equation (10.21):

$$\tilde{G}^A(p,\omega) = (\tilde{G}^R(p,\omega))^\dagger = (\omega - i\eta)^{-1}\sigma_z. \tag{10.22}$$

Thus, the fast oscillation of the anomalous terms in the Keldysh Green's function vanishes in the interaction picture and the Wigner approximation can still be used.

10.2.2 Single Condensate vs. Relative/Absolute Condensate Basis

We now continue to consider a good choice of basis to describe the two uncoupled condensates.[28,58–64] The global system of two uncoupled interacting Luttinger Liquids can be described in a single condensate basis with operators $\hat{b}^\dagger_{p,\alpha}/\hat{b}_{p,\alpha}$ and $\hat{b}^\dagger_{p,\beta}/\hat{b}_{p,\beta}$, where the two condensates are labeled by the indices $\{\alpha,\beta\} \in \{1,2\}$, or in a relative/absolute basis $\{\hat{b}^\dagger_p, \hat{b}_p\}/\{\hat{a}^\dagger_p, \hat{a}_p\}$. We define the following unitary transformation between both:

$$\hat{b}_{p,1} = \frac{\hat{a}_p + \hat{b}_p}{\sqrt{2}} \text{ and } \hat{b}_{p,2} = \frac{\hat{a}_p - \hat{b}_p}{\sqrt{2}}. \tag{10.23}$$

According to this, we conclude the following relations:

$$\left\langle \hat{b}^\dagger_{p,1}\hat{b}_{p,1}\right\rangle = \left\langle \hat{b}^\dagger_{p,2}\hat{b}_{p,2}\right\rangle = \frac{1}{2}(\left\langle \hat{a}^\dagger_p\hat{a}_p\right\rangle + \left\langle \hat{b}^\dagger_p\hat{b}_p\right\rangle), \tag{10.24}$$

$$\left\langle \hat{b}^\dagger_{p,1}\hat{b}_{p,2}\right\rangle = \left\langle \hat{b}^\dagger_{p,2}\hat{b}_{p,1}\right\rangle = \frac{1}{2}(\left\langle \hat{a}^\dagger_p\hat{a}_p\right\rangle - \left\langle \hat{b}^\dagger_p\hat{b}_p\right\rangle), \tag{10.25}$$

$$\left\langle \hat{b}^\dagger_{p,1}\hat{b}^\dagger_{-p,1}\right\rangle = \left\langle \hat{b}^\dagger_{p,2}\hat{b}^\dagger_{-p,2}\right\rangle = \frac{1}{2}\left\langle \hat{b}^\dagger_p\hat{b}^\dagger_{-p}\right\rangle, \tag{10.26}$$

$$\left\langle \hat{b}^\dagger_{p,1}\hat{b}^\dagger_{-p,2}\right\rangle = -\frac{1}{2}\left\langle \hat{b}^\dagger_p\hat{b}^\dagger_{-p}\right\rangle. \tag{10.27}$$

For the computations of the kinetic equations we use the single condensate basis, because of the following advantages: The mixed sector of the retarded and advanced Green's functions vanish in the single condensate basis, since operators of different condensates commute. Thus, the number of propagators for two uncoupled interacting Luttinger Liquids is reduced in the single condensate basis.
Furthermore, we benefit from the invariance of the global system by $1 \leftrightarrow 2$, which comes from the indistinguishability of both condensates.

However, we need to transform at each point in forward time from the occupations in the single condensate basis to the relative/absolute basis in order to compute the RPC (cf. equation (10.16)), which is useful for the experiment.

10.2.3 Green's Functions of Two Uncoupled Condensates

In this section, we define the notation and determine the bare Green's function for two uncoupled interacting Luttinger Liquids.
The Green's functions have in the Nambu space representation a 4×4 structure. For instance, the bare Keldysh Green's function reads:

$$i\tilde{G}^K(t,t') = \{\left(i\tilde{G}^K_{\alpha,\beta}(t,t')\right)\}|_{\alpha,\beta} = \begin{pmatrix} i\tilde{G}^K_{1,1}(t,t') & i\tilde{G}^K_{1,2}(t,t') \\ i\tilde{G}^K_{2,1}(t,t') & i\tilde{G}^K_{2,2}(t,t') \end{pmatrix}, \tag{10.28}$$

where we neglected for simplicity any space dependence.
We represent the Keldysh Green's function in the interaction picture and use that the annihilation/creation operators of different condensates commute in order to determine each block in the bare Keldysh Green's function (10.28):

$$i\tilde{G}^K_{1,2}(p,\omega) = \delta(\omega) \begin{pmatrix} 2n_{p,1,2} & 2m_{p,1,2} \\ 2m^\dagger_{p,1,2} & 2n_{p,1,2} \end{pmatrix}, \tag{10.29}$$

$$i\tilde{G}^K_{1,1}(p,\omega) = \delta(\omega) \begin{pmatrix} 2n_{p,1,1}+1 & 2m_{p,1,1} \\ 2m^\dagger_{p,1,1} & 2n_{p,1,1}+1 \end{pmatrix}, \tag{10.30}$$

where $n_{p,\alpha,\beta} = \left\langle b^\dagger_\alpha b_\beta \right\rangle (p)$ and $m_{p,\alpha,\beta} = \left\langle \hat{b}^\dagger_\alpha(p)\hat{b}^\dagger_\beta(-p) \right\rangle$.
Since both subsystems are indistinguishable, the global system is invariant under exchange of labels $1 \leftrightarrow 2$ and thus we conclude the following relations:

$$\tilde{G}^K_{2,1} = \tilde{G}^K_{1,2}|_{1\leftrightarrow 2}, \tag{10.31}$$

$$\tilde{G}^K_{2,2} = \tilde{G}^K_{1,1}|_{1\leftrightarrow 2}. \tag{10.32}$$

We continue to derive the retarded Green's function in the rotating frame for the two uncoupled interacting Luttinger Liquids and start from the following definition:

$$\tilde{G}^R(t,t') = \{\left(\tilde{G}^R_{\alpha,\beta}(t,t')\right)\}|_{\alpha,\beta} = \begin{pmatrix} \tilde{G}^R_{1,1}(t,t') & \tilde{G}^R_{1,2}(t,t') \\ \tilde{G}^R_{2,1}(t,t') & \tilde{G}^R_{2,2}(t,t') \end{pmatrix}, \tag{10.33}$$

where

$$i\tilde{G}^R_{\alpha,\beta}(t,t') = \Theta(t-t') \begin{pmatrix} \left\langle [\hat{b}^\dagger_\alpha(t), \hat{b}_\beta(t')] \right\rangle & \left\langle [\hat{b}^\dagger_\alpha(t), \hat{b}^\dagger_\beta(t')] \right\rangle \\ \left\langle [\hat{b}_\alpha(t), \hat{b}_\beta(t')] \right\rangle & \left\langle [\hat{b}_\alpha(t), \hat{b}^\dagger_\beta(t')] \right\rangle \end{pmatrix}. \tag{10.34}$$

The operators from both subsystems commute and thus the off-diagonal elements in equation (10.34) are zero:

$$\tilde{G}^R_{1,2}(p,\omega) = \tilde{G}^R_{2,1}(p,\omega) = \begin{pmatrix} 0 & 0 \\ 0 & 0 \end{pmatrix}. \tag{10.35}$$

On the other hand, the diagonal elements are equivalent to the retarded Green's function for a single condensate (cf. equation (10.21)):

$$\tilde{G}^R_{1,1}(p,\omega) = \tilde{G}^R_{2,2}(p,\omega) = (\omega + i\eta)^{-1}\sigma_z. \tag{10.36}$$

Since advanced and retarded Green's functions are hermitian, we conclude from equation (10.34 - 10.36) the following:

$$\tilde{G}^A_{1,2}(p,\omega) = \tilde{G}^A_{2,1}(p,\omega) = \begin{pmatrix} 0 & 0 \\ 0 & 0 \end{pmatrix}, \tag{10.37}$$

$$\tilde{G}^A_{1,1}(p,\omega) = \tilde{G}^A_{2,2}(p,\omega) = (\omega - i\eta)^{-1}\sigma_z. \tag{10.38}$$

In conclusion, we have determined the Green's functions in the Keldysh framework for the system of two uncoupled condensates.

10.3 Fluctuation-Dissipation Theorem in Nambu Space

In this section, the fluctuation-dissipation theorem for two uncoupled interacting Luttinger Liquids is derived.
We separate the bare Keldysh Green's function as follows:

$$\tilde{G}^K = \tilde{G}^R\, T - M\, \tilde{G}^A. \tag{10.39}$$

Since the Keldysh propagator is antihermitian, $T^\dagger = M$ is required:

$$\tilde{G}^K = \tilde{G}^R\, T - T^\dagger\, \tilde{G}^A = \begin{pmatrix} \tilde{G}^R_{1,1} & 0 \\ 0 & \tilde{G}^R_{2,2} \end{pmatrix} T - T^\dagger \begin{pmatrix} \tilde{G}^A_{1,1} & 0 \\ 0 & \tilde{G}^A_{2,2} \end{pmatrix}. \tag{10.40}$$

We use a general structure for T in order to solve equation (10.40):

$$T = \begin{pmatrix} a & b \\ c & d \end{pmatrix}, \tag{10.41}$$

where a,b,c and d are complex numbers.
Together with the explicit representation of the Keldysh, retarded and advanced Green's functions for two uncoupled condensates in Nambu space, we determine the following structure for T:

$$T = \begin{pmatrix} \sigma_z & 0 \\ 0 & \sigma_z \end{pmatrix} \begin{pmatrix} F_{1,1} & F_{1,2} \\ F_{2,1} & F_{2,2} \end{pmatrix} = \Sigma_z F, \tag{10.42}$$

where

$$F_{\alpha,\alpha} = \begin{pmatrix} 2n_{p,\alpha,\alpha} + 1 & 2m_{p,\alpha,\alpha} \\ 2m^{\dagger}_{p,\alpha,\alpha} & 2n_{p,\alpha,\alpha} + 1 \end{pmatrix} \tag{10.43}$$

and

$$F_{\alpha,\beta}|_{\alpha\neq\beta} = \begin{pmatrix} 2n_{p,\alpha,\beta} & 2m_{p,\alpha,\beta} \\ 2m^{\dagger}_{p,\alpha,\beta} & 2n_{p,\alpha,\beta} \end{pmatrix}. \tag{10.44}$$

According to this, the fluctuation-dissipation theorem for two condensates in Nambu space reads:

$$\tilde{G}^K = \tilde{G}^R \, \Sigma_z F - F \Sigma_z \, \tilde{G}^A. \tag{10.45}$$

We generalize equation (10.45) in the same manner as for a single condensate and define the following relation with a hermitian operator $\Sigma_z F$:

$$G^K = G^R \circ \Sigma_z \circ F - F \circ \Sigma_z \circ G^A, \tag{10.46}$$

where $G^{R/A}$ and G^K are the dressed Green's functions. Relation (10.46) equals the fluctuation-dissipation theorem for a time and space translation invariant system.
In the following sections, we make use of this relation in order to derive the kinetic equations for two uncoupled interacting Luttinger Liquids.

10.4 Kinetic Equations for Two Uncoupled Condensates

We define the inverse dressed Green's function as the difference of the inverse bare Green's function and the self-energy. The self-energy is generated by the interactions, which renormalizes the bare theory (cf. equation (5.10)).

According to chapter 4, we consider that the self-energies are purely imaginary and their frequencies are pinned on the dispersion relation.
Then, we define the retarded, advanced and Keldysh self-energy:

$$\Sigma^K(p) = \{\left(\Sigma^K_{\alpha,\beta}(p)\right)\}|_{\alpha,\beta} = \begin{pmatrix} \Sigma^K_{1,1}(p) & \Sigma^K_{1,2}(p) \\ \Sigma^K_{2,1}(p) & \Sigma^K_{2,2}(p) \end{pmatrix}, \tag{10.47}$$

with

$$\Sigma^K_{\alpha,\beta}(p) = -i \begin{pmatrix} 2\sigma^K_{\alpha,\beta}(p) & 2\Phi^K_{\alpha,\beta}(p) \\ 2\Phi^K_{\alpha,\beta}(p) & 2\sigma^K_{\alpha,\beta}(p) \end{pmatrix}, \tag{10.48}$$

$$\Sigma^{R/A}(p) = \{\left(\Sigma^{R/A}_{\alpha,\beta}(p)\right)\}|_{\alpha,\beta} = \begin{pmatrix} \Sigma^{R/A}_{1,1}(p) & 0 \\ 0 & \Sigma^{R/A}_{2,2}(p) \end{pmatrix}, \tag{10.49}$$

with

$$\Sigma^{R/A}_{\alpha,\beta}(p) = -i \begin{pmatrix} \pm\sigma^{R/A}(p) & \pm\Phi^{R/A}(p) \\ \pm\Phi^{R/A}(p) & \pm\sigma^{R/A}(p) \end{pmatrix}. \tag{10.50}$$

The off-diagonal entries of the retarded and advanced self-energy in equation (10.50) are zero.[30] We evaluate the convolution integrals in Wigner approximation (cf. chapter 3) in order to derive the kinetic equations for the uncoupled condensates. In the first step, we separate each dressed Green's function in equation (10.46) into its bare and self-energy component:

$$(\tilde{G}^R)^{-1} \circ F \circ \Sigma_z - \Sigma_z \circ F \circ (\tilde{G}^A)^{-1} = \Sigma^K - (\Sigma^R \circ F \circ \Sigma_z - \Sigma_z \circ F \circ \Sigma^A) = I_{\text{coll}}. \tag{10.51}$$

In order to evaluate the convolution integrals, we use the following relation[51]:

$$C(x,p) = A(x,p) e^{\frac{i}{2}(\overleftarrow{\partial}_x \overrightarrow{\partial}_p - \overleftarrow{\partial}_p \overrightarrow{\partial}_x)} B(x,p), \tag{10.52}$$

where $C(x_1,x_2) = A(x_1,x_3) \circ B(x_3,x_2)$ and $A(x,p) = WT\{A(x_1,x_2)\}$ and $B(x,p) = WT\{B(x_1,x_2)\}$, where $x = \{\vec{r},\tau\}$ and $p = \{\vec{p},\omega\}$.
We expand the collision integral in equation (10.51) to first order (cf. equation (5.29)) and apply the Wigner approximation, which is valid for the following inequality:

$$\frac{(\partial_\omega \Sigma^{R/A} \partial_\tau (\Sigma_z F))|_{ij}}{(\Sigma^{R/A}\Sigma_z F)|_{ij}} \ll 1, \tag{10.53}$$

where $|_{ij}$ indicates the element $\{i,j\}$ of the 4×4 matrix in the denominator/nominator of equation (10.53). The inequality must hold for all elements,

which is simplified here, since all components have the same time scale. In this case, the collision integral reads:

$$I_{\text{coll}} = \Sigma^K - (\Sigma^R \circ F \circ \Sigma_z - \Sigma_z \circ F \circ \Sigma^A) \approx \Sigma^K - (\Sigma^R \Sigma_z F - F \Sigma_z \Sigma^A). \tag{10.54}$$

The left hand side of equation (10.51) is evaluated to first order and reads:

$$(\tilde{G}^R)^{-1} \circ F \circ \Sigma_z - \Sigma_z \circ F \circ (\tilde{G}^A)^{-1} \approx -i\partial_\tau (\Sigma_z F \Sigma_z). \tag{10.55}$$

In conclusion, the following kinetic equation describes the dynamics of two uncoupled interacting Luttinger Liquids:

$$-i\partial_\tau \tilde{F} = \Sigma^K - (\Sigma^R \tilde{F} \Sigma_z - \Sigma_z \tilde{F} \Sigma^A), \tag{10.56}$$

where $\tilde{F} = \Sigma_z F \Sigma_z$.
The external frequency is now pinned on the singularity $\omega = \pm i\sigma^R(p)|_{\omega=0}$ of $\mathcal{B}(\mathbf{p}) = G^R(\mathbf{p}) - G^A(\mathbf{p})$ as follows:

$$\frac{i}{2\pi} \int_\omega \mathcal{B}(\mathbf{p}) \tilde{F}(\mathbf{p}) = \Sigma_z \tilde{F}(\mathbf{p})|_{\omega = +i\sigma^R(p)}. \tag{10.57}$$

According to this, the following kinetic equations are derived from equation (10.56):

$$\partial_\tau n_{p,1,1}(\tau) = \sigma^K_{1,1}(p) - \sigma^R(p)(2n_{p,1,1}(\tau) + 1), \tag{10.58}$$

$$\partial_\tau n_{p,2,1}(\tau) = \sigma^K_{2,1}(p) - \sigma^R(p) 2n_{p,2,1}(\tau), \tag{10.59}$$

$$\partial_\tau m_{p,1,1}(\tau) = \Phi^K_{1,1}(p) - \sigma^R(p) 2m_{p,1,1}(\tau). \tag{10.60}$$

Equation (10.58) is equivalent to the kinetic equation (6.31) for a single condensate, where $n_p \to n_{p,1,1}$. As we have shown in section 8.5, the Wigner approximation holds for a single interacting Luttinger Liquid as long as the low-energy description is correct. The same approximation is valid for the diagonal occupation $n_{p,1,1}$. Since all occupations in (10.58 - 10.60) have the same time scale, the Wigner approximation breaks down after the interacting Luttinger Liquid description.
We continue to analyse the diagrammatic structure of the Keldysh self-energy $(10.47 - 10.48)$ in order to determine the kinetic equation for $n_{p,2,1}$ and $m_{p,1,1}$.

10.5 Self-Energy in a Diagrammatic Approach

We consider a generalized diagram in order to determine the necessary diagrammatic contributions to the Keldysh self-energies $\sigma^K_{2,1}(p)$ and $\Phi^K_{1,1}(p)$. In this chapter we neglect vertex corrections.[30]

10.5.1 Generalized Diagram

In the presence of diagonal and off-diagonal occupations we need to consider nine different possible propagators, which are summarized in Fig. 10.4 with the index q in $\hat{b}^\dagger_{q,\alpha},\ \hat{b}_{q,\alpha}$ for a quantum field line.

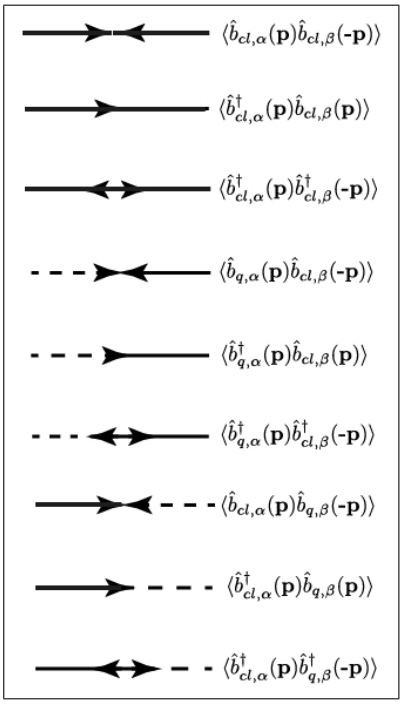

Figure 10.4: *Propagators due to the off-diagonal and diagonal occupations in a uncoupled interacting Luttinger Liquid.*

A generalized diagram of the Keldysh self-energy (cf. Fig. 10.5) is used to identify the possible combinations of propagators. The single field lines in Fig. 10.5 are labeled by a momentum $\{\tilde{\mathbf{p}}, \tilde{\mathbf{q}}, \tilde{\mathbf{k}}, \mathbf{p}, \mathbf{q}, \mathbf{k}\}$ and a direction index $r_i^\alpha = \pm 1$, where $\alpha \in \{1, 2\}$ stands for the condensate and i for the momentum. The direction index r_i^α indicates the type of operator associated with the field line:

$$r_i^\alpha = 1 \leftrightarrow \hat{a}^\dagger_{cl/q}(i), \tag{10.61}$$

$$r_i^\alpha = -1 \leftrightarrow \hat{a}_{cl/q}(i). \tag{10.62}$$

Since any vertex correction is neglected, the outgoing and ingoing lines connected with the same vertex need to have the same condensate index (cf. Fig. 10.5). The resonance conditions at each vertex and the frequency / momentum conservation in the propagators (cf. Fig. 10.5) require the

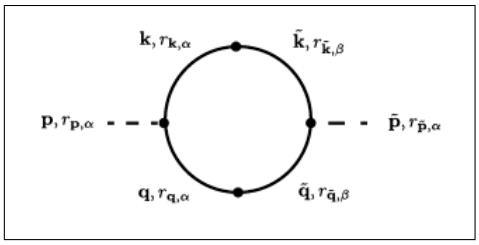

Figure 10.5: *Generalized Diagram of the Keldysh Self-Energy.*

following constraints[30]:

$$\mathbf{k} r^{\alpha}_{\mathbf{k}} = \tilde{\mathbf{k}} r^{\beta}_{\tilde{\mathbf{k}}}, \tag{10.63}$$

$$\mathbf{q} r^{\alpha}_{\mathbf{q}} = \tilde{\mathbf{q}} r^{\beta}_{\tilde{\mathbf{q}}}, \tag{10.64}$$

$$\mathbf{p} r^{\alpha}_{\mathbf{p}} = \tilde{\mathbf{p}} r^{\beta}_{\tilde{\mathbf{p}}}, \tag{10.65}$$

$$\mathbf{p} r^{\alpha}_{\mathbf{p}} + \mathbf{k} r^{\alpha}_{\mathbf{k}} + \mathbf{q} r^{\alpha}_{\mathbf{q}} = 0, \tag{10.66}$$

$$\tilde{\mathbf{p}} r^{\beta}_{\tilde{\mathbf{p}}} + \tilde{\mathbf{k}} r^{\beta}_{\tilde{\mathbf{k}}} + \tilde{\mathbf{q}} r^{\beta}_{\tilde{\mathbf{q}}} = 0, \tag{10.67}$$

$$r^{\alpha}_{\mathbf{q}} r^{\beta}_{\tilde{\mathbf{q}}} + r^{\alpha}_{\mathbf{p}} r^{\beta}_{\tilde{\mathbf{p}}} = 2 r^{\alpha}_{\mathbf{k}} r^{\beta}_{\tilde{\mathbf{k}}}. \tag{10.68}$$

The last condition (10.68) is a consequence of the two independent resonance conditions at each vertex. From this relation we directly conclude:

$$r^{\alpha}_{\mathbf{q}} r^{\beta}_{\tilde{\mathbf{q}}} = r^{\alpha}_{\mathbf{p}} r^{\beta}_{\tilde{\mathbf{p}}} = r^{\alpha}_{\mathbf{k}} r^{\beta}_{\tilde{\mathbf{k}}}. \tag{10.69}$$

We continue to evaluate the self-energies $\sigma^{K}_{2,1}(p)$, $\Phi^{K}_{1,1}(p)$ and use equation (10.69) to simplify the computations.

10.5.2 Keldysh Self-Energy for Two Uncoupled Condensates

The following diagrammatic approach is due to the argumentation in chapter 6 performed in a self-consistent Born approximation.

Diagrammatic Approach for $\sigma^{K}_{2,1}(p)$ and the Kinetic Equation for the Mixed Diagonal Occupation $n_{p,2,1}$

The retarded and advanced self-energy are zero in the mixed blocks $\Sigma^{R/A}_{2,1}(p)$ and $\Sigma^{R/A}_{1,2}(p)$ (cf. equation (10.49)). Furthermore, just diagonal Green's functions contribute due to relation (10.69) to the diagonal elements of the Keldysh self-energy (cf. Fig. 10.6): $r^{\alpha}_{\mathbf{q}} r^{\beta}_{\mathbf{q}} = r^{\alpha}_{\mathbf{p}-\mathbf{q}} r^{\beta}_{\mathbf{p}-\mathbf{q}} = r^{\alpha}_{\mathbf{p}} r^{\beta}_{\mathbf{p}} = 1$.

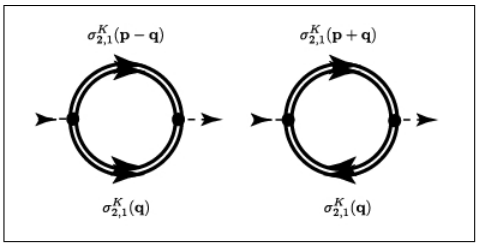

Figure 10.6: *Mixed diagonal Keldysh self-energy.*

According to this, we determine the following analytic equation for the mixed diagonal Keldysh self-energy:

$$\begin{aligned}&-\sigma^K_{2,1}(p) \qquad (10.70)\\ &=\frac{1}{4\pi^2}\int_{\mathbf{q}}[2\sigma^K_{2,1}(\mathbf{p}-\mathbf{q})\sigma^K_{2,1}(\mathbf{q})|qp(p-q)|v_0^2+4\sigma^K_{2,1}(\mathbf{p}+\mathbf{q})\sigma^K_{2,1}(\mathbf{q})|qp(p+q)|v_0^2]\end{aligned}$$

The kinetic equation for the mixed diagonal occupation

$$\partial_\tau n_{p,2,1}(\tau)=\sigma^K_{2,1}(p)-\sigma^R(p)2n_{p,2,1}(\tau) \qquad (10.71)$$

consists of the retarded self-energy, which is due to relation (10.69) identical to the case of a single condensate (6.35). According to this, we derive in the same manner as in chapter 6 the following kinetic equation:

$$\begin{aligned}&\partial_{\tilde\tau} n_{p,2,1}(\tau) \qquad (10.72)\\ &=\frac{1}{2\pi}\int_{0<q<p}\frac{qp(p-q)}{\tilde\sigma^R(p)+\tilde\sigma^R(q)+\tilde\sigma^R(p-q)}[n_{p-q,2,1}n_{q,2,1}-n_{p,2,1}(n_{p-q,1,1}+n_{q,1,1}+1)]\\ &+\frac{1}{2\pi}\int_{0<q}\frac{2qp(p+q)}{\tilde\sigma^R(p)+\tilde\sigma^R(q)+\tilde\sigma^R(p+q)}[n_{p+q,1,1}n_{p,2,1}+n_{p+q,2,1}n_{q,2,1}-n_{q,1,1}n_{p,2,1}],\end{aligned}$$

where v_0 is absorbed in the forward time and the self energy.

Diagrammatic Approach for $\Phi^K_{1,1}(p)$ and the Kinetic Equation for the Off-Diagonal Occupation $m_{p,1,1}$

The off-diagonal self-energy $\Phi^K_{1,1}(p)$ is due to relation (10.69) computed from the two diagrams in Fig. 10.7 and reads:

$$\begin{aligned}&-\Phi^K_{1,1}(p) \qquad (10.73)\\ &=\frac{1}{4\pi^2}\int_{\mathbf{q}}[2\Phi^K_{1,1}(\mathbf{p}-\mathbf{q})\Phi^K_{1,1}(\mathbf{q})|qp(p-q)|v_0^2+4\Phi^K_{1,1}(\mathbf{p}+\mathbf{q})\Phi^K_{1,1}(\mathbf{q})|qp(p+q)|v_0^2]\end{aligned}$$

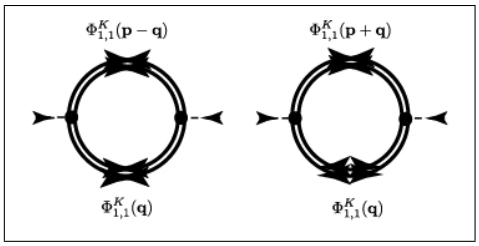

Figure 10.7: *Off-diagonal Keldysh self-energy.*

Since the retarded self-energy is identical to the case of a single condensate in equation (6.35), we conclude for the kinetic (10.60):

$$\begin{aligned}&\partial_{\bar{\tau}} m_{p,1,1}(\tau) \qquad (10.74)\\ &= \frac{1}{2\pi}\int_{0<q<p} \frac{qp(p-q)}{\tilde{\sigma}^R(p)+\tilde{\sigma}^R(q)+\tilde{\sigma}^R(p-q)}[m_{p-q,1,1}m_{q,1,1} - m_{p,1,1}(n_{p-q,1,1}+n_{q,1,1}+1)]\\ &+ \frac{1}{2\pi}\int_{0<q} \frac{2qp(p+q)}{\tilde{\sigma}^R(p)+\tilde{\sigma}^R(q)+\tilde{\sigma}^R(p+q)}[n_{p+q,1,1}m_{p,1,1} + m_{p+q,1,1}m_{q,1,1} - n_{q,1,1}m_{p,1,1}],\end{aligned}$$

where v_0 is according to chapter 8 absorbed in the forward time and the self-energy.
In conclusion, we have computed the kinetic equations for the single condensate distributions $n_{p,1,1}$, $n_{p,2,1}$ and $m_{p,1,1}$. The self-consistent equation for the retarded self-energy is identical to the case of a single interacting Luttinger Liquid, since the diagrams of the diagonal self-energies consist due to constraint (10.69) just of diagonal propagators.

10.6 Numerical Implementation

In this section, we discuss the numerical implementation of the retarded self-energy and the kinetic equations (8.1), (10.66), (10.68).

10.6.1 Phenomenological Initial Conditions

The phenomenological initial values for the relative phase and density correlations (cf. equations (10.8) and (10.9)) are transformed in the single condensate basis of annihilation and creation operators.
We use the Bogoliubov transformation (2.20 - 2.21) in order to represent the relative phase and density correlations in terms of relative anomalous and

normal occupations:

$$2\left\langle \hat{b}_p^\dagger \hat{b}_p \right\rangle + 1 = \frac{\pi}{K|p|}\left\langle \hat{\rho}_p \hat{\rho}_{-p} \right\rangle + \frac{K|p|}{\pi}\left\langle \hat{\theta}_p \hat{\theta}_{-p} \right\rangle, \tag{10.75}$$

$$2\left\langle \hat{b}_p^\dagger \hat{b}_{-p}^\dagger \right\rangle + 2\left\langle \hat{b}_{-p} \hat{b}_p \right\rangle = \frac{2\pi}{K|p|}\left\langle \hat{\rho}_p \hat{\rho}_{-p} \right\rangle - \frac{2K|p|}{\pi}\left\langle \hat{\theta}_p \hat{\theta}_{-p} \right\rangle. \tag{10.76}$$

Due to the initial conditions for the relative phase correlation $\left\langle \hat{\theta}_p \hat{\theta}_{-p} \right\rangle(\tilde{\tau} = 0) = \frac{2}{\rho_0}$ and the relative density correlation $\langle \hat{\rho}_p \hat{\rho}_{-p} \rangle(\tilde{\tau} = 0) = \frac{\rho_0}{2}$, we conclude from equations (10.75 - 10.76) the following[28,58–60]:

$$2\left\langle \hat{b}_p^\dagger \hat{b}_p \right\rangle(\tilde{\tau} = 0) + 1 = \frac{\pi}{K|p|}\frac{\rho_0}{2} + \frac{K|p|}{\pi}\frac{2}{\rho_0}, \tag{10.77}$$

$$2\left\langle \hat{b}_p^\dagger \hat{b}_{-p}^\dagger \right\rangle(\tilde{\tau} = 0) + 2\left\langle \hat{b}_p \hat{b}_{-p} \right\rangle(\tilde{\tau} = 0) = \frac{\pi}{K}\frac{\rho_0}{|p|} - \frac{K|p|}{\pi}\frac{4}{\rho_0}. \tag{10.78}$$

The diagonal distribution in the absolute basis is after the splitting thermal with a temperature T[63,64]:

$$\left\langle \hat{a}_p^\dagger \hat{a}_p \right\rangle(\tilde{\tau} = 0) \approx \frac{T}{u|p|} \text{ and } \langle \hat{a}_p \hat{a}_{-p} \rangle(\tilde{\tau} = 0) = \left\langle \hat{a}_p^\dagger \hat{a}_{-p}^\dagger \right\rangle(\tilde{\tau} = 0) = 0. \tag{10.79}$$

We represent these phenomenological initial values with equations (10.24 - 10.27) in the single condensate basis:

$$\left\langle \hat{b}_{p,\alpha}^\dagger \hat{b}_{p,\alpha} \right\rangle(\tilde{\tau} = 0) = \frac{1}{2}\left(\frac{T}{u|p|} + \frac{\pi}{K|p|}\frac{\rho_0}{2} + \frac{K|p|}{\pi}\frac{2}{\rho_0} - \frac{1}{2}\right), \tag{10.80}$$

$$\left\langle \hat{b}_{p,\alpha}^\dagger \hat{b}_{p,\beta} \right\rangle(\tilde{\tau} = 0) = \frac{1}{2}\left(\frac{T}{u|p|} - \frac{\pi}{K|p|}\frac{\rho_0}{2} - \frac{K|p|}{\pi}\frac{2}{\rho_0} + \frac{1}{2}\right), \tag{10.81}$$

$$\left\langle \hat{b}_{p,\alpha}^\dagger \hat{b}_{-p,\alpha}^\dagger \right\rangle(\tilde{\tau} = 0) = \frac{\pi}{4K|p|}\rho_0 - \frac{K|p|}{\pi\rho_0}. \tag{10.82}$$

10.6.2 Numerical Routine for Two Uncoupled Interacting Luttinger Liquids

We apply a similar numerical routine as in chapter 8 to determine the dynamics of the two uncoupled interacting Luttinger Liquids. First, the retarded self-energy is computed by the self-consistent equation (8.2). The numerical evaluation is implemented with the initial values (10.80 - 10.82).

Subsequently, we solve the kinetic equations (8.1),(10.72) and (10.74) in order to determine the corresponding distributions at time step $\tilde{\tau} + \delta\tilde{\tau}$ in

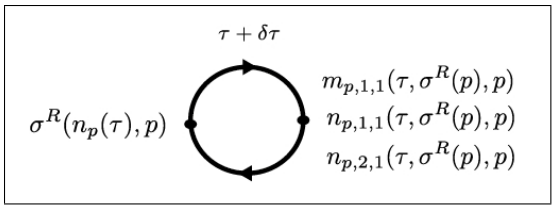

Figure 10.8: *Routine for solving a system of differential equations for two uncoupled interacting Luttinger Liquids.*

the single condensate basis. These are then represented in the relative and absolute condensate basis.
We continue to compute the RPC at $\tilde{\tau} + \delta\tilde{\tau}$:

$$C(\bar{z} = z - z', \tilde{\tau} + \delta\tilde{\tau}) \propto e^{-\frac{1}{2}\left\langle[\hat{\theta}(\bar{z},\tilde{\tau}+\delta\tilde{\tau})-\hat{\theta}(0,\tilde{\tau}+\delta\tilde{\tau})]^2\right\rangle}, \tag{10.83}$$

where

$$\begin{aligned}&\left\langle[\hat{\theta}(\bar{z},\tilde{\tau}+\delta\tilde{\tau})-\hat{\theta}(0,\tilde{\tau}+\delta\tilde{\tau})]^2\right\rangle\\ =&\int_p \frac{1}{2Kp}e^{-\alpha p^2}[1-\cos(p\bar{z})](2n_p(\tilde{\tau}+\delta\tilde{\tau})+1-m_p(\tilde{\tau}+\delta\tilde{\tau})-m_p^\dagger(\tilde{\tau}+\delta\tilde{\tau})).\end{aligned}$$

Afterwards, the retarded self-energy is evaluated from $n_{p,1,1}$ at $\tilde{\tau} + \delta\tilde{\tau}$. This numerical routine is repeated until the evaluation reaches the final forward time $\tilde{\tau}_f$.

10.6.3 Numerical Results

In the following the numerical results of the uncoupled interacting Luttinger Liquids are summarized in the case of two different initial conditions.
First, we consider the initial values for the correlations in the single condensate basis in the large density limit:

$$\left\langle\hat{b}_{p,\alpha}^\dagger\hat{b}_{p,\alpha}\right\rangle(\tilde{\tau}=0) \approx \frac{1}{2}(\frac{T}{u|p|}+\frac{\pi}{K|p|}\frac{\rho_0}{2}-\frac{1}{2}), \tag{10.84}$$

$$\left\langle\hat{b}_{p,\alpha}^\dagger\hat{b}_{p,\beta}\right\rangle(\tilde{\tau}=0) \approx \frac{1}{2}(\frac{T}{u|p|}-\frac{\pi}{K|p|}\frac{\rho_0}{2}+\frac{1}{2}), \tag{10.85}$$

$$\left\langle\hat{b}_{p,\alpha}^\dagger\hat{b}_{-p,\alpha}^\dagger\right\rangle(\tilde{\tau}=0) = \frac{\pi}{4K|p|}\rho_0. \tag{10.86}$$

We can make a separation of the behaviour of the RPC into three different regimes. Fig. 10.9 a) shows the RPC (10.83) for a Luttinger Liquid. We observe that the dephasing of the anomalous occupations $m_p(\tilde{\tau})$, $m_p^\dagger(\tilde{\tau})$ causes

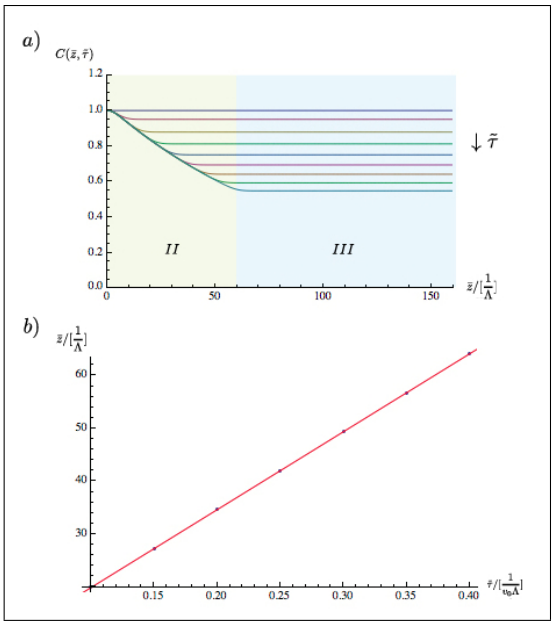

Figure 10.9: *Dephasing in a Luttinger Liquid without interactions* ($\frac{T}{p_L} = \frac{10}{\pi}$)*: a) RPC at different times with step size* $\Delta\tilde{\tau} = 0.05\frac{1}{v_0\Lambda}$*. For each time step the correlation is constant above a certain threshold in the relative distance (regime III). The RPC decreases below this point linearly in space (regime II). b) Light-cone propagation due to the dephasing process in a Luttinger Liquid.*

a continuous increase of the relative distance, above which the relative phase is constant. At $\tilde{\tau} = 0$ the RCP equals one, since the relative phase after the splitting is perfectly correlated. However, the correlation decays linearly for $\tilde{\tau} > 0$ as a consequence of dephasing (regime II) and is constant above a distinct threshold (regime III). This local spreading of the dephasing process is well known as a light-cone propagation. Fig. 10.9 b) shows the relative distance as a function of the forward time, which has a characteristic linear increase of 2ν.

On the other hand, we determine a new regime in the RPC for an interacting Luttinger Liquid, where the decay of the correlation is caused by dephasing and scattering (cf. Fig. 10.10, regime I). This regime shows an exponential decay of the RPC caused by the interaction. However, the dephasing happens on much faster time scales than the interaction and thus propagates further. Thus, at longer relative distances a second regime is determined, where the RPC decays linearly due to the bare dephasing. Finally, the RPC is again constant above a certain threshold in the relative distance.

The value of the RPC at $\bar{z} \to \infty$ is determined by the exponential decay due to the interactions in regime I (cf. Fig. 10.10). Indeed, we show in Fig.

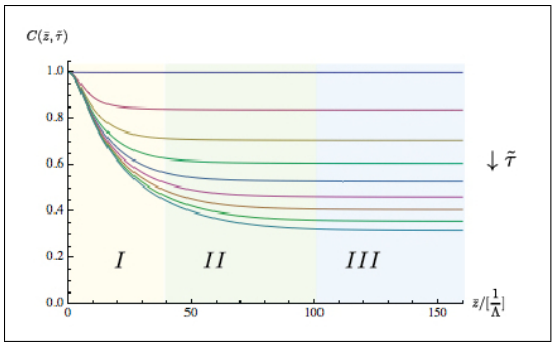

Figure 10.10: *Dephasing in an interacting Luttinger Liquid* ($\frac{T}{p_L} = \frac{10}{\pi}$)*: RPC at different times with step size* $\Delta\tilde{\tau} = 0.05\frac{1}{v_0\Lambda}$*. Due to the interactions in the system the RPC decays in regime I exponentially. In an intermediate regime II the correlation decays linearly, since the effect of interactions has not reached this distance but dephasing has. Above a certain threshold in the relative distance the RPC is constant (regime III).*

10.11 that $C(\bar{z} \to \infty, \tilde{\tau}) \propto e^{-2.58\tilde{\tau}}$. For a Luttinger Liquid without interactions $C(\bar{z} \to \infty, \tilde{\tau})$ decays algebraically (cf. Appendix C).
In conclusion, dephasing and interactions spread locally through each condensate. On small relative distances the overlap of both effects cause an exponential decay of the RPC. Since the dephasing propagates faster than the interactions through the condensate, we observe an algebraic regime on intermediate relative distances, where dephasing is present but no interactions. Finally, for large relative distances the RPC is constant.
We now initialize the numerical evaluation with the full equations (10.80 -

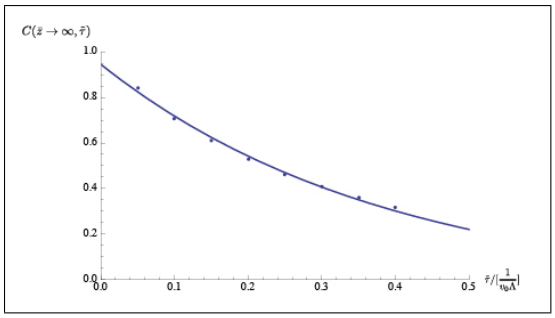

Figure 10.11: *The correlation* $C(\bar{z} \to \infty, \tilde{\tau})$ *based on the data in Fig. 10.10 decays exponential as a function of forward time* $\tilde{\tau}$ *for an interacting Luttinger Liquid.*

10.82). According to this, the correlations in the single and relative condensate basis are approximately thermal for low momenta and increase linearly above a certain threshold.

For a pure Luttinger Liquid without interactions the RPC separates into two regimes (cf. Fig. 10.12): It starts at small relative distances to decrease by dephasing and reaches a local minimum (cf. Fig. 10.12, regime I). Afterwards, the phase correlation increases again for a short relative distance and stays above a threshold constant (regime III).
We now switch on the interactions in the two uncoupled Luttinger Liquids.

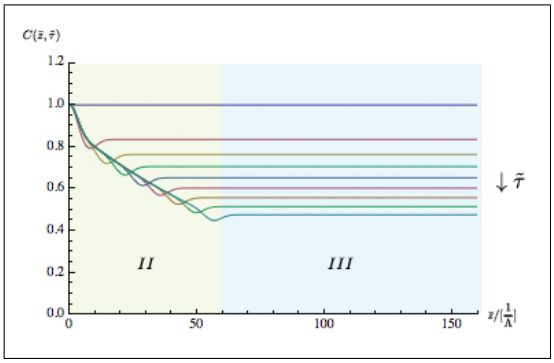

Figure 10.12: *Dephasing in a Luttinger Liquid without interactions* ($\frac{T}{p_L} = \frac{10}{\pi}$)*: RPC at different times with step size* $\Delta\tilde{\tau} = 0.05\frac{1}{v_0\Lambda}$*. The correlation is for each time step constant above a certain threshold in the relative distance (regime III). Below this point in space the RPC decreases linearly in space until a local minimum is reached, above which it increases until regime III.*

As a consequence, higher momentum occupations are redistributed, which influences the decay of the RPC (cf. Fig. 10.13). Again, we determine a

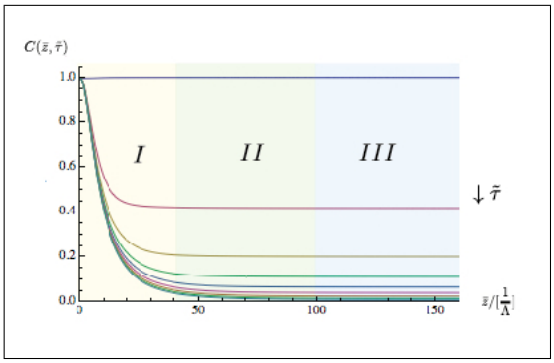

Figure 10.13: *Dephasing in an interacting Luttinger Liquid* ($\frac{T}{p_L} = \frac{10}{\pi}$)*: RPC at different times with step size* $\Delta\tilde{\tau} = 0.05\frac{1}{v_0\Lambda}$*. The RPC decays in regime I exponential due to the interaction in the system. In an intermediate regime II the correlation runs linear, since the dephasing passed the interaction. And above a certain threshold in the relative distance the RPC is constant (regime III).*

regime for small relative distances, where the RPC drops of exponentially. We determine from the data in Fig. 10.13 $C(\bar{z} \to \infty, \tilde{\tau}) \propto e^{-15\tilde{\tau}}$, which confirms this assumption. In comparison to the case of fully thermal initial values, the exponential decay is much stronger (cf. Fig. 10.11).
In conclusion, we analysed the RPC for two different initial values and showed that the presence of interaction lead to a new regime in the RPC with an exponetial decay. The RPC is above a certain threshold in the relative distance constant.
Further analysis is needed to characterize the interplay of dephasing and interaction in order to find an analytic expression for the strength of the exponential decay.

Chapter 11

Conclusion

In chapter 1 to 9 we have investigated a thermalization mechanism in a driven interacting Luttinger Liquid derived from a microscopic model of interacting bosons in an optical lattice subjected to a permanent heating due to spontaneous emission. For this purpose, from the Keldysh path integral formalism we determined a quantum Boltzmann equation for the phonon density and computed the time evolution for a low and finite temperature initial state. The numerical results show that for both initial states, in the high momentum regime the diagonal phonon density effectively thermalizes to a time dependent effective temperature. Moreover, below a certain crossover momentum $p_0(\tau) \propto \tau^{-\frac{4}{5}}$ the phonon density shows a universal scaling regime for which it scales linearly in momentum, which does not correspond to any equilibrium counterpart and is a clear nonequilibrium scaling regime. This behaviour is protected by the vertex structure of the phonon scattering processes and is generic for an interacting Luttinger Liquid.
In the case of an initial finite temperature state the numerical results of the phonon density show a thermal regime for low momenta. In an analytic approach we verified that for small momenta the phonon density is pinned to its initial value.
Finally, we derived a relation between the scaling exponents of the phonon density and the quasiparticle lifetime. We identified a new universal scaling exponent for the quasiparticle lifetime from the linear regime in the phonon density: $\tau_{qp} \propto p^{-\frac{5}{3}}$.
In view of this work it would be interesting to study the modification of the phonon lifetime by interactions in an appropriate experiment. Moreover, the question arises if and in which way more classes of driven one dimensional systems are able to show universal nonequilibrium behaviour and could be even summarized in universality classes.
In chapter 10 we have investigated two uncoupled interacting Luttinger Liq-

uids initialized in a state with perfect phase coherence between the liquids. We derived the quantum Boltzmann equations in the Keldysh framework for the kinetics of the normal and anomalous occupations. In the large density limit, the initial relative phonon occupation is to a good approximation thermal. The numerical results show that without interactions the relative phase correlation decays locally with the characteristic velocity 2ν. In the presence of interactions, we identify a new regime in the relative phase correlation function for low relative distances, where the initial perfect phase correlation decays exponentially.
Moreover, for a finite mean density, above a certain momentum threshold the phenomenological initial values show a linearly increasing occupation of the relative excitations, which is responsible for a large energy of the system after the quench, stored in the UV regime. This induces a faster thermalization process with a stronger exponential decay of the relative phase function for low relative distances.
As a future work it would be interesting to compare the findings with experimental results and to observe signatures of thermalization in experiments. Furthermore, the precise initial state after the splitting has not been computed theoretically. The model of two uncoupled interacting Luttinger Liquids are a promising system for further theoretical and experimental analysis of the interplay between interaction and dephasing.

Appendices

Appendix A

Luttinger Liquid Formalism

A.1 Field Operators in Real Space

Restricting the mobility of atoms to one dimension, e.g. ordering them in a quantum wire, effects strongly the excitation spectrum of the physical system.[19,20,38] Single particle-hole excitations are strongly surpressed and replaced by collective modes comparable to newton's cradle. In 1981 Haldane took this intuitive picture and proposed a new universality class, called Luttinger Liquids[16–19], including a large number of massless one dimensional systems that are well described at low temperatures in a hydrodynamic theory. The two significant properties of these models are:

1. Linear dispersion.
2. Algebraic decay of correlation functions at zero temperature with exponents only depending on the two system parameters.

In this theory the collective fields are defined in a polar description by

$$\hat{b}^{\dagger}(x) = \sqrt{\hat{\rho}(x)} e^{-i\hat{\theta}(x)}, \tag{A.1}$$

where $\hat{\rho}(x) = \sum_i \delta(x - x_i)$. The density is rewritten using the field $\hat{\phi}(x)$

$$\hat{\rho}(x) = [\rho_0 - \frac{1}{\pi}\partial_x \hat{\phi(x)}] \sum_l e^{i2l(\pi\rho_0 x - \hat{\phi}(x))}, \tag{A.2}$$

where the average dennsity is $\rho_0 = \langle\hat{\rho}(x)\rangle$. The conservation of the bosonic commutation relation forces the fields $\hat{\phi}(x)$ and $\hat{\theta}(x)$ to fullfill

$$[\hat{\rho}(x), \hat{\theta}(x^{'})] = i\delta(x - x^{'}).$$

This relation is well known in the superfluid theory, where phase and density are canonical conjugated fields. In summary the complete bosonic annihilation operator in the Luttinger Liquid theory is given by

$$\hat{b}^{\dagger}(x) = \sqrt{[\rho_0 - \frac{1}{\pi}\partial_x\hat{\phi}(x)]}\sum_l e^{i2l(\pi\rho_0 x - \hat{\phi}(x))}e^{-i\hat{\theta}(x)}. \tag{A.3}$$

In the case of low energy excitations the derivation of the density from the average value ρ_0 is negligible and just the term $l = 0$ remains

$$\hat{b}^{\dagger}(x) \simeq \sqrt{[\rho_0 - \frac{1}{\pi}\partial_x\hat{\phi}(x)]}e^{-i\hat{\theta}(x)}. \tag{A.4}$$

For instance we determine from equation (A.4) the probability current in a one dimensional system of bosons in the low-energy regime:

$$\hat{j}(x) = \frac{\hbar}{m}\mathrm{Im}(\hat{b}^{\dagger}(x)\partial_x\hat{b}(x)) = \frac{\hbar}{m}\sqrt{\hat{\rho}(x)}[\nabla\hat{\Theta}(x)]\sqrt{\hat{\rho}(x)}, \tag{A.5}$$

where $[\hat{\rho}(x), \hat{j}(x')] = i\frac{\hbar}{m}(\partial_{x'}\delta(x - x'))\hat{\rho}(x')$.

A.2 Quadratic Hamiltonian

The free bosonic Hamiltonian is represented in Luttinger Liquid formalism as follows

$$\begin{aligned} H_{\mathrm{kin}} &= \frac{1}{2m}\int_x [\partial_x\hat{\psi}_B^{\dagger}(x)\partial_x\hat{\psi}_B(x)] \\ &= \frac{1}{2m}\int_x [\frac{1}{4}\frac{(\partial_x\hat{\rho}(x))^2}{\hat{\rho}(x)} + \sqrt{\hat{\rho}(x)}(\partial_x\hat{\theta}(x))^2\sqrt{\hat{\rho}(x)}], \end{aligned} \tag{A.6}$$

where we used that the Hamiltonian is invariant under space inversion ($x \to -x$) and thus just an even power of $\partial_x\hat{\theta}(x)$ is allowed to appear. The kinetic Hamiltonian in a zero order expansion with respect to $\hat{\rho}(x)$ is

$$\hat{H}_{\mathrm{kin}} = \frac{1}{2m}\int_x [\frac{\rho_0}{\pi}(\partial_x\hat{\theta}(x))^2 + \frac{1}{4\pi\rho_0}(\partial_x\hat{\phi}(x))^2]. \tag{A.7}$$

Considering an additional four point contact interation $\hat{H}_{\mathrm{int}} = g\int_x(\hat{\rho}(x))^2$, we can write the low-energy Hamiltonian of interacting bosons in a one dimensional system in a quadratic theory of the Luttinger Liquid fields $\hat{\theta}(x)$ and $\hat{\phi}(x)$. The prefactors of the two terms are modified in the presence of

interactions and are therefore in general replaced by the two parameters u and K[19,20]:

$$\hat{H}_{\mathrm{LL}} = \frac{u}{2\pi}\int [K(\partial_x\hat{\theta}(x))^2 + \frac{1}{K}(\partial_x\hat{\phi}(x))^2]\mathrm{d}x, \tag{A.8}$$

where $u = \frac{v_f}{K}$.
The low-energy excitations of the Luttinger Liquid system are phonons. We define the Luttinger Liquid fields in terms of the phonon eigenbasis $\{\hat{b}_p^\dagger, \hat{b}_p\}$ via

$$\hat{\theta}(x) = (N_R - N_L)\frac{\pi x}{L\sqrt{K}} + \frac{i\pi}{L}\sum_{p\neq 0}\sqrt{(\frac{L|p|}{2\pi K})}\frac{1}{|p|}e^{-\frac{1}{2}a|p|-ipx}(\hat{b}_p^\dagger - \hat{b}_{-p}), \tag{A.9}$$

$$\hat{\phi}(x) = -(N_R + N_L)\frac{\pi x\sqrt{K}}{L} - \frac{i\pi}{L}\sum_{p\neq 0}\sqrt{(\frac{L|p|K}{2\pi})}\frac{1}{p}e^{-\frac{1}{2}a|p|-ipx}(\hat{b}_p^\dagger + \hat{b}_{-p}), \tag{A.10}$$

where a is an ultra-violet cutoff.
The inclusion of K in this definition avoids off-diagonal terms $\hat{b}_{-p}^\dagger\hat{b}_p^\dagger$ and $\hat{b}_{-p}\hat{b}_p$. After the Bogoliubov transformation (A.9 - A.10), the diagonlized Hamiltonian in the bosonic operator basis reads:

$$\hat{H}_{\mathrm{LL}} = \sum_{p\neq 0} u|p|\hat{b}_p^\dagger\hat{b}_p = \sum_{p\neq 0}\epsilon(p)\hat{b}_p^\dagger\hat{b}_p, \tag{A.11}$$

where $\epsilon(p)$ is a linear dispersion and we neglect the constant energy shift.

Appendix B

Keldysh Formalism in a Nutshell

B.1 Time Evolution of the Density Operator

The dynamics of a many-body density operator at equilibrium is described by the following equation of motion:

$$\partial_t \hat{\rho}(t) = -i[\hat{H}, \hat{\rho}(t)] \Rightarrow \hat{\rho}(t) = \hat{U}\rho_0\hat{U}^\dagger \tag{B.1}$$

The time evolution operator U for the evolution from an inital point t_0 to t_f is unitary and therefore its hermitian conjugate $\hat{U}^\dagger$ describes the reverse time evolution $t_f \to t_0$. As a consequence forward and backward time evolution are not separable. If the system evolves on a circle in time space, the state does not differ at t_0 and t_f.
However, if the time evolution of the many-body quantum system reaches states out of equilibrium, the time evolution is not unitary any more and the reverse process of going backward in time does not necessarily lead to the initial state. Any circle in time space needs to be split in a forward $+$, respectively backward time contour $-$, and the physical information on both are independent.[51] Therefore the field integral representation (4.11) for a many-body system out of equilibrium is necessarily represented in a $\pm$ - basis.

B.2 Keldysh Field Integral Formalism

This section of the appendix is devoted to the explanation and motivation of the Keldysh path integral formalism[49–52], which is used to describe many-body quantum systems out of equilibrium. In contrast to the main text, we

restrict the explanations to systems without dissipation to put greater focus on the physical motivation of the formalism. We start from the field integral representation that is derived in section 4.1 and assume free bosonic particles with a quadratic dispersion:

$$\mathscr{Z} = \int \mathscr{D}\{\bar{\phi}^-, \phi^-, \bar{\phi}^+, \phi^+\} e^{iS[\bar{\phi}^+, \phi^+, \bar{\phi}^-, \phi^-]}, \tag{B.2}$$

$$\text{where } S[\bar{\phi}^+, \phi^+, \bar{\phi}^-, \phi^-] = \int_t \int_{x,x'} \tag{B.3}$$
$$[\bar{\phi}^+(x,t)(i\partial_t - \frac{\partial_x^2}{2m})\phi^+(x',t) - \bar{\phi}^-(x,t)(i\partial_t - \frac{\partial_x^2}{2m})\phi^-(x',t)].$$

The correlation functions are defined

$$i\,\langle \bar{\phi}^i(x,t)\phi^j(x',t')\rangle = \int \mathscr{D}\{\bar{\phi}^-, \phi^-, \bar{\phi}^+, \phi^+\} \bar{\phi}^i(x,t)\phi^j(x',t') e^{iS[\bar{\phi}^+, \phi^+, \bar{\phi}^-, \phi^-]}, \tag{B.4}$$

where $i, j \in \{-, +\}$. The corresponding correlation functions for the action of free bosons with a quadratic dispersion relation $\epsilon(q)$ is[51]

$$iG_\pm = \langle \bar{\phi}^+(x,t)\phi^-(x',t')\rangle = n_B(\omega) e^{-i\epsilon(q)(t-t')}, \tag{B.5}$$
$$iG_\mp = \langle \bar{\phi}^-(x,t)\phi^+(x',t')\rangle = (n_B(\omega)+1) e^{-i\epsilon(q)(t-t')}, \tag{B.6}$$
$$iG_+ = \langle \bar{\phi}^+(x,t)\phi^+(x',t')\rangle = \Theta(t-t')iG_\pm + \Theta(t'-t)iG_\mp, \tag{B.7}$$
$$iG_- = \langle \bar{\phi}^-(x,t)\phi^-(x',t')\rangle = \Theta(t'-t)iG_\pm + \Theta(t-t')iG_\mp, \tag{B.8}$$

where $n_B(\omega)$ is the bosonic occupation number,
On the + - contour the fields are symmetric ordered in time, whereas on the − - contour antisymmetric. For $G_\mp$ and $G_\pm$ the time ordering follows straightforward from the notation of the contours.
We conclude from comparison of the action (B.3) on the ± - contour and the corresponding correlations (B.5 - B.8) the following:

1. Continuum action in (B.3) does not directly show the correlations between the ± - contour at $t = t_0$ and $t = t_N$, where the contours are connected.

2. Green's function need to be specifically defined for $t = t'$.[51]

Therefore the action is transformed into a Keldysh representation, where the correlations between the two contours are directly observable and simultane-

ously the number of propagators is minimized:

$$\begin{pmatrix}\phi_+(x,t)\\ \phi_-(x,t)\end{pmatrix} = \frac{1}{\sqrt{2}}\begin{pmatrix}1 & 1\\ 1 & -1\end{pmatrix}\begin{pmatrix}\phi_{cl}(x,t)\\ \phi_q(x,t)\end{pmatrix}, \qquad \begin{pmatrix}\bar{\phi}_+(x,t)\\ \bar{\phi}_-(x,t)\end{pmatrix} = \frac{1}{\sqrt{2}}\begin{pmatrix}1 & 1\\ 1 & -1\end{pmatrix}\begin{pmatrix}\bar{\phi}_{cl}(x,t)\\ \bar{\phi}_q(x,t)\end{pmatrix}. \tag{B.9}$$

As a consequence the Keldysh action (B.8) is

$$S[\bar{\phi}_{cl},\phi_{cl},\bar{\phi}_q,\phi_q] = \int_{t,t'}\int_{x,x'} \bar{\Phi}(x,t)\begin{pmatrix}0 & P^R(x,t,x',t')\\ P^A(x,t,x',t') & P^K(x,t,x',t')\end{pmatrix}\Phi(x',t'), \tag{B.10}$$

where $\Phi(x,t) = (\phi_{cl}(x,t),\phi_q(x,t))^T$.
The bare propagators in the Keldysh basis read due to definition (B.9) and the Keldysh action (B.10):

$$iG^R(x,t,x',t') = \langle\bar{\phi}_{cl}(x,t)\phi_q(x',t')\rangle = \Theta(t-t')e^{-i\epsilon(q)(t-t')}, \tag{B.11}$$

$$iG^A(x,t,x',t') = \langle\bar{\phi}_q(x,t)\phi_{cl}(x',t')\rangle = -\Theta(t'-t)e^{-i\epsilon(q)(t-t')}, \tag{B.12}$$

$$iG^K(x,t,x',t') = \langle\bar{\phi}_{cl}(x,t)\phi_{cl}(x',t')\rangle = (2n_B(\omega)+1)e^{-i\epsilon(q)(t-t')}. \tag{B.13}$$

The choice of the Keldysh basis is also motivated by the advantage of better revealing the physical information of the many-body quantum system. For instance the Keldysh propagator is at equiibrium proportional to the occupation distribution. Furthermore the system's spectrum is stored in the retarded, respectively advanced Green's function.
The Keldysh Green's function G^K is antihermitian:

$$(G^K(x,t,x',t'))^\dagger = i(2n_B(\omega)+1)e^{i\epsilon(q)(t'-t)} = -G^K(x,t,x',t'). \tag{B.14}$$

Advanced and retarded Green's function are by definition hermition conjugate , i.e. $(G^A)^\dagger = -G^R$. The properties of the three propagators are used to define the following relation[51]

$$\begin{aligned}&G^K(x,t,x',t')\\ =&G^R(x,t,x_1,t_1)\circ F(x_1,t_1,x',t') - F(x,t,x_1,t_1)\circ G^A(x_1,t_1,x',t')\end{aligned} \tag{B.15}$$

where F must be due to (B.14) a hermitian operator.
At equilibrium the system is time and space translation invariant. Thus the operators in equation (B.15) just depend on the ralative time and space coordinates and we transform equation (B.15) into the Fourier space:

$$G^K(p,\omega) = [G^R(p,\omega) - G^A(p,\omega)]F(p,\omega). \tag{B.16}$$

From equations (B.11 - B.13) we get the retarded, advanced and Keldysh Green's functions in Fourier space:

$$G^R(p,\omega) = \omega - \epsilon(p) + i\eta)^{-1}, \tag{B.17}$$

$$G^A(p,\omega) = (\omega - \epsilon(p) - i\eta)^{-1}, \tag{B.18}$$

$$G^K(p,\omega) = (2n_B(\epsilon(p)) + 1), \tag{B.19}$$

where η is an infinitesimal regularization and we find

$$F(p,\omega) = 2n_B(\epsilon(p)) + 1 = \coth(\beta\epsilon(p)). \tag{B.20}$$

In conclusion the relation (B.15) turns in the limit, where the system reaches equilibrium, into the fluctuation-dissipation theorem.
If the system is out of equilibrium, the convolution operation between two functions is not simply the product of their Fourier representations. In this case the distribution function $F(x_1, t_1, x^{'}, t^{'})$ is unspecified and differs from the stationary Bose-Einstein distribution. We analyse this in more detail in connection with the kinetic equation for a many-body quantum system far from equilibrium in chapter 5.

Appendix C

Correlations in a Luttinger Liquid

In this appendix we compute the relative phase correlation function for a thermal Luttinger Liquid.[19]
At equilibrium the two point correlation functions of the bosonic operators in the Keldysh representation (B.17 - B.19) are

$$\langle \hat{b}_{p,cl}(t)\hat{b}^{\dagger}_{p,cl}(t^{'})\rangle = e^{-i\epsilon(p)(t-t^{'})}\coth(\frac{\epsilon(p)\beta}{2}), \tag{C.1}$$

$$\langle \hat{b}_{p,cl}(t)\hat{b}^{\dagger}_{p,q}(t^{'})\rangle = \Theta(t-t^{'})e^{-i\epsilon(p)(t-t^{'})}, \tag{C.2}$$

$$\langle \hat{b}_{p,q}(t)\hat{b}^{\dagger}_{p,cl}(t^{'})\rangle = -\Theta(t^{'}-t)e^{-i\epsilon(p)(t-t^{'})}. \tag{C.3}$$

The correlations of the Luttinger Liquid fields on the $\pm$ - contour is determined via (B.9) and (A.9 - A.10):

$$\begin{aligned}
&\langle \hat{\phi}_{-}(x,t)\hat{\phi}_{-}(y,t^{'})\rangle \qquad\qquad (C.4)\\
&= -\tfrac{\pi^2}{L^2}K\sum_{p,q\neq 0}\tfrac{L}{2\pi}\tfrac{\sqrt{|p||q|}}{pq}e^{\frac{-\alpha(|p|+|q|)}{2}}e^{-i(px+qy)}(\langle \hat{b}^{\dagger}_{p,-}(t)\hat{b}_{-q,-}(t^{'})\rangle + \langle \hat{b}_{-p,-}(t)\hat{b}^{\dagger}_{q,-}(t^{'})\rangle)\\
&= \tfrac{\pi}{L}K\sum_{p\neq 0}\tfrac{\sqrt{|p||p|}}{p^2}e^{-\alpha|p|}e^{-ip(x-y)}[\cos(\epsilon(p)(t-t^{'}))\coth(\tfrac{\epsilon(p)\beta}{2}) - i\ \mathrm{sign}(t-t^{'})\sin(\epsilon(p)(t-t^{'}))]
\end{aligned}$$

$$\begin{aligned}
&\langle \hat{\phi}_{+}(x,t)\hat{\phi}_{+}(y,t^{'})\rangle \qquad\qquad (C.5)\\
&= -\tfrac{\pi^2}{L^2}K\sum_{p,q\neq 0}\tfrac{L}{2\pi}\tfrac{\sqrt{|p||q|}}{pq}e^{\frac{-\alpha(|p|+|q|)}{2}}e^{-i(px+qy)}(\langle \hat{b}^{\dagger}_{p,+}(t)\hat{b}_{-q,+}(t^{'})\rangle + \langle \hat{b}_{-p,+}\hat{b}^{\dagger}_{q,+}(t^{'})\rangle)\\
&= \tfrac{\pi}{L}K\sum_{p\neq 0}\tfrac{\sqrt{|p||p|}}{p^2}e^{-\alpha|p|}e^{-ip(x-y)}[\cos(\epsilon(p)(t-t^{'}))\coth(\tfrac{\epsilon(p)\beta}{2}) + i\ \mathrm{sign}(t-t^{'})\sin(\epsilon(p)(t-t^{'}))]
\end{aligned}$$

$$\begin{aligned}
&\langle\hat{\phi}_-(x,t)\hat{\phi}_+(y,t')\rangle \qquad\qquad (C.6)\\
&= -\tfrac{\pi^2}{L^2}K\sum_{p,q\neq 0}\tfrac{L}{2\pi}\tfrac{\sqrt{|p||q|}}{pq}e^{\frac{-\alpha(|p|+|q|)}{2}}e^{-i(px+qy)}(\langle\hat{b}^\dagger_{p,-}(t)\hat{b}_{-q,+}(t')\rangle+\langle\hat{b}_{-p,-}(t)\hat{b}^\dagger_{q,+}(t')\rangle)\\
&= \tfrac{\pi}{L}K\sum_{p\neq 0}\tfrac{\sqrt{|p||p|}}{p^2}e^{-\alpha|p|}e^{-ip(x-y)}[\cos(\epsilon(p)(t-t'))\coth(\tfrac{\epsilon(p)\beta}{2})+i\sin(\epsilon(p)(t-t'))]
\end{aligned}$$

In the zero temperature limit the occupation distribution is $F(\epsilon(p),\beta)=\coth(\frac{\epsilon(p)\beta}{2})\overset{T\to 0}{=}1$. In this limit the definition of the relative phase correlators reads[19]:

$$C_{\hat{\phi}_\pm\hat{\phi}_\pm}=\langle e^{i\gamma\hat{\phi}_\pm(x,t)}e^{-i\gamma\hat{\phi}_\pm(y,t')}\rangle=e^{-\frac{\gamma^2}{2}\langle(\hat{\phi}_\pm(x,t)-\hat{\phi}_\pm(y,t'))^2\rangle}. \qquad (C.7)$$

The relative phase correlators can be calculated using relations (C.1 - C.3):

$$\begin{aligned}
&C_{\hat{\phi}_-\hat{\phi}_-}= \qquad\qquad (C.8)\\
&\big(\tfrac{((x-y)+u(t-t'))^2+\alpha^2)}{\alpha^2}\big)^{-K_{eq}}\big(\tfrac{((x-y)-u(t-t'))^2+\alpha^2)}{\alpha^2}\big)^{-K_{eq}}\\
&e^{-2K_{eq}i\ \mathrm{sign}(t-t')[\tan^{-1}\frac{u(t-t')+(x-y)}{\alpha}+\tan^{-1}\frac{u(t-t')-(x-y)}{\alpha}]}
\end{aligned}$$

$$\begin{aligned}
&C_{\hat{\phi}_+\hat{\phi}_+}= \qquad\qquad (C.9)\\
&\big(\tfrac{((x-y)+u(t-t'))^2+\alpha^2)}{\alpha^2}\big)^{-K_{eq}}\big(\tfrac{((x-y)-u(t-t'))^2+\alpha^2)}{\alpha^2}\big)^{-K_{eq}}\\
&e^{2K_{eq}i\ \mathrm{sign}(t-t')[\tan^{-1}\frac{u(t-t')+(x-y)}{\alpha}+\tan^{-1}\frac{u(t-t')-(x-y)}{\alpha}]}
\end{aligned}$$

$$\begin{aligned}
&C_{\hat{\phi}_-\hat{\phi}_+}= \qquad\qquad (C.10)\\
&\big(\tfrac{((x-y)+u(t-t'))^2+\alpha^2)}{\alpha^2}\big)^{-K_{eq}}\big(\tfrac{((x-y)-u(t-t'))^2+\alpha^2)}{\alpha^2}\big)^{-K_{eq}}\\
&e^{2K_{eq}i[\tan^{-1}\frac{u(t-t')+(x-y)}{\alpha}+\tan^{-1}\frac{u(t-t')-(x-y)}{\alpha}]}
\end{aligned}$$

The results (C.8 - C.10) show an algebraic decay of the correlation functions with exponent

$$K_{eq}=\frac{K\gamma^2}{8}, \qquad (C.11)$$

which is characteristic for models of the universality class of Luttinger Liquids.
Finally, we check that for this thermalized system the fluctuation-dissipation

theorem (B.16) in the Keldysh framework is fullfilled.
The Keldysh and retarded correlation functions in the Keldysh basis (B.9) are:

$$
\begin{aligned}
&iC^K_{\phi\phi}(x,t;y,t') = \\
&\tfrac{1}{2}(C_{\hat{\phi}_-\hat{\phi}_-}(x,t;y,t') + C_{\hat{\phi}_+\hat{\phi}_+}(x,t;y,t')) = \\
&\big(\tfrac{((x-y)+u(t-t'))^2+\alpha^2)}{\alpha^2}\big)^{-K_{eq}}\big(\tfrac{((x-y)-u(t-t'))^2+\alpha^2)}{\alpha^2}\big)^{-K_{eq}} \\
&\cos(K_{eq}[\tan^{-1}\tfrac{u(t-t')+(x-y)}{\alpha} + \tan^{-1}\tfrac{u(t-t')-(x-y)}{\alpha}]),
\end{aligned}
\tag{C.12}
$$

$$
\begin{aligned}
&iC^R_{\phi\phi}(x,t;y,t') = \\
&\frac{1}{2}(C_{\hat{\phi}_-\hat{\phi}_-}(x,t;y,t') - C_{\hat{\phi}_-\hat{\phi}_+}(x,t;y,t') = \\
&-i\theta(t-t')\big(\tfrac{((x-y)+u(t-t'))^2+a^2)}{\alpha^2}\big)^{-K_{eq}}\big(\tfrac{((x-y)-u(t-t'))^2+\alpha^2)}{\alpha^2}\big)^{-K_{eq}} \\
&\sin(K_{eq}[\tan^{-1}\tfrac{u(t-t')+(x-y)}{\alpha} + \tan^{-1}\tfrac{u(t-t')-(x-y)}{\alpha}]).
\end{aligned}
\tag{C.13}
$$

The fluctuation-dissipation theorem is according to

$$
C^K_{\phi\phi} \overset{T=0}{=} [C^R_{\phi\phi} - C^A_{\phi\phi}] = [C^R_{\phi\phi} - C^{R\dagger}_{\phi\phi}] = 2i\mathrm{Im}(C^R_{\phi\phi}) \tag{C.14}
$$

fulfilled.

References

[1]D. Jaksch, C. Bruder, J. I. Cirac, C. W. Gardiner, and P. Zoller, "Cold bosonic atoms in optical lattices", Physical Review Letters **81**, 3108 (1998).

[2]I. Bloch, J. Dalibard, and W. Zwerger, "Many-body physics with ultracold gases", Reviews of Modern Physics **80**, 885 (2008).

[3]R. Nandkishore and D. A. Huse, "Many body localization and thermalization in quantum statistical mechanics", arXiv:1404.0686 (2014).

[4]M. Rigol, V. Dunjko, and M. Olshanii, "Thermalization and its mechanism for generic isolated quantum systems", Nature **452**, 854–858 (2008).

[5]M. Cheneau, P. Barmettler, D. Poletti, M. Endres, P. Schauß, T. Fukuhara, C. Gross, I. Bloch, C. Kollath, and S. Kuhr, "Light-cone-like spreading of correlations in a quantum many-body system", Nature **481**, 484–487 (2012).

[6]T. Langen, R. Geiger, M. Kuhnert, B. Rauer, and J. Schmiedmayer, "Local emergence of thermal correlations in an isolated quantum many-body system", Nature Physics **9**, 640–643 (2013).

[7]D. Poletti, J.-S. Bernier, A. Georges, and C. Kollath, "Interaction-induced impeding of decoherence and anomalous diffusion", Physical Review Letters **109**, 045302 (2012).

[8]Z. Cai and T. Barthel, "Algebraic versus exponential decoherence in dissipative many-particle systems", Physical Review Letters **111**, 150403 (2013).

[9]P. Calabrese and J. Cardy, "Time dependence of correlation functions following a quantum quench", Physical Review Letters **96**, 136801 (2006).

[10]M. Rigol, V. Dunjko, V. Yurovsky, and M. Olshanii, "Relaxation in a completely integrable many-body quantum system: An ab initio study of the dynamics of the highly excited states of 1D lattice hard-core bosons", Physical Review Letters **98**, 050405 (2007).

[11]M. Cazalilla, "The Luttinger model following a sudden interaction switch-on", arXiv:cond-mat/0606236 (2006).

[12]J.-S. Caux and R. M. Konik, "Constructing the generalized Gibbs ensemble after a quantum quench", Physical Review Letters **109**, 175301 (2012).

[13]E. Altman and A. Auerbach, "Oscillating superfluidity of bosons in optical lattices", Physical Review Letters **89**, 250404 (2002).

[14]C. Kollath, U. Schollwöck, J. Von Delft, and W. Zwerger, "One-dimensional density waves of ultracold bosons in an optical lattice", Physical Review A **71**, 053606 (2005).

[15]R. Barankov and L. Levitov, "Dynamical projection of atoms to Feshbach molecules at strong coupling", arXiv:cond-mat/0506323 (2005).

[16]F. Haldane, "Effective harmonic-fluid approach to low-energy properties of one-dimensional quantum fluids", Physical Review Letters **47**, 1840 (1981).

[17]J. Luttinger, "An exactly soluble model of a many-fermion system", Journal of Mathematical Physics **4**, 1154–1162 (1963).

[18]S.-I. Tomonaga, "Remarks on Bloch's method of sound waves applied to many-fermion problems", Progress of Theoretical Physics **5**, 544–569 (1950).

[19]T. Giamarchi, *Quantum physics in one dimension*, International Series of Monographs on Physics (Oxford University Press, 2004).

[20]M. Cazalilla, R. Citro, T. Giamarchi, E. Orignac, and M. Rigol, "One dimensional bosons: From condensed matter systems to ultracold gases", Reviews of Modern Physics **83**, 1405 (2011).

[21]J. Berges, S. Borsányi, and C. Wetterich, "Prethermalization", Physical Review Letters **93**, 142002 (2004).

[22]M. Eckstein, M. Kollar, and P. Werner, "Thermalization after an interaction quench in the Hubbard model", Physical Review Letters **103**, 056403 (2009).

[23]M. Moeckel and S. Kehrein, "Real-time evolution for weak interaction quenches in quantum systems", Annals of Physics **324**, 2146–2178 (2009).

[24]E. T. Jaynes, "Information theory and statistical mechanics 2", Physical Review **108**, 171 (1957).

[25]F. Schwabl, *Statistische Mechanik* (Springer-Verlag, 2006).

[26]J.-S. Caux and P. Calabrese, "Dynamical density-density correlations in the one-dimensional Bose gas", Physical Review A **74**, 031605 (2006).

[27]T. Kinoshita, T. Wenger, and D. S. Weiss, "A quantum Newton's cradle", Nature **440**, 900–903 (2006).

[28]T. Kitagawa, A. Imambekov, J. Schmiedmayer, and E. Demler, "The dynamics and prethermalization of one-dimensional quantum systems probed through the full distributions of quantum noise", New Journal of Physics **13**, 073018 (2011).

[29]A. Andreev, "The hydrodynamics of two- and one-dimensional liquids", Soviet Journal of Experimental and Theoretical Physics **51**, 1038 (1980).

[30]M. Buchhold and S. Diehl, "Kinetic theory for interacting Luttinger liquids", arXiv:1501.01027 (2015).

[31]M. Buchhold and S. Diehl, "Non-equilibrium universality in the heating dynamics of interacting Luttinger liquids", arXiv:1404.3740 (2014).

[32]H. Pichler, A. Daley, and P. Zoller, "Nonequilibrium dynamics of bosonic atoms in optical lattices: Decoherence of many-body states due to spontaneous emission", Physical Review A **82**, 063605 (2010).

[33]K. Samokhin, "Lifetime of excitations in a clean Luttinger liquid", Journal of Physics: Condensed Matter **10**, 533–538 (1998).

[34]O. Narayan and S. Ramaswamy, "Anomalous heat conduction in one-dimensional momentum-conserving systems", Physical Review Letters **89**, 200601_1–200601_4 (2002).

[35]S. Lepri, R. Livi, and A. Politi, "Universality of anomalous one-dimensional heat conductivity", Physical Review E **68**, 067102 (2003).

[36]R. G. Pereira, J. Sirker, J.-S. Caux, R. Hagemans, J. M. Maillet, S. White, and I. Affleck, "Dynamical spin structure factor for the anisotropic spin-1/2 Heisenberg chain", Physical Review Letters **96**, 257202 (2006).

[37]M. Punk and W. Zwerger, "Collective mode damping and viscosity in a 1D unitary Fermi gas", New Journal of Physics **8**, 168 (2006).

[38]J. Von Delft and H. Schoeller, "Bosonization for beginners—Refermionization for experts", arXiv:cond-mat/9805275 (1998).

[39]M. P. Fisher, P. B. Weichman, G. Grinstein, and D. S. Fisher, "Boson localization and the superfluid-insulator transition", Physical Review B **40**, 546 (1989).

[40]M. Greiner, O. Mandel, T. Esslinger, T. W. Hänsch, and I. Bloch, "Quantum phase transition from a superfluid to a Mott insulator in a gas of ultracold atoms", Nature **415**, 39–44 (2002).

[41]E. Haller, R. Hart, M. J. Mark, J. G. Danzl, L. Reichsöllner, M. Gustavsson, M. Dalmonte, G. Pupillo, and H.-C. Nägerl, "Pinning quantum phase transition for a Luttinger liquid of strongly interacting bosons", Nature **466**, 597–600 (2010).

[42]A. Altland and B. D. Simons, *Condensed matter field theory* (Cambridge University Press, 2010).

[43]F. Petruccione and H.-P. Breuer, *The theory of open quantum systems* (Oxford University Press, 2002).

[44]M. Lewenstein, J. I. Cirac, and P. Zoller, "Master equation for sympathetic cooling of trapped particles", Physical Review A **51**, 4617 (1995).

[45]S. Diehl, A. Micheli, A. Kantian, B. Kraus, H. Büchler, and P. Zoller, "Quantum states and phases in driven open quantum systems with cold atoms", Nature Physics **4**, 878–883 (2008).

[46]C. Gardiner and P. Zoller, *Quantum noise: A handbook of markovian and non-markovian quantum stochastic methods with applications to quantum optics* (Springer Science & Business Media, 2004).

[47]F. Gerbier and Y. Castin, "Heating rates for an atom in a far-detuned optical lattice", Physical Review A **82**, 013615 (2010).

[48]W. Rohringer, D. Fischer, F. Steiner, I. E. Mazets, J. Schmiedmayer, and M. Trupke, "Scaling of phonons and shortcuts to adiabaticity in a one-dimensional quantum system", arXiv:1312.5948 (2013).

[49]L. Sieberer, S. Huber, E. Altman, and S. Diehl, "Dynamical critical phenomena in driven-dissipative systems", Physical Review Letters **110**, 195301 (2013).

[50]L. Sieberer, S. Huber, E. Altman, and S. Diehl, "Nonequilibrium functional renormalization for driven-dissipative Bose-Einstein condensation", Physical Review B **89**, 134310 (2014).

[51]A. Kamenev, *Field theory of non-equilibrium systems* (Cambridge University Press, 2011).

[52]E. G. Dalla Torre, S. Diehl, M. D. Lukin, S. Sachdev, and P. Strack, "Keldysh approach for nonequilibrium phase transitions in quantum optics: Beyond the Dicke model in optical cavities", Physical Review A **87**, 023831 (2013).

[53]M. Buchhold, PhD thesis (TU Dresden, 2015).

[54]A. L. Fetter and J. D. Walecka, *Quantum theory of many-particle systems* (Courier Corporation, 2003).

[55]J. L. Lebowitz and E. W. Montroll, "Nonequilibrium phenomena I: The Boltzmann equation", Nonequilibrium Phenomena I: The Boltzmann Equation **1** (1983).

[56]U. Stroth, *Plasmaphysik* (Springer-Verlag, 2011).

[57]J. Schachenmayer, L. Pollet, M. Troyer, and A. J. Daley, "Spontaneous emission and thermalization of cold bosons in optical lattices", Physical Review A **89**, 011601 (2014).

[58]T. Langen, S. Erne, R. Geiger, B. Rauer, T. Schweigler, M. Kuhnert, W. Rohringer, I. E. Mazets, T. Gasenzer, and J. Schmiedmayer, "Experimental observation of a generalized Gibbs ensemble", arXiv:1411.7185 (2014).

[59]M. Gring, M. Kuhnert, T. Langen, T. Kitagawa, B. Rauer, M. Schreitl, I. Mazets, D. A. Smith, E. Demler, and J. Schmiedmayer, "Relaxation and prethermalization in an isolated quantum system", Science **337**, 1318–1322 (2012).

[60]R. Geiger, T. Langen, I. Mazets, and J. Schmiedmayer, "Local relaxation and light-cone-like propagation of correlations in a trapped one-dimensional Bose gas", New Journal of Physics **16**, 053034 (2014).

[61]E. G. Dalla Torre, E. Demler, and A. Polkovnikov, "Universal rephasing dynamics after a quantum quench via sudden coupling of two initially independent condensates", Physical Review Letters **110**, 090404 (2013).

[62]N. K. Whitlock and I. Bouchoule, "Relative phase fluctuations of two coupled one-dimensional condensates", Physical Review A **68**, 053609 (2003).

[63]A. Burkov, M. Lukin, and E. Demler, "Decoherence dynamics in low-dimensional cold atom interferometers", Physical Review Letters **98**, 200404 (2007).

[64]L. Foini and T. Giamarchi, "Non-equilibrium dynamics of coupled Luttinger liquids", arXiv:1412.6377 (2014).